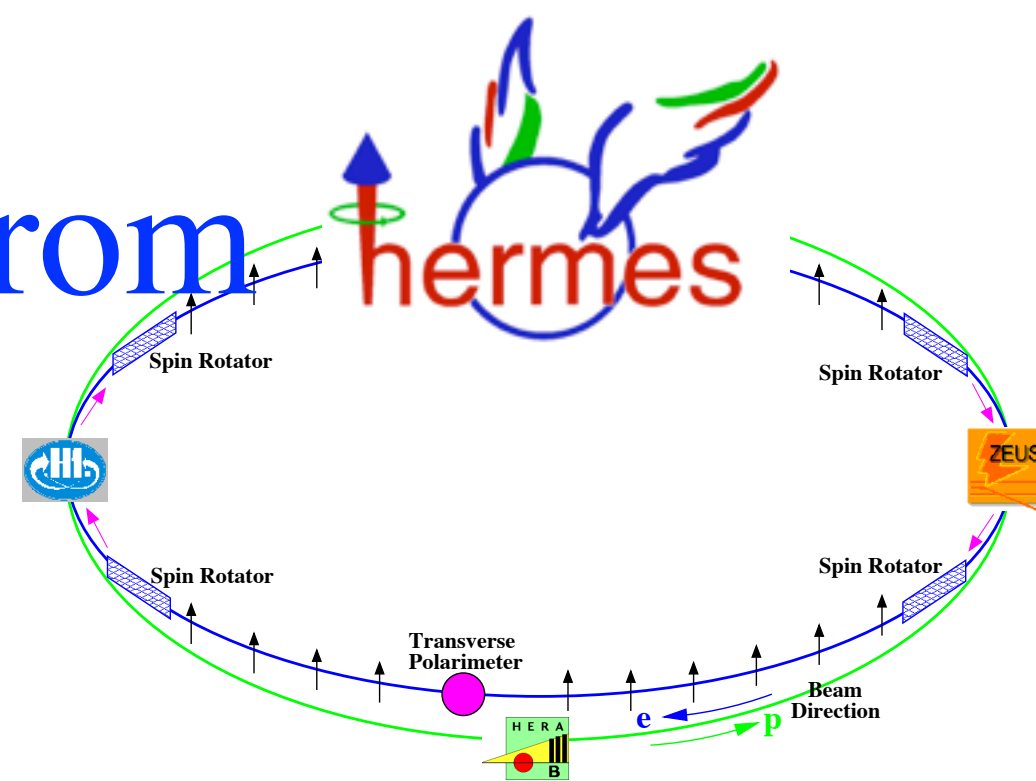


Recent results from



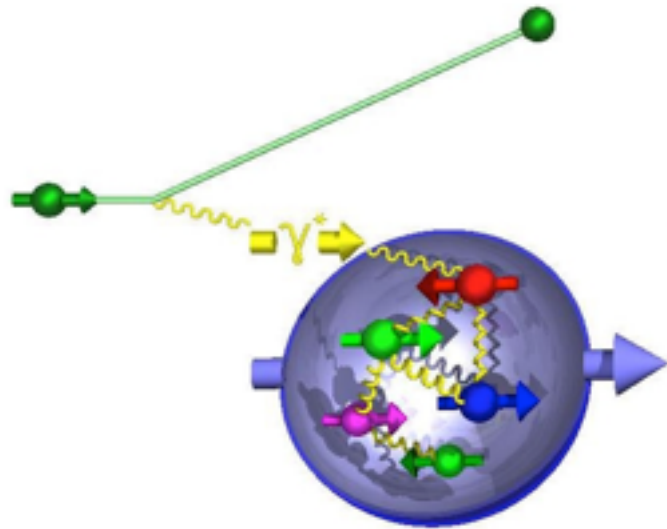
DSPIN 2013

Dubna, Russia, October 8 - 12, 2013

Wolf-Dieter Nowak,

Ami Rostomyan, Charlotte Van Hulse
(for the HERMES Collaboration)

spin and hadronization



HERMES main research topics:

✓ origin of nucleon spin

- ☞ longitudinal spin/momentum structure
- ☞ transverse spin/momentum structure

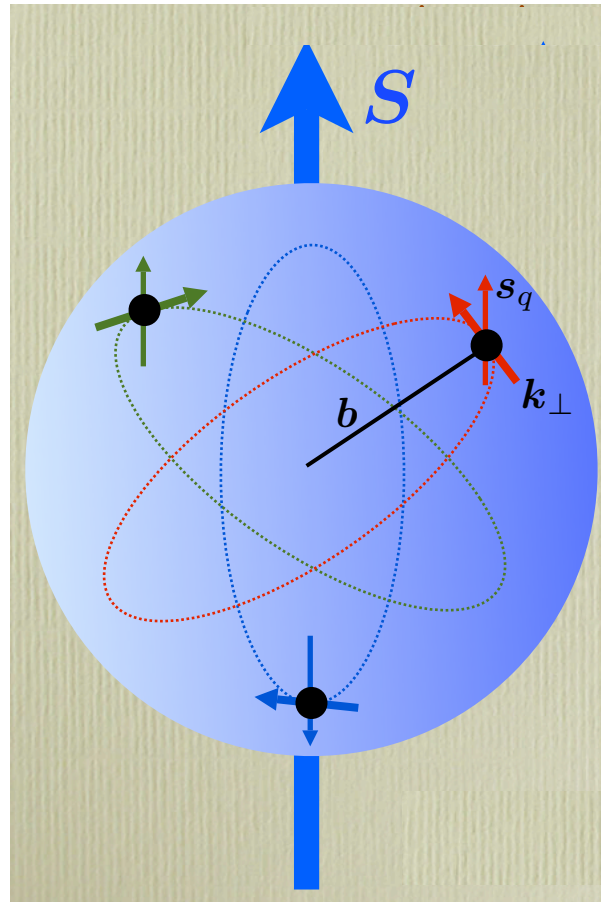
✓ hadronization/fragmentation

- ✓ nucleon properties (mass, charge, momentum, magnetic moment, spin...) should be explained by its constituents
- ☞ momentum: quarks carry $\sim 50\%$ of the proton momentum
- ☞ spin: total quark spin contribution only $\sim 30\%$

quantum phase-space “tomography” of the nucleon

Wigner functions: $W^q(\mathbf{k}, \mathbf{b})$

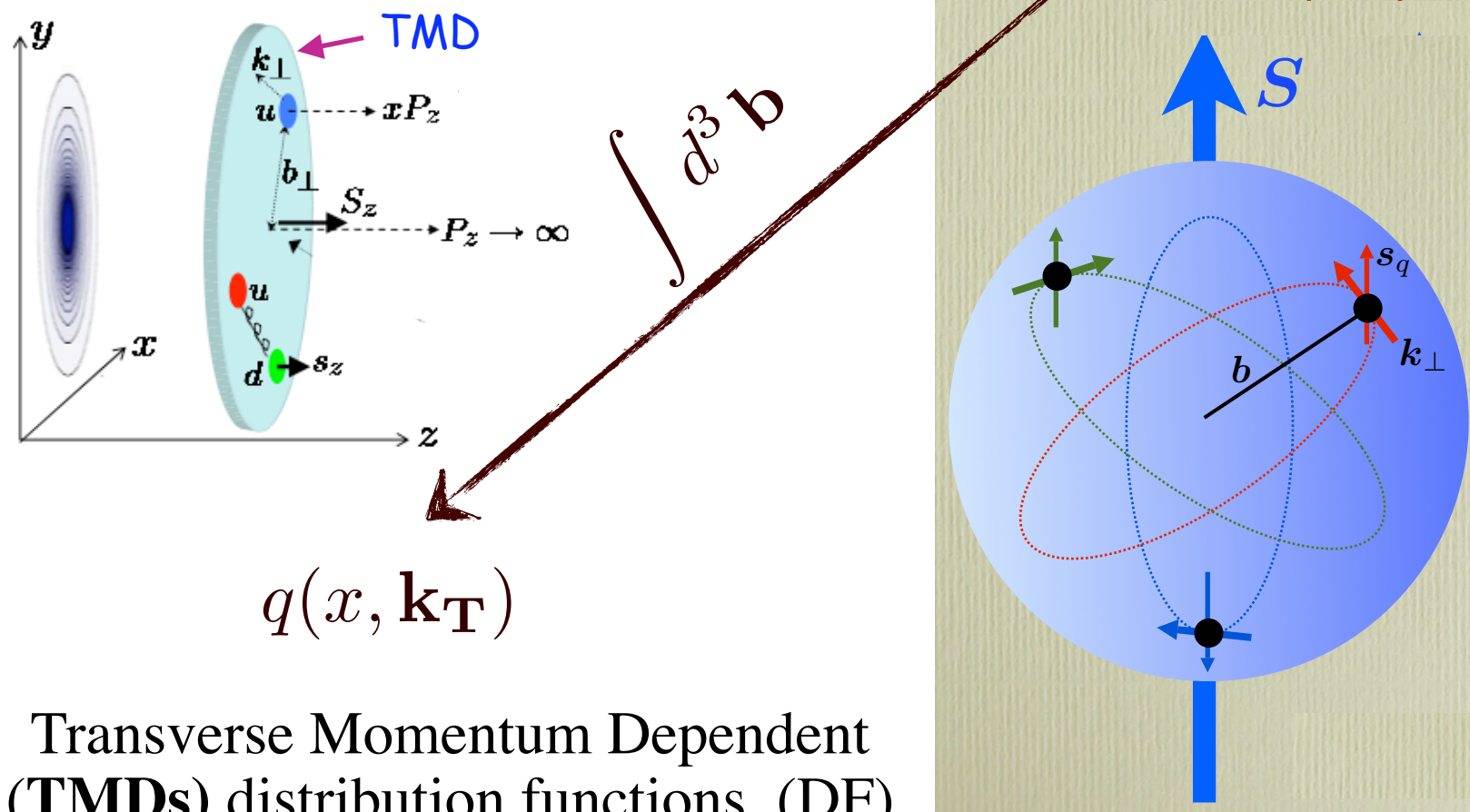
probability to find a quark in a nucleon with a certain polarization in a position \mathbf{b} and momentum \mathbf{k}



quantum phase-space “tomography” of the nucleon

Wigner functions: $W^q(\mathbf{k}, \mathbf{b})$

probability to find a quark in a nucleon with a ~~certain~~ polarization in a position \mathbf{b} and momentum \mathbf{k}

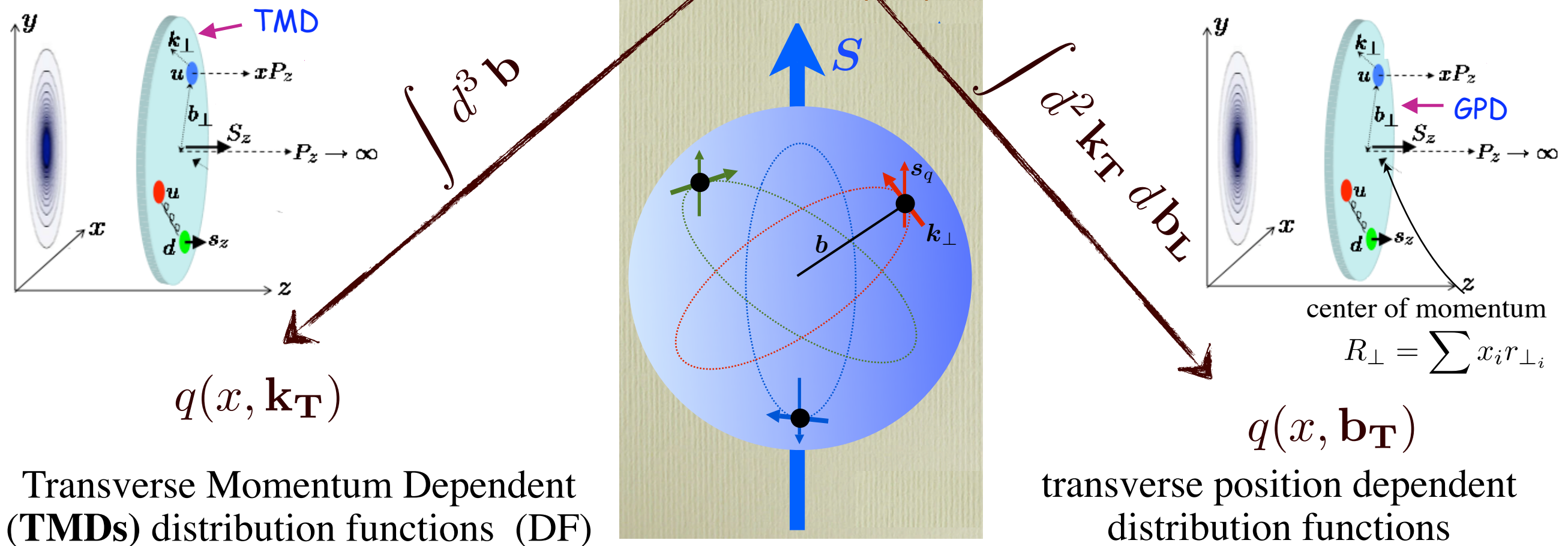


Transverse Momentum Dependent (TMDs) distribution functions (DF)

quantum phase-space “tomography” of the nucleon

Wigner functions: $W^q(\mathbf{k}, \mathbf{b})$

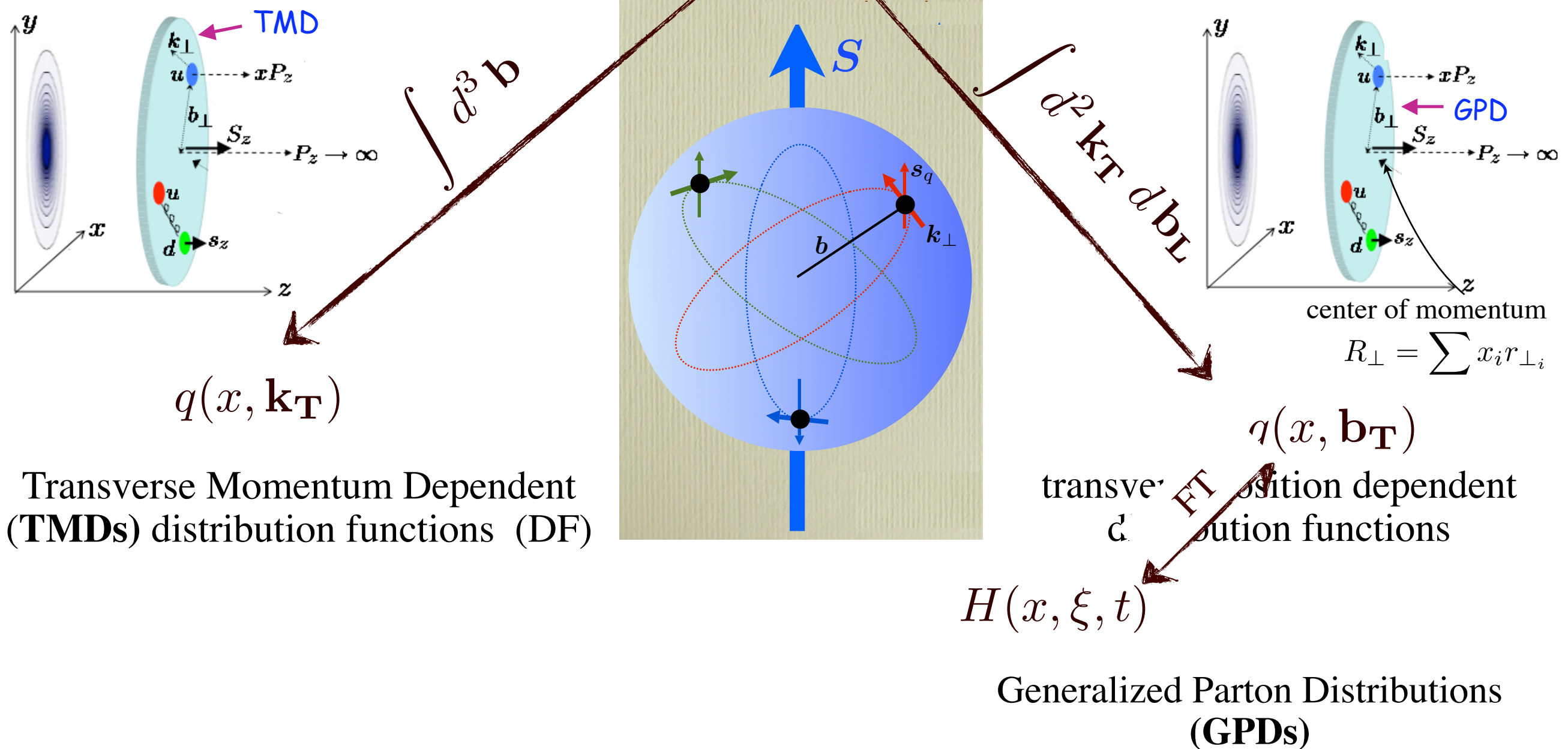
probability to find a quark in a nucleon with a certain polarization in a position \mathbf{b} and momentum \mathbf{k}



quantum phase-space “tomography” of the nucleon

Wigner functions: $W^q(\mathbf{k}, \mathbf{b})$

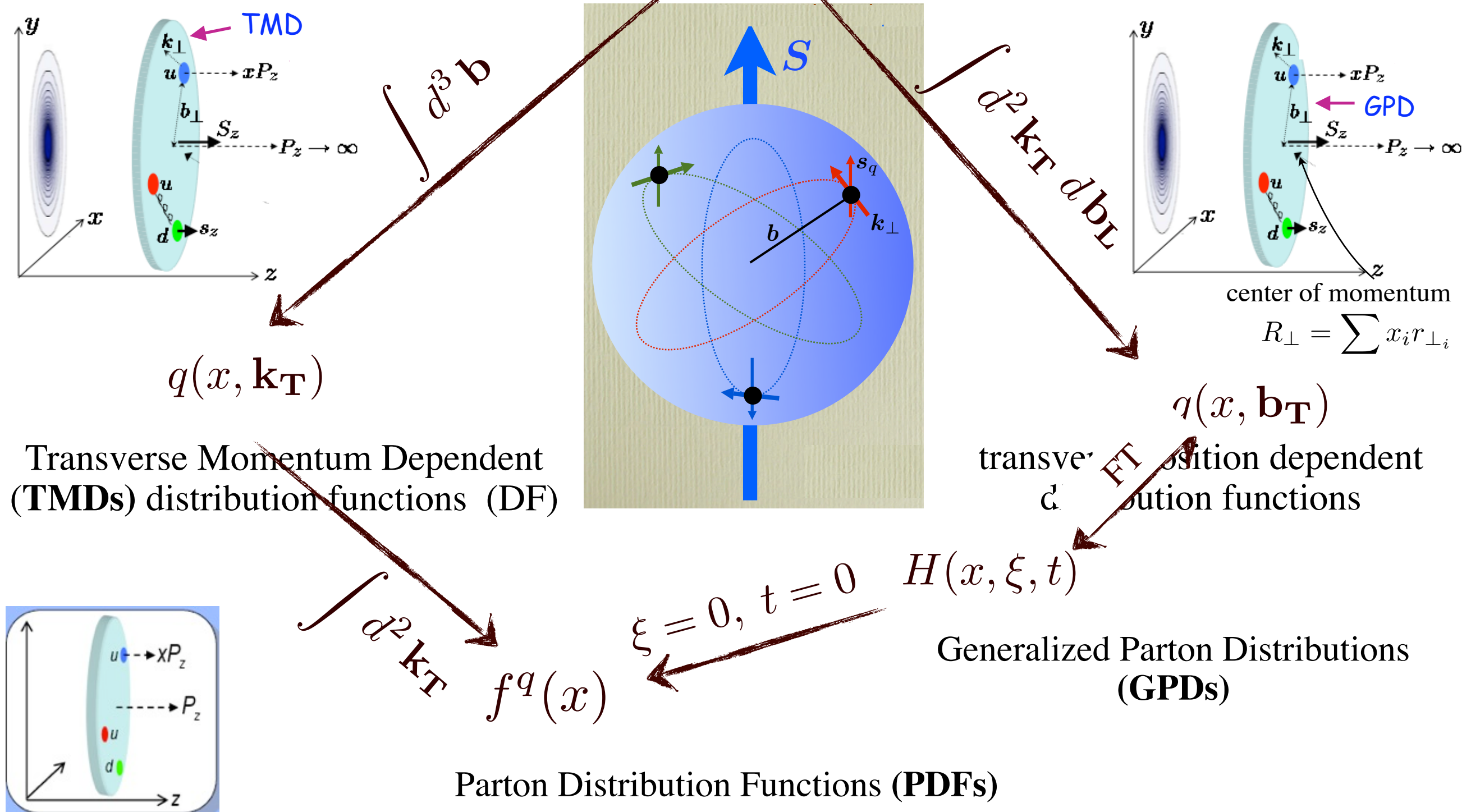
probability to find a quark in a nucleon with a certain polarization in a position \mathbf{b} and momentum \mathbf{k}



quantum phase-space “tomography” of the nucleon

Wigner functions: $W^q(\mathbf{k}, \mathbf{b})$

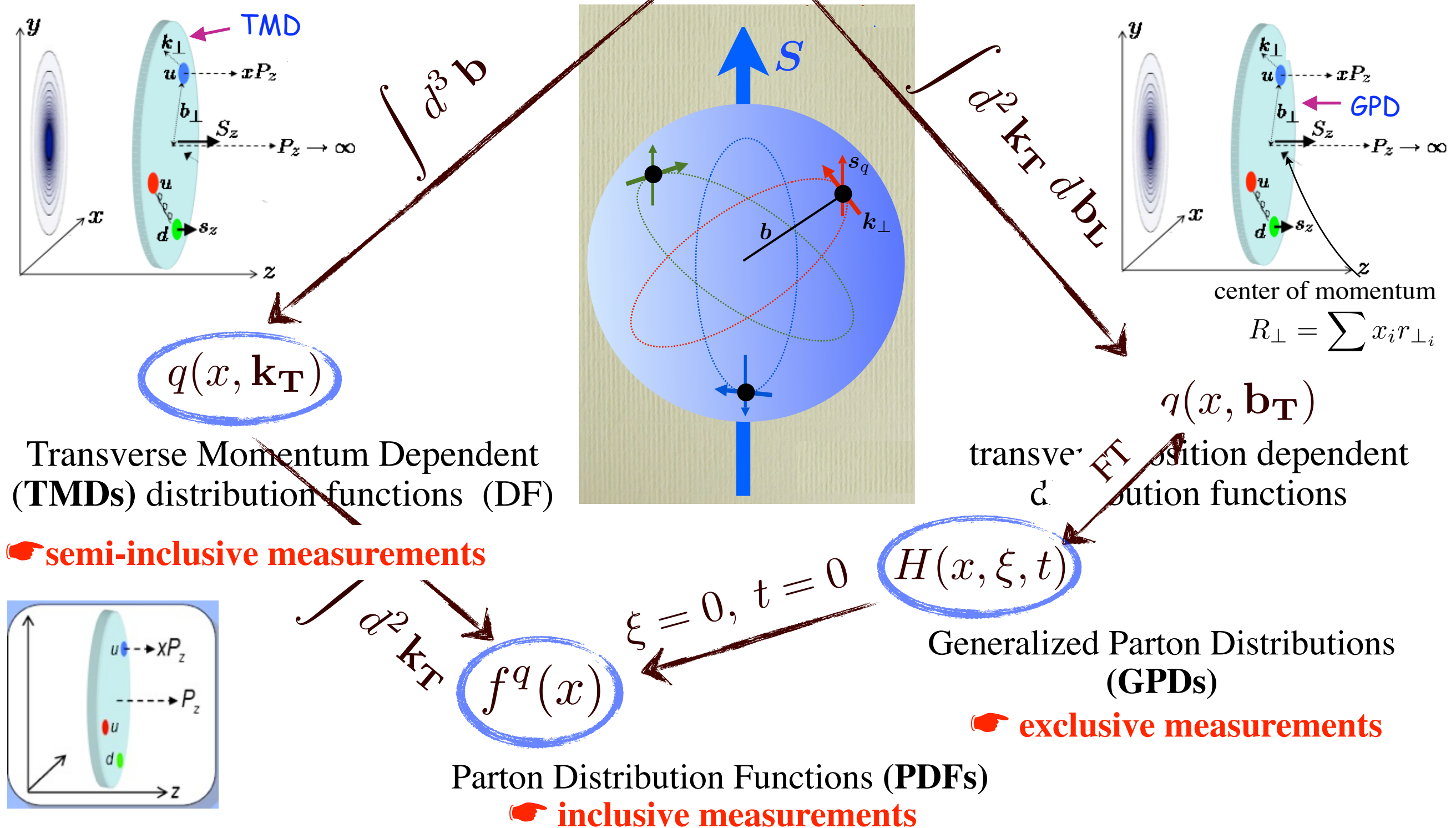
probability to find a quark in a nucleon with a certain polarization in a position \mathbf{b} and momentum \mathbf{k}



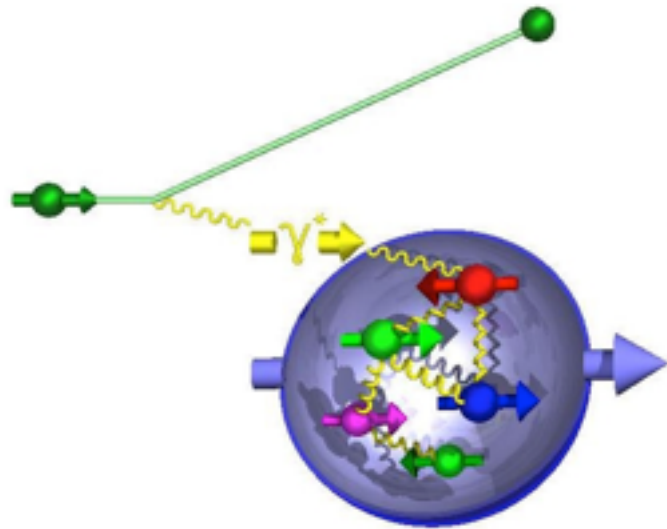
quantum phase-space “tomography” of the nucleon

Wigner functions: $W^q(\mathbf{k}, \mathbf{b})$

probability to find a quark in a nucleon with a certain polarization in a position \mathbf{b} and momentum \mathbf{k}



spin and hadronization



HERMES main research topics:

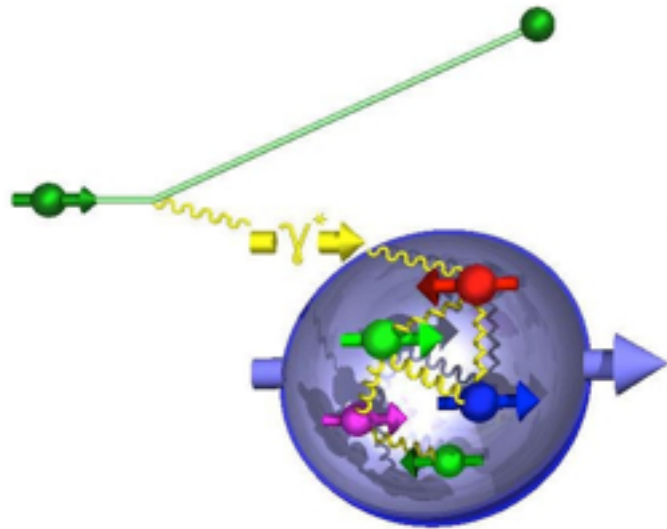
✓ origin of nucleon spin

- ☞ longitudinal spin/momentum structure
- ☞ transverse spin/momentum structure

✓ hadronization/fragmentation

- ✓ nucleon properties (mass, charge, momentum, magnetic moment, spin...) should be explained by its constituents
- ☞ momentum: quarks carry ~ 50 % of the proton momentum
- ☞ spin: total quark spin contribution only ~30%
- ➡ study of TMD DFs and GPDs

spin and hadronization



HERMES main research topics:

✓ origin of nucleon spin

- ☞ longitudinal spin/momentum structure
- ☞ transverse spin/momentum structure

✓ hadronization/fragmentation

- ✓ nucleon properties (mass, charge, momentum, magnetic moment, spin...) should be explained by its constituents
- ☞ momentum: quarks carry ~ 50 % of the proton momentum
- ☞ spin: total quark spin contribution only ~30%
- ➡ **study of TMD DFs and GPDs**

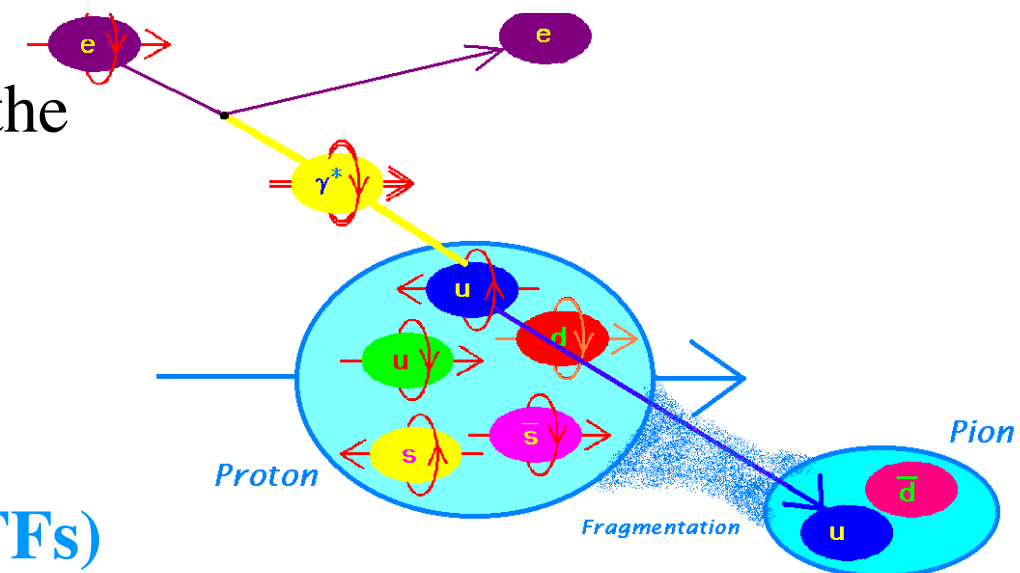
✓ isolated quarks have never been observed in nature

✓ fragmentation functions were introduced to describe the hadronization

☞ non-pQCD objects

☞ universal but not well known functions

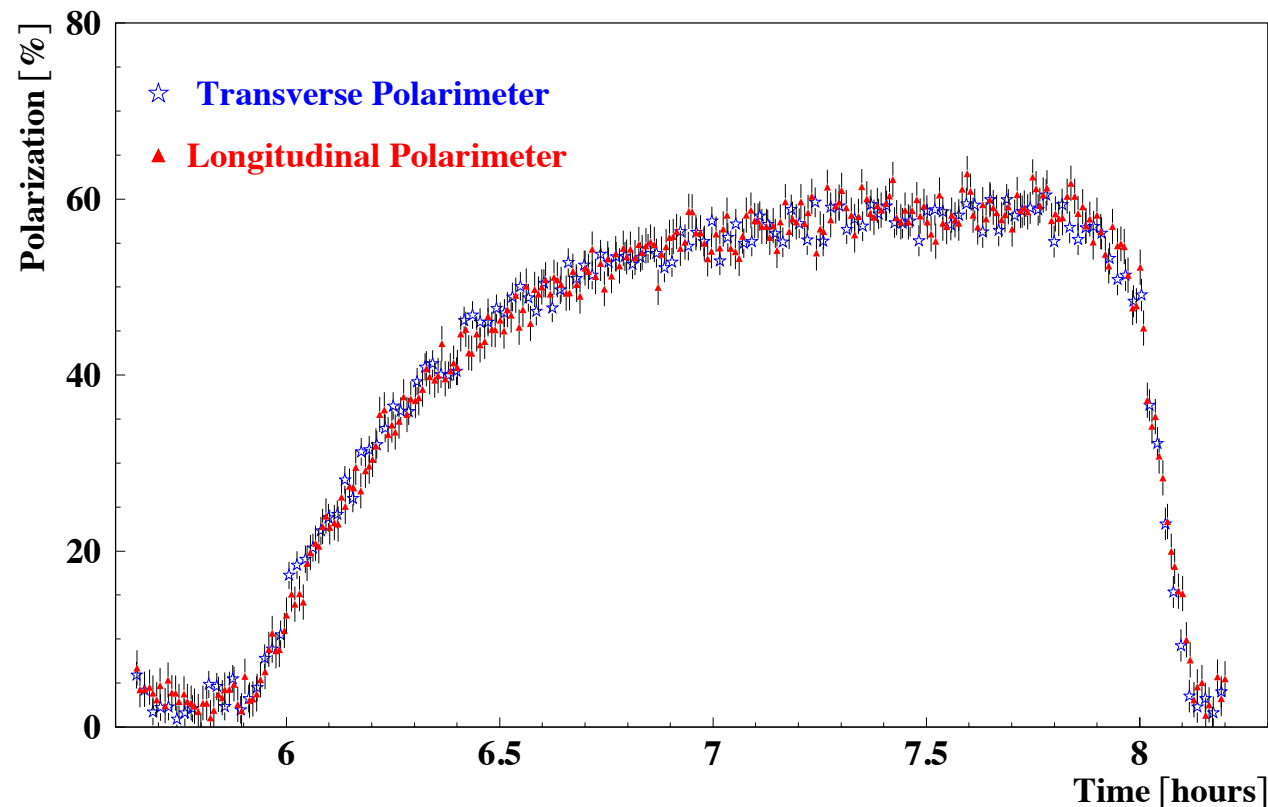
➡ **advantage of lepton-nucleon scattering data → flavour separation of fragmentation functions (FFs)**



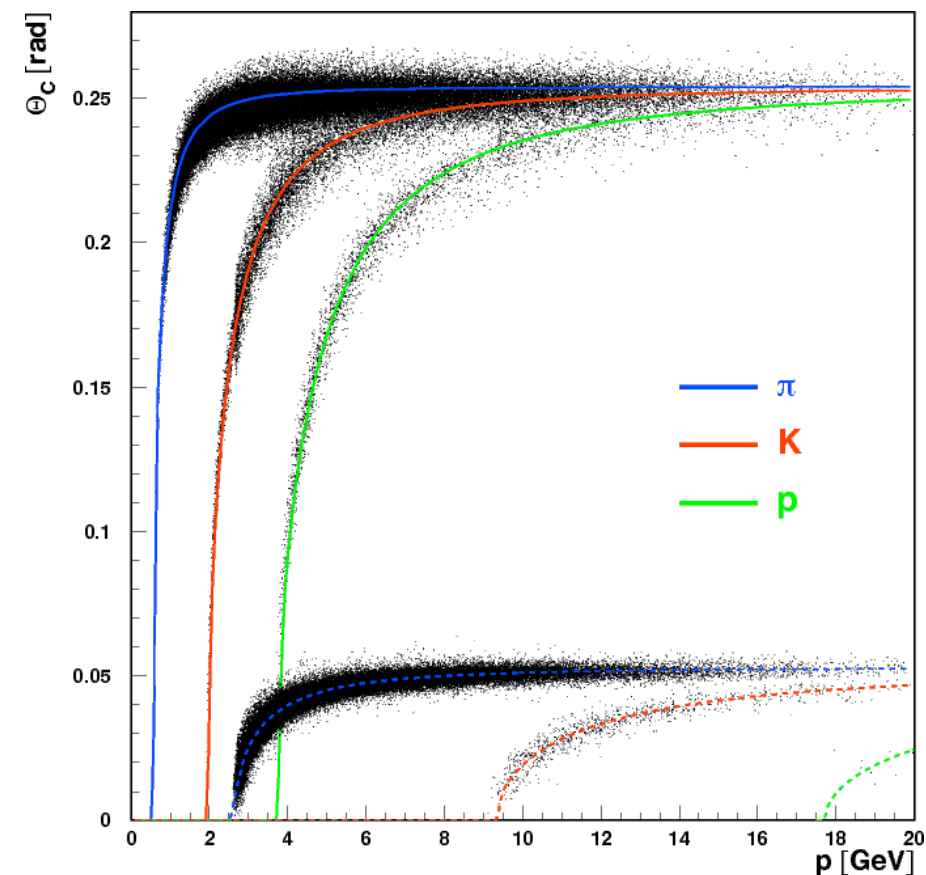
advantages of the experiment

The HERMES experiment, located at HERA, with its pure gas targets and advanced particle identification (π , K, p) is well suited for TMD and GPD measurements.

self-polarized e^+/e^- beam



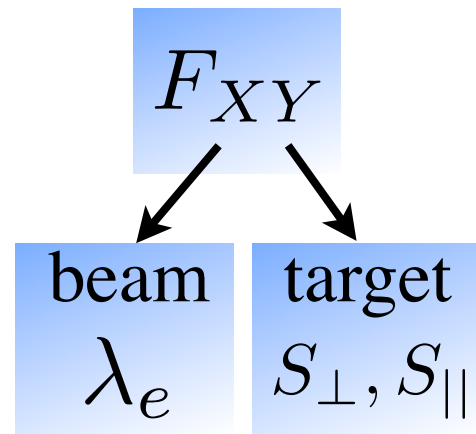
hadron identification with RICH detector



- ➡ **longitudinal** target polarization (H, D, ^3He)
- ➡ **transverse** target polarization (H)
- ➡ **unpolarized** targets: H, D, ^4He , ^{14}N , ^{20}Ne , ^{84}Kr , ^{131}Xe
- ➡ **unpolarized** H, D targets with **recoil detector**

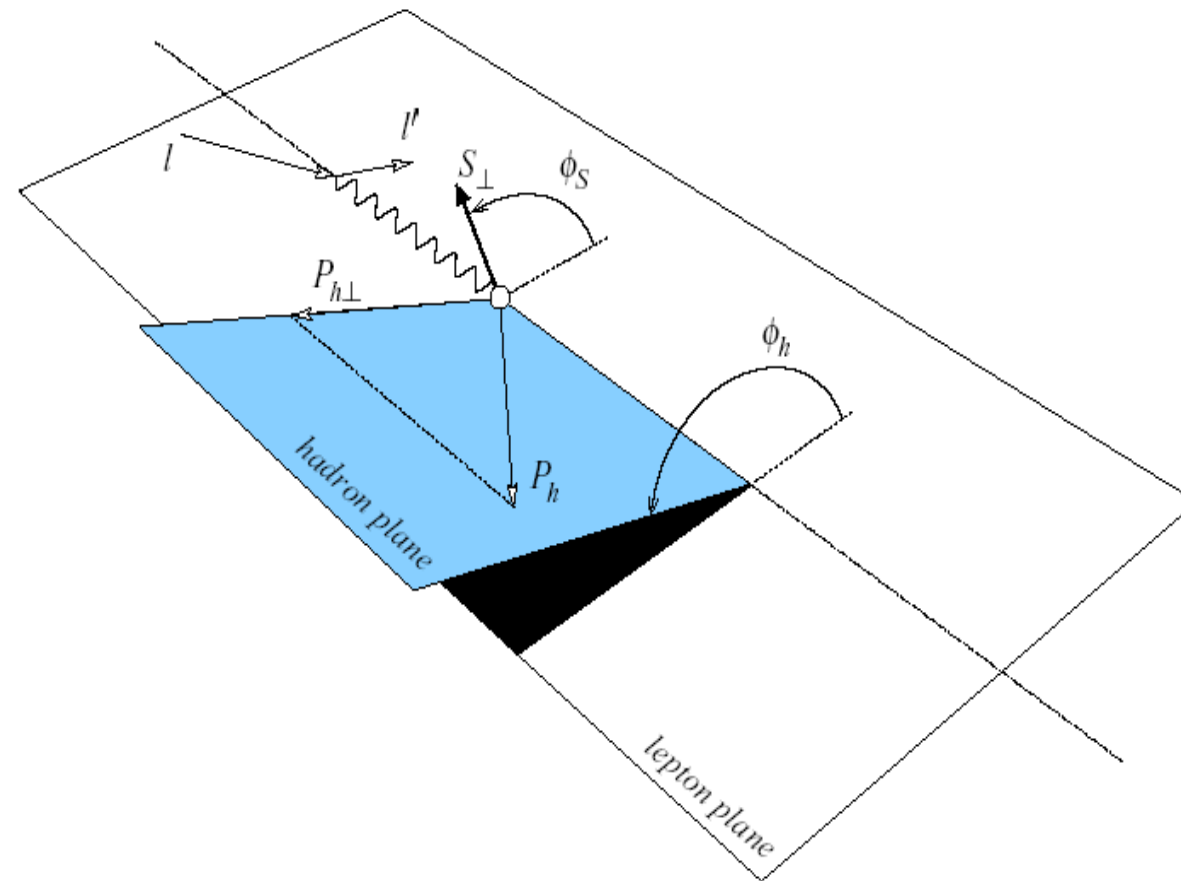
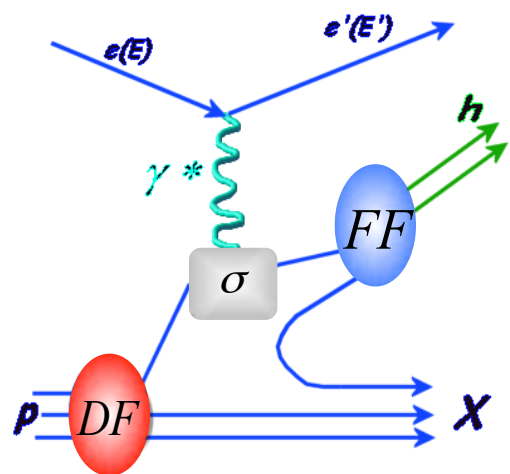
semi-inclusive measurements
(probing TMDs)

semi-inclusive DIS cross section and TMDs

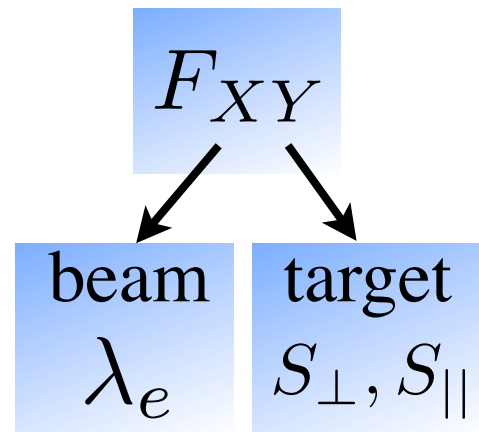


$$\frac{d^4\sigma}{dx dy dz d\phi_s} \propto F_{UU} + S_{\parallel} \lambda_e \sqrt{1 - \epsilon^2} F_{LL} + S_{\perp} \{ \dots \}$$

$$f_1 \otimes D_1$$



semi-inclusive DIS cross section and TMDs

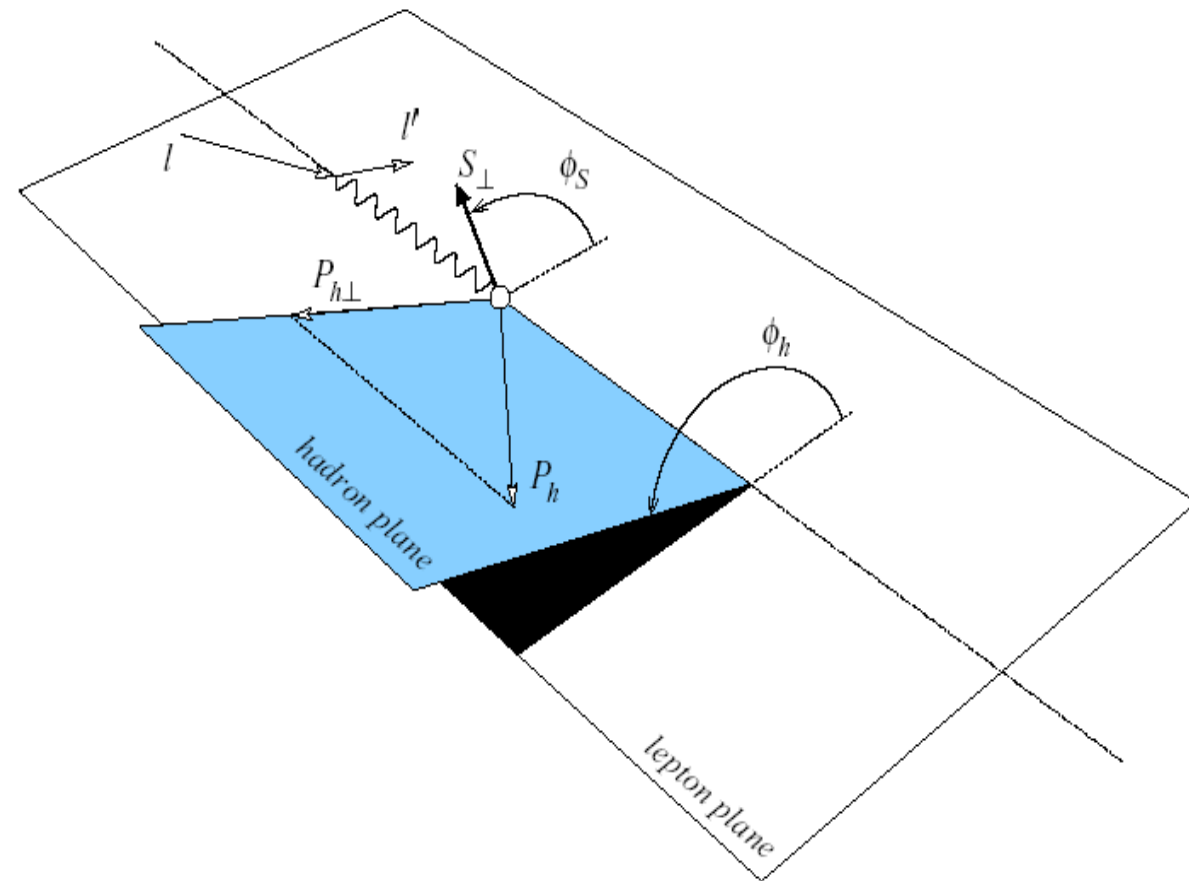
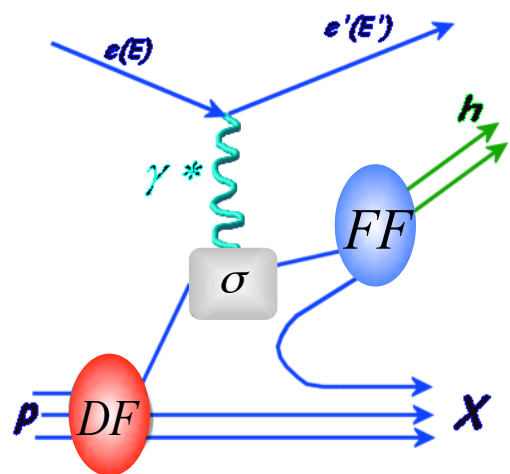


$$\frac{d^6\sigma}{dx dy dz dP_{h\perp}^2 d\phi d\phi_s}$$

$$\frac{d^4\sigma}{dx dy dz d\phi_s} \propto F_{UU} + S_{\parallel} \lambda_e \sqrt{1 - \epsilon^2} F_{LL} + S_{\perp} \{ \dots \}$$

$$f_1 \otimes D_1$$

$$\begin{aligned} \propto & \left\{ F_{UU} + \sqrt{2\epsilon(1+\epsilon)} F_{UU}^{\cos\phi} \cos\phi + \epsilon F_{UU}^{\cos 2\phi} \cos 2\phi \right\} \\ + & \lambda_e \left\{ \sqrt{2\epsilon(1-\epsilon)} F_{LU}^{\sin\phi} \sin\phi \right\} + S_{\parallel} \{ \dots \} + S_{\perp} \{ \dots \} \end{aligned}$$

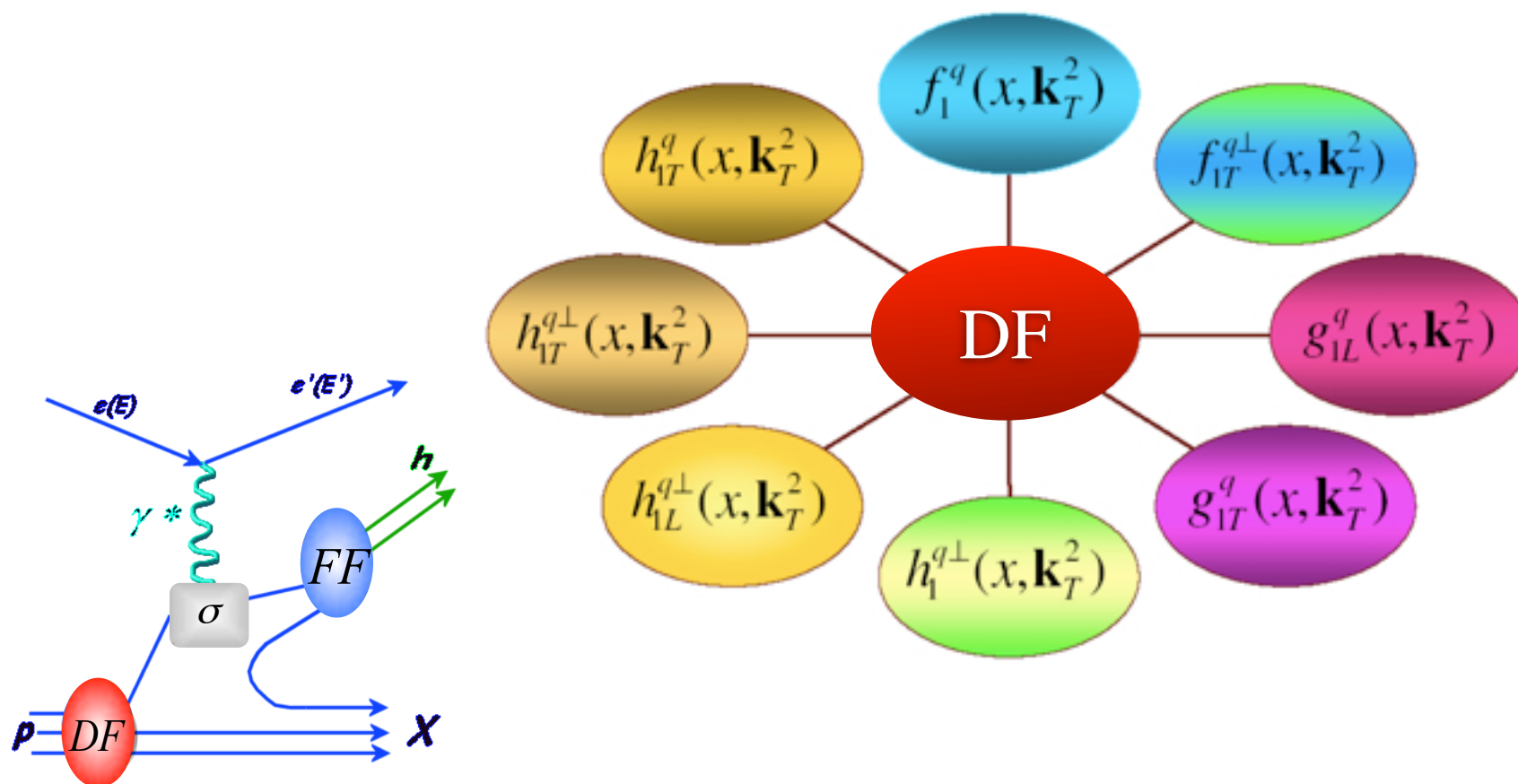


semi-inclusive DIS cross section and TMDs

$$\frac{d^6 \sigma}{dx dy dz dP_{h\perp}^2 d\phi d\phi_s} \propto \left\{ F_{UU} + \sqrt{2\epsilon(1+\epsilon)} F_{UU}^{\cos \phi} \cos \phi + \epsilon F_{UU}^{\cos 2\phi} \cos 2\phi \right\} \\ + \lambda_e \left\{ \sqrt{2\epsilon(1-\epsilon)} F_{UL}^{\sin \phi} \sin \phi \right\} + S_{||} \{ \dots \} + S_{\perp} \{ \dots \} + \dots$$

leading twist TMD DF:

parameterize the quark-flavor
structure of the nucleon



semi-inclusive DIS cross section and TMDs

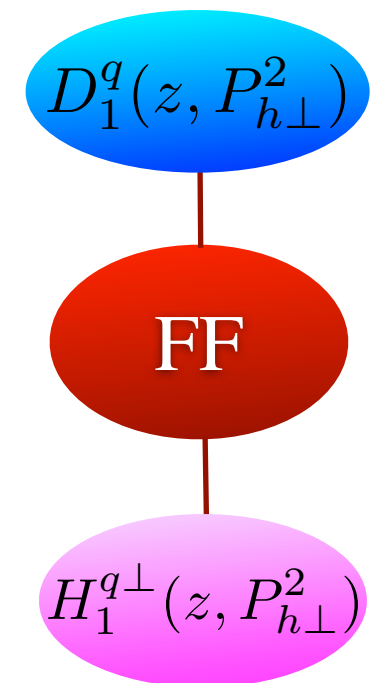
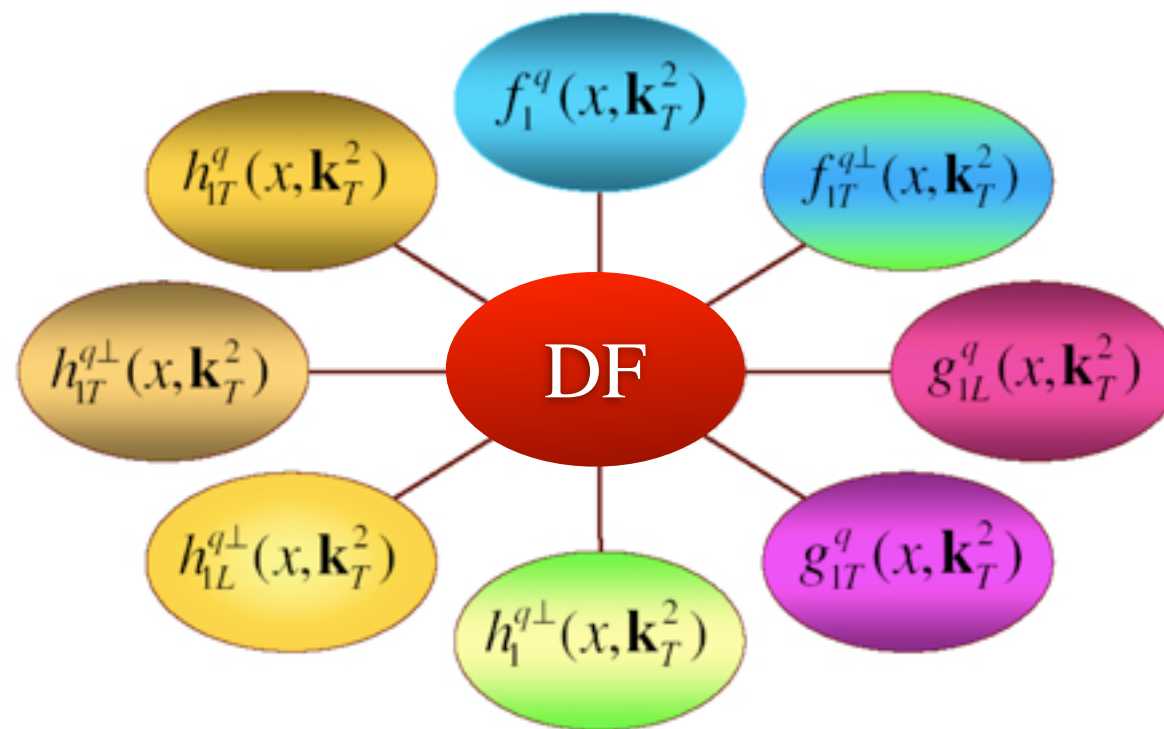
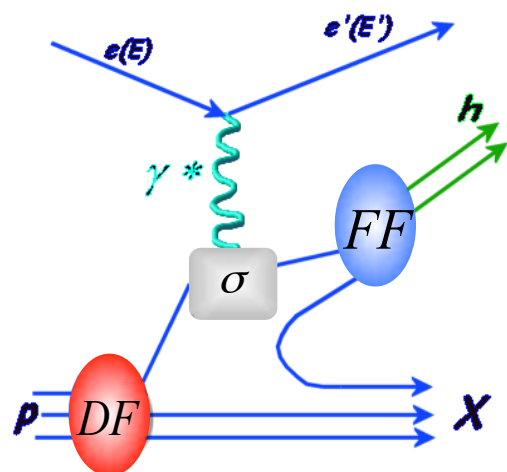
$$\frac{d^6\sigma}{dx dy dz dP_{h\perp}^2 d\phi d\phi_s} \propto \left\{ F_{UU} + \sqrt{2\epsilon(1+\epsilon)} F_{UU}^{\cos\phi} \cos\phi + \epsilon F_{UU}^{\cos 2\phi} \cos 2\phi \right\} \\ + \lambda_e \left\{ \sqrt{2\epsilon(1-\epsilon)} F_{UL}^{\sin\phi} \sin\phi \right\} + S_{||} \left\{ \dots \right\} + S_{\perp} \left\{ \dots \right\} + \dots$$

leading twist TMD DF:

parameterize the quark-flavor structure of the nucleon

leading twist TMD FF:

number densities for the conversion of a quark of a certain type to a specific hadron



semi-inclusive DIS cross section and TMDs

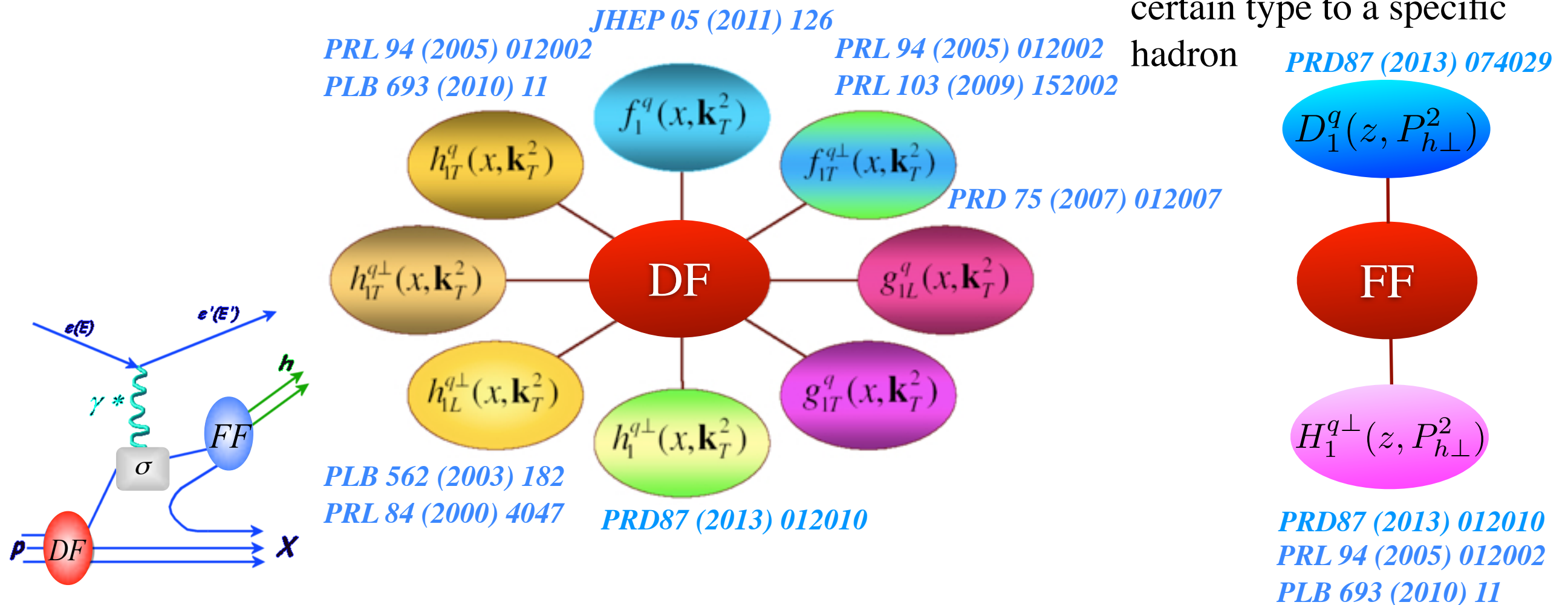
$$\frac{d^6\sigma}{dx dy dz dP_{h\perp}^2 d\phi d\phi_s} \propto \left\{ F_{UU} + \sqrt{2\epsilon(1+\epsilon)} F_{UU}^{\cos\phi} \cos\phi + \epsilon F_{UU}^{\cos 2\phi} \cos 2\phi \right\} \\ + \lambda_e \left\{ \sqrt{2\epsilon(1-\epsilon)} F_{UL}^{\sin\phi} \sin\phi \right\} + S_{||} \left\{ \dots \right\} + S_{\perp} \left\{ \dots \right\} + \dots$$

leading twist TMD DF:

parameterize the quark-flavor structure of the nucleon

leading twist TMD FF:

number densities for the conversion of a quark of a certain type to a specific hadron



HERMES: access to all TMDs thanks to polarized beam and target

DSPIN 2013

semi-inclusive DIS cross section and TMDs

$$\frac{d^6\sigma}{dx dy dz dP_{h\perp}^2 d\phi d\phi_s} \propto \left\{ F_{UU} + \sqrt{2\epsilon(1+\epsilon)} F_{UU}^{\cos\phi} \cos\phi + \epsilon F_{UU}^{\cos 2\phi} \cos 2\phi \right\} + \lambda_e \left\{ \sqrt{2\epsilon(1-\epsilon)} F_{UL}^{\sin\phi} \sin\phi \right\} + S_{||} \{ \dots \} + S_{\perp} \{ \dots \} + \dots$$

$f_1 \otimes D_1$

twist-3

$h_1^\perp \otimes H_1^\perp$

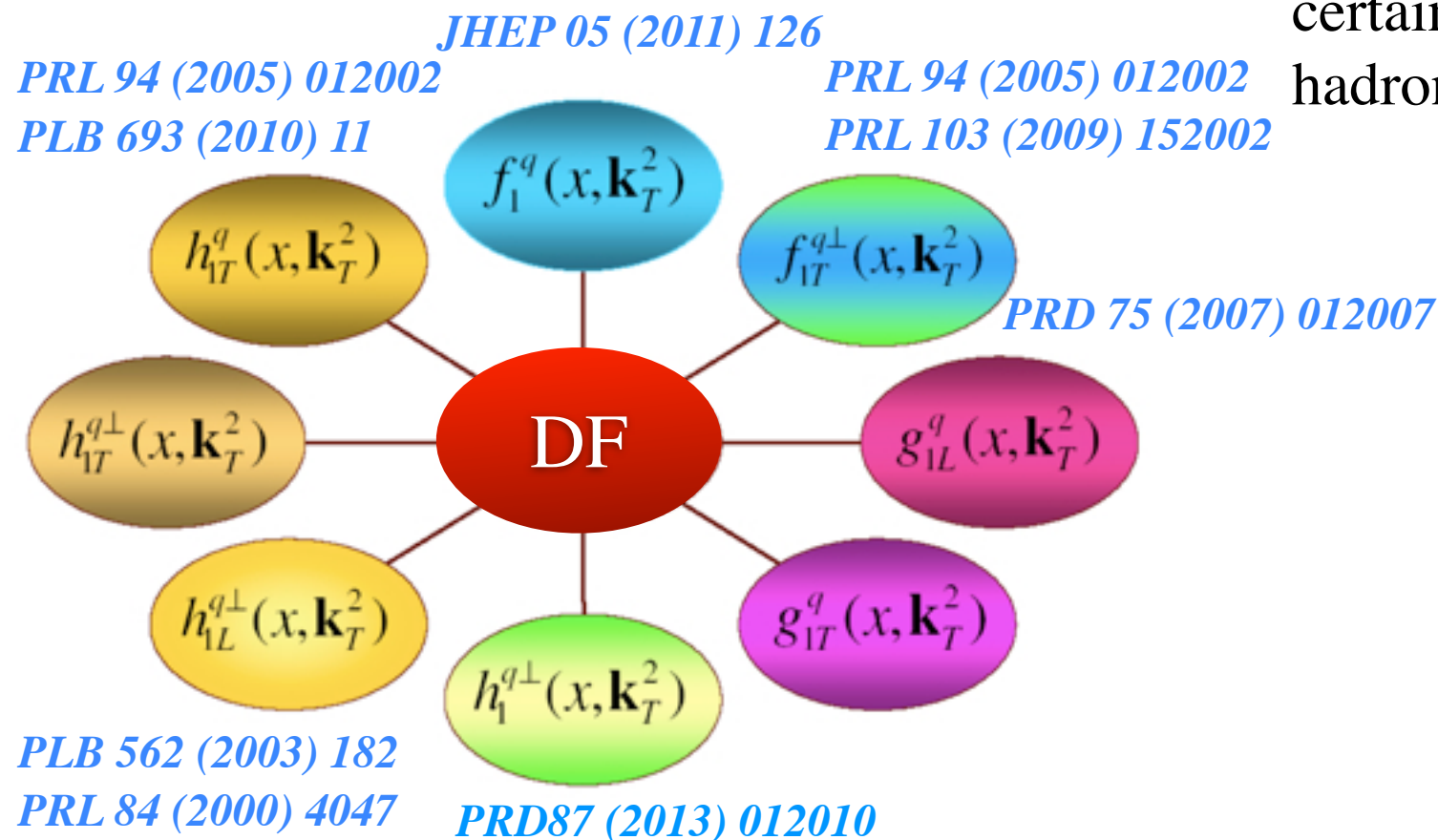
twist-3

leading twist TMD DF:

parameterize the quark-flavor structure of the nucleon

leading twist TMD FF:

number densities for the conversion of a quark of a certain type to a specific hadron



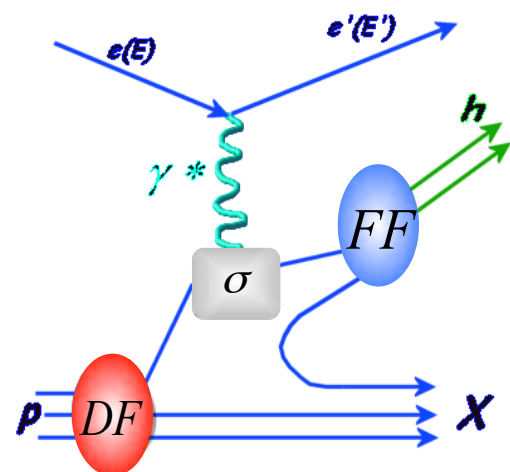
PRD87 (2013) 074029

$D_1^q(z, P_{h\perp}^2)$

FF

$H_1^{q\perp}(z, P_{h\perp}^2)$

PRD87 (2013) 012010
PRL 94 (2005) 012002
PLB 693 (2010) 11



HERMES: access to all TMDs thanks to polarized beam and target

DSPIN 2013


unpolarized quarks

$$\sigma_{UU} \propto f_1 \otimes D_1$$

$$f_1 = \text{img}$$

unpolarized quarks

$$\sigma_{UU} \propto f_1 \otimes D_1$$


$$f_1 =$$


$$M^h = \frac{d\sigma_{SIDIS}^h(x, Q^2, z, P_{h\perp})}{d\sigma_{DIS}(x, Q^2)}$$

$$\sigma_{UU} \propto f_1 \otimes D_1$$

LO interpretation of multiplicity results (integrated over $\mathbf{P}_{h\perp}$):

$$M^h \propto \frac{\sum_q e_q^2 \int dx f_{1q}(x, Q^2) D_{1q}^h(z, Q^2)}{\sum_q e_q^2 \int dx f_{1q}(x, Q^2)}$$

$$f_1 =$$


$$M^h = \frac{d\sigma_{SIDIS}^h(x, Q^2, z, P_{h\perp})}{d\sigma_{DIS}(x, Q^2)}$$

✓ charge-separated multiplicities of pions and kaons sensitive to the individual quark and antiquark flavours in the fragmentation process

unpolarized quarks

$$\sigma_{UU} \propto f_1 \otimes D_1$$

LO interpretation of multiplicity results (integrated over $\mathbf{P}_{h\perp}$):

$$M^h \propto \frac{\sum_q e_q^2 \int dx f_{1q}(x, Q^2) D_{1q}^h(z, Q^2)}{\sum_q e_q^2 \int dx f_{1q}(x, Q^2)}$$

$$f_1 =$$


$$M^h = \frac{d\sigma_{SIDIS}^h(x, Q^2, z, P_{h\perp})}{d\sigma_{DIS}(x, Q^2)}$$

- HERMES Collaboration -
Phys. Rev. D87 (2013) 074029

✓ charge-separated multiplicities of pions and kaons sensitive to the individual quark and antiquark flavours in the fragmentation process

π^+ and K^+ :

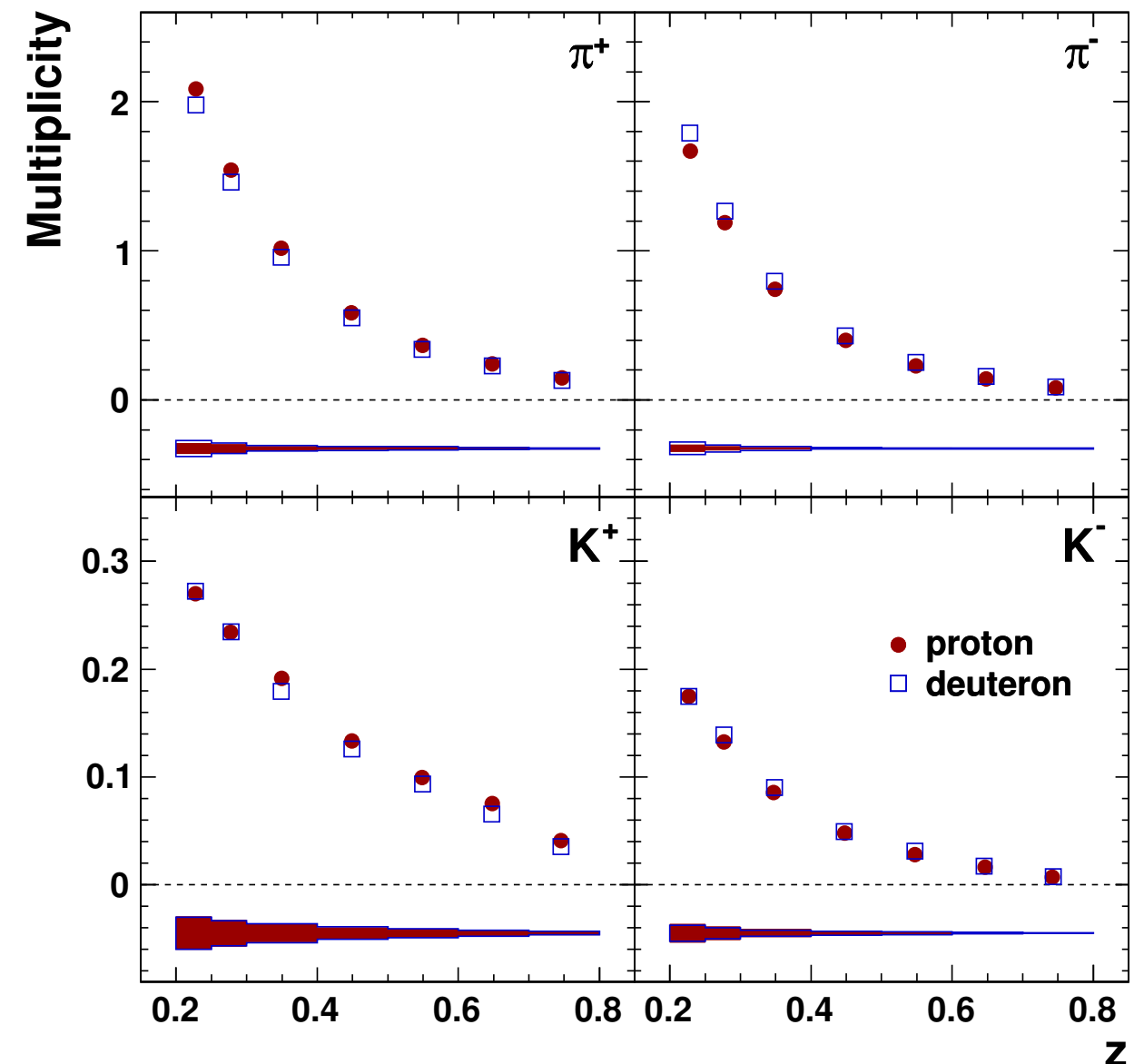
➡ favoured fragmentation on proton

π^- :

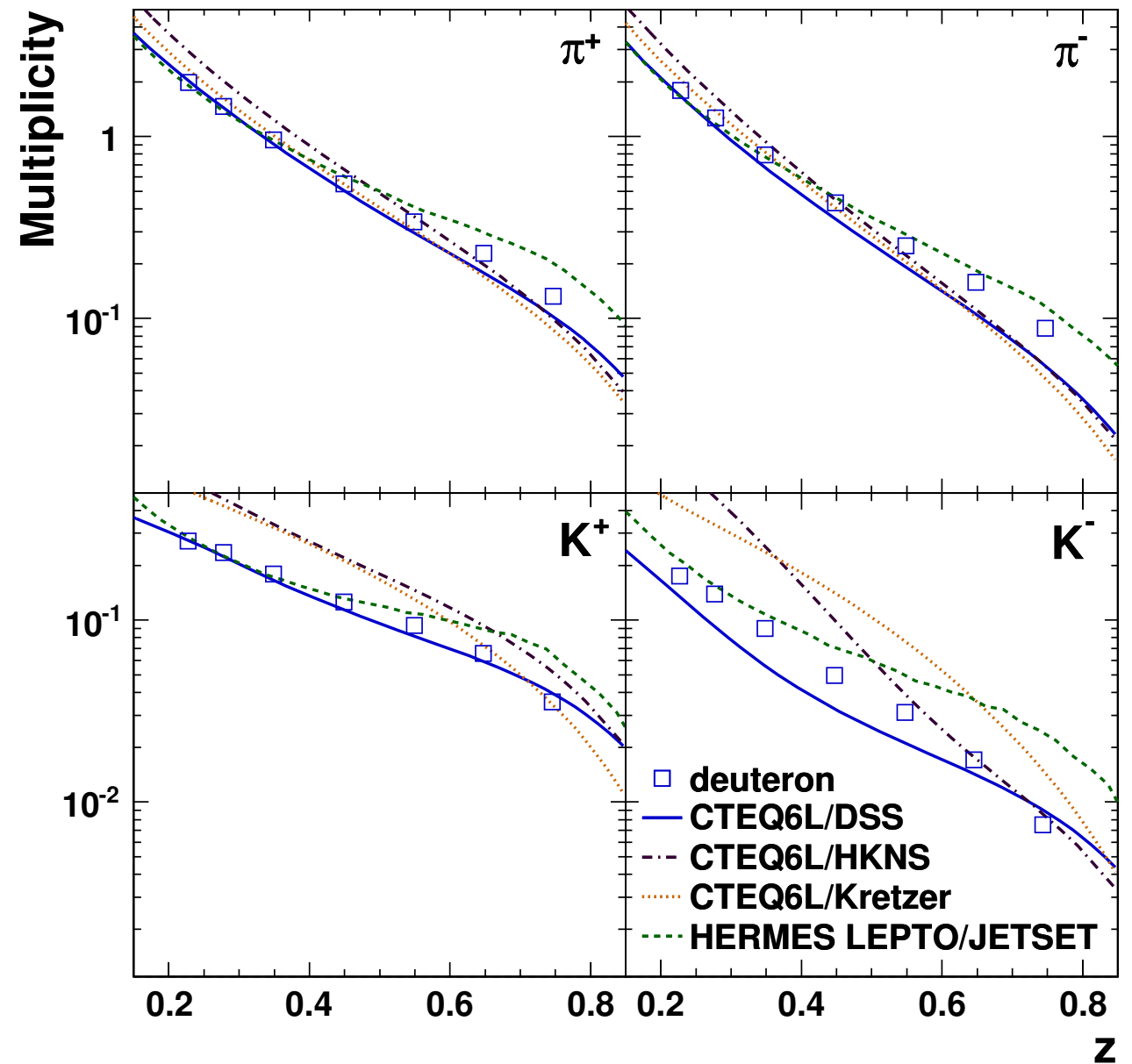
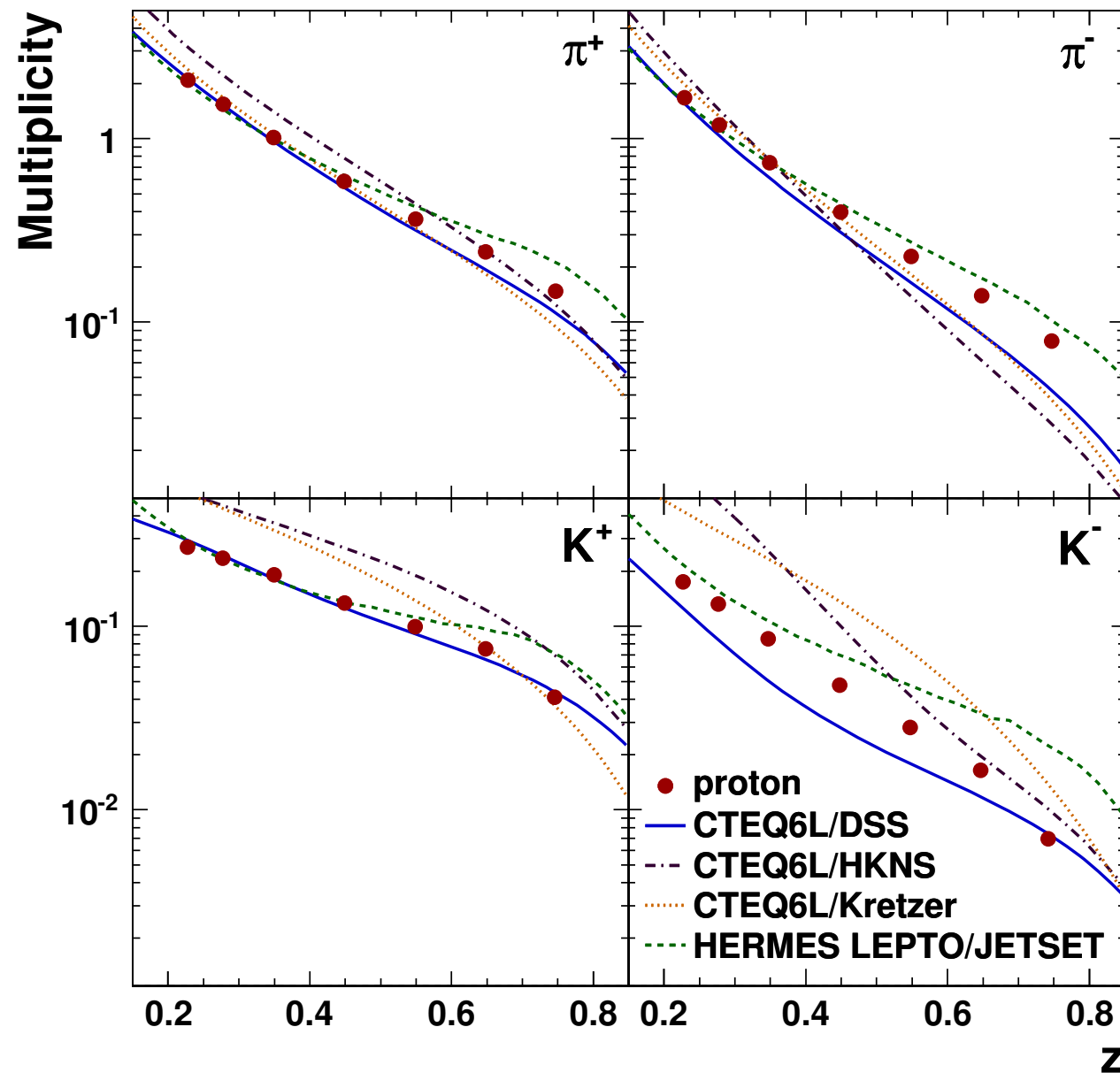
➡ increased number of d-quarks in D target and favoured fragmentation on neutron

K^- :

➡ cannot be produced through favoured fragmentation from the nucleon valence quarks



$$\sigma_{UU} \propto f_1 \otimes D_1$$



✓ calculations using DSS, HNKS and Kretzer FF fits together with CTEQ6L PDFs

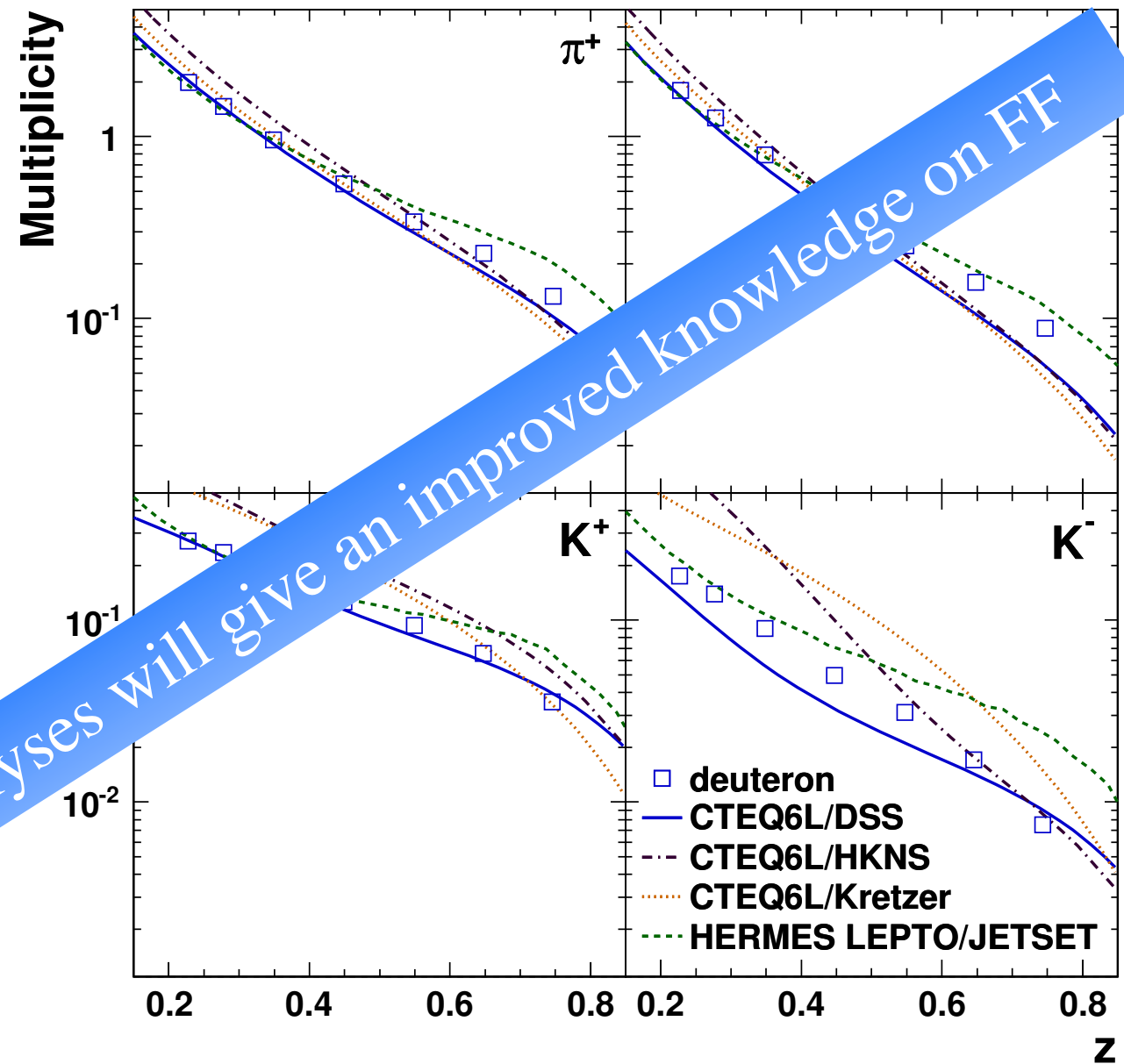
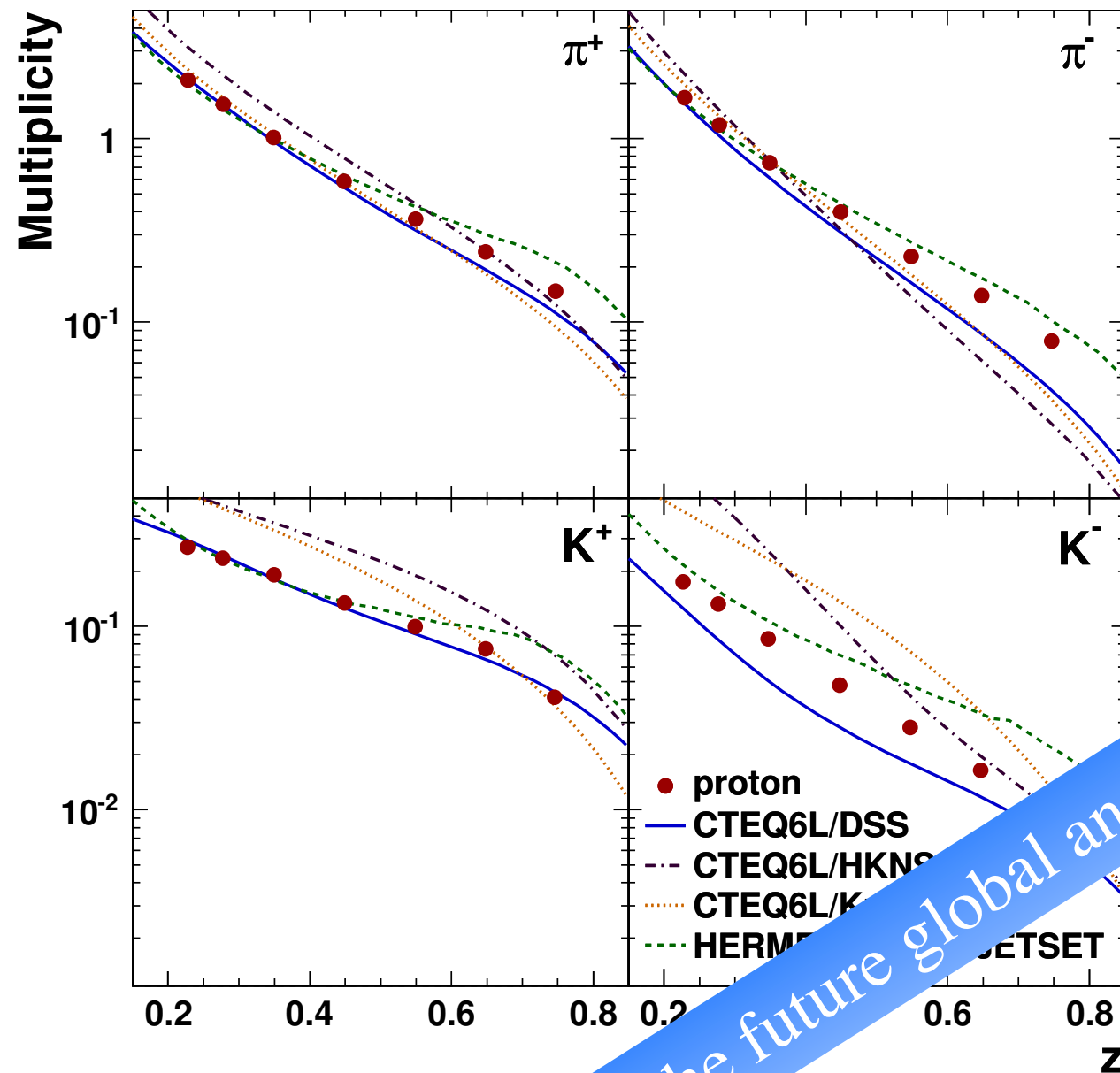
proton:

- ✎ fair agreement for positive hadrons
- ✎ disagreement for negative hadrons

deuteron:

- ✎ results are in general in better agreement with the various predictions

$$\sigma_{UU} \propto f_1 \otimes D_1$$



✓ calculations using HKNS and Kretzer FF fits together with CTEQ6L PDFs

proton:

✗ fair agreement for positive hadrons

✗ fair agreement for negative hadrons

deuteron: results are in general in better agreement with the various predictions

inclusion of the data in the future global analyses will give an improved knowledge on FF

evaluation of strange quark PDFs

✓ in the absence of experimental constraints, many global QCD fits of PDFs assume

$$s(x) = \bar{s}(x) = r[\bar{u}(x) + \bar{d}(x)]/2$$

✓ isoscalar extraction of $S(x)\mathcal{D}_S^\mathcal{K}$ based on the multiplicity data of K^+ and K^- on D

$$S(x) \int \mathcal{D}_S^K(z) dz \simeq Q(x) \left[5 \frac{d^2 N^K(x)}{d^2 N^{DIS}(x)} - \int \mathcal{D}_Q^K(z) dz \right]$$

$$S(x) = s(x) + \bar{s}(x)$$

$$Q(x) = u(x) + \bar{u}(x) + d(x) + \bar{d}(x)$$

$$\mathcal{D}_S^\mathcal{K} = D_1^{s \rightarrow K^+} + D_1^{\bar{s} \rightarrow K^+} + D_1^{s \rightarrow K^-} + D_1^{\bar{s} \rightarrow K^-}$$

$$\mathcal{D}_Q^\mathcal{K} = D_1^{u \rightarrow K^+} + D_1^{\bar{u} \rightarrow K^+} + D_1^{d \rightarrow K^+} + D_1^{\bar{d} \rightarrow K^+} + \dots$$

evaluation of strange quark PDFs

✓ in the absence of experimental constraints, many global QCD fits of PDFs assume

$$s(x) = \bar{s}(x) = r[\bar{u}(x) + \bar{d}(x)]/2$$

✓ isoscalar extraction of $S(x)\mathcal{D}_S^K$ based on the multiplicity data of K^+ and K^- on D

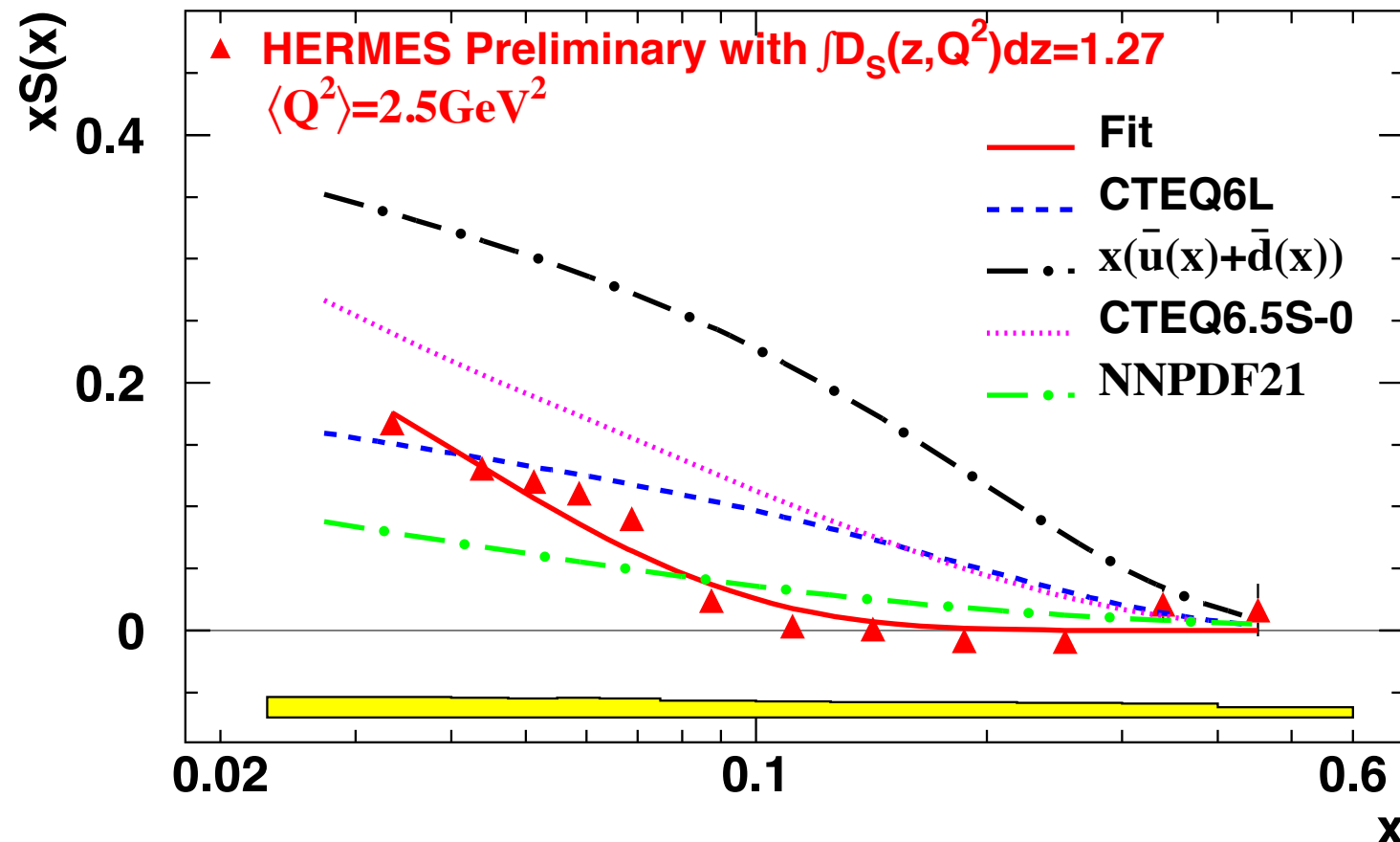
$$S(x) \int \mathcal{D}_S^K(z) dz \simeq Q(x) \left[5 \frac{d^2 N^K(x)}{d^2 N^{DIS}(x)} - \int \mathcal{D}_Q^K(z) dz \right]$$

$$S(x) = s(x) + \bar{s}(x)$$

$$Q(x) = u(x) + \bar{u}(x) + d(x) + \bar{d}(x)$$

$$\mathcal{D}_S^K = D_1^{s \rightarrow K^+} + D_1^{\bar{s} \rightarrow K^+} + D_1^{s \rightarrow K^-} + D_1^{\bar{s} \rightarrow K^-}$$

$$\mathcal{D}_Q^K = D_1^{u \rightarrow K^+} + D_1^{\bar{u} \rightarrow K^+} + D_1^{d \rightarrow K^+} + D_1^{\bar{d} \rightarrow K^+} + \dots$$



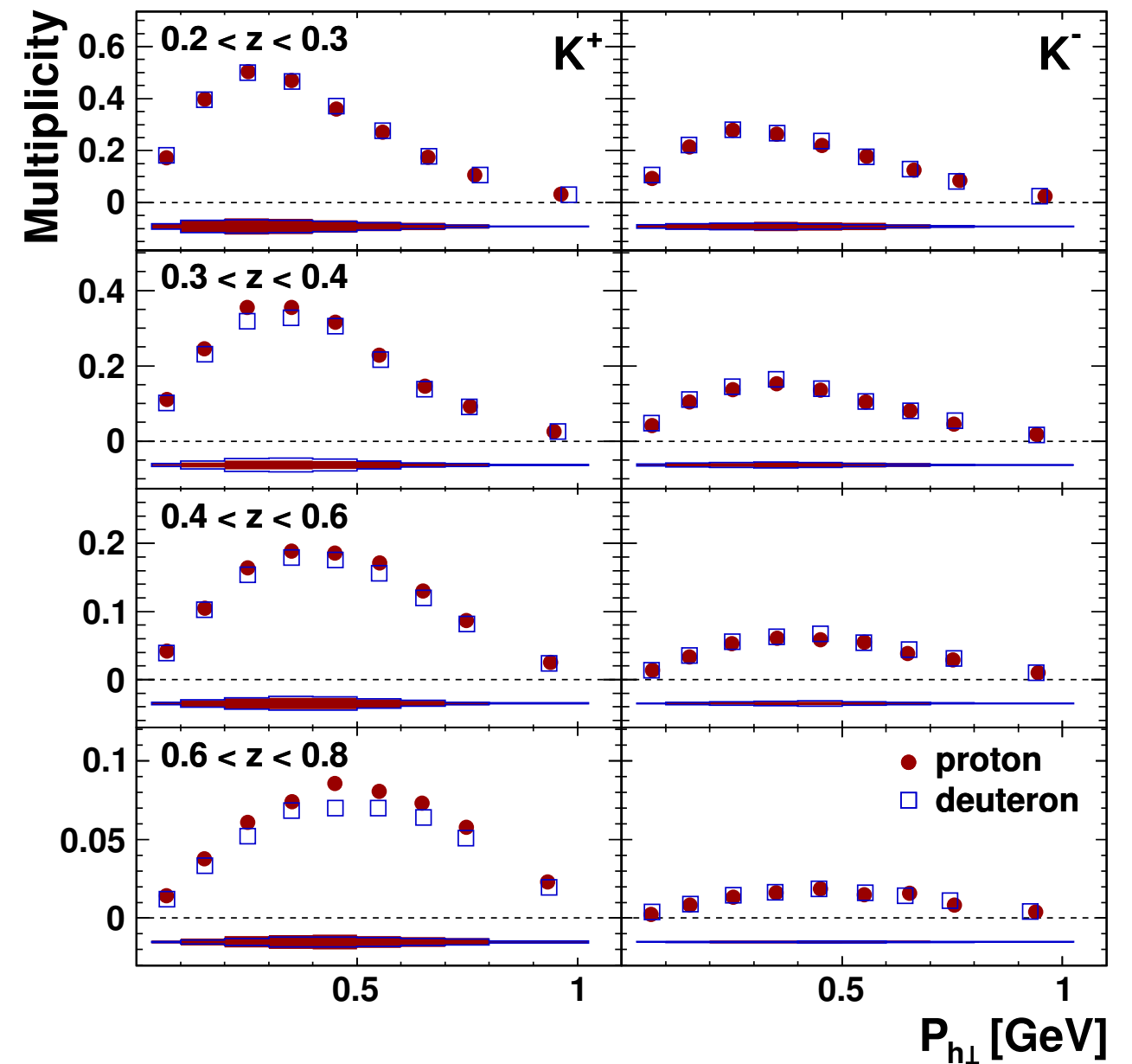
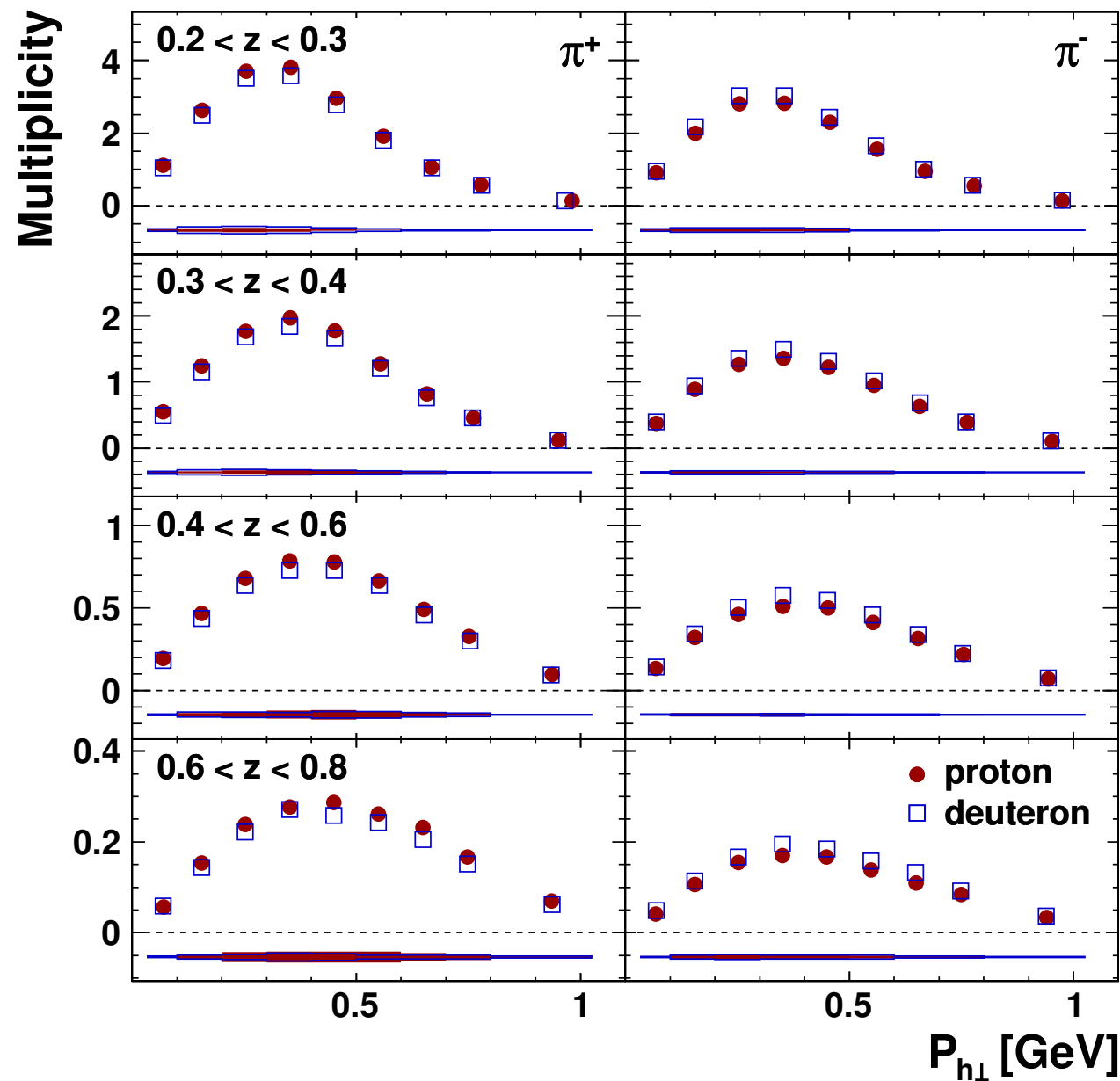
✓ the distribution of $S(x)$ is obtained for a certain value of \mathcal{D}_S^K

✓ the normalization of the data is given by that value

✓ whatever the normalization, the shape is incompatible with the predictions

beyond the collinear factorization

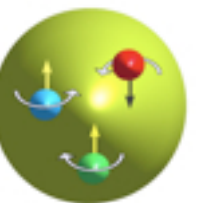
- HERMES Collaboration-
Phys.Rev.D87 (2013) 074029



- ✓ multi-dimensional analysis allows exploration of new kinematic dependences
- ✓ broader $P_{h\perp}$ distribution for K^-

quark's transverse degrees of freedom

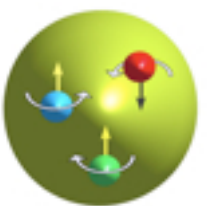
$$\sigma_{UU} \propto h_1^\perp \otimes H_1^\perp$$

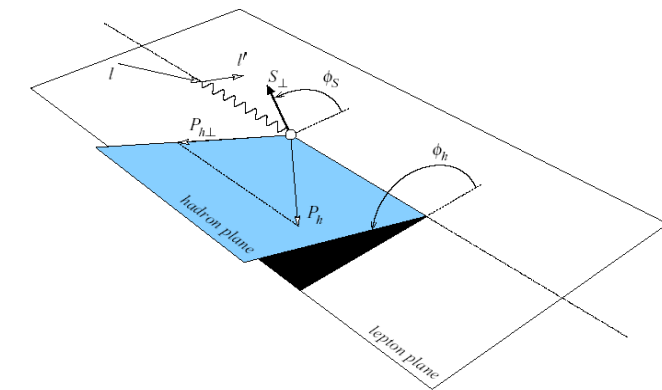
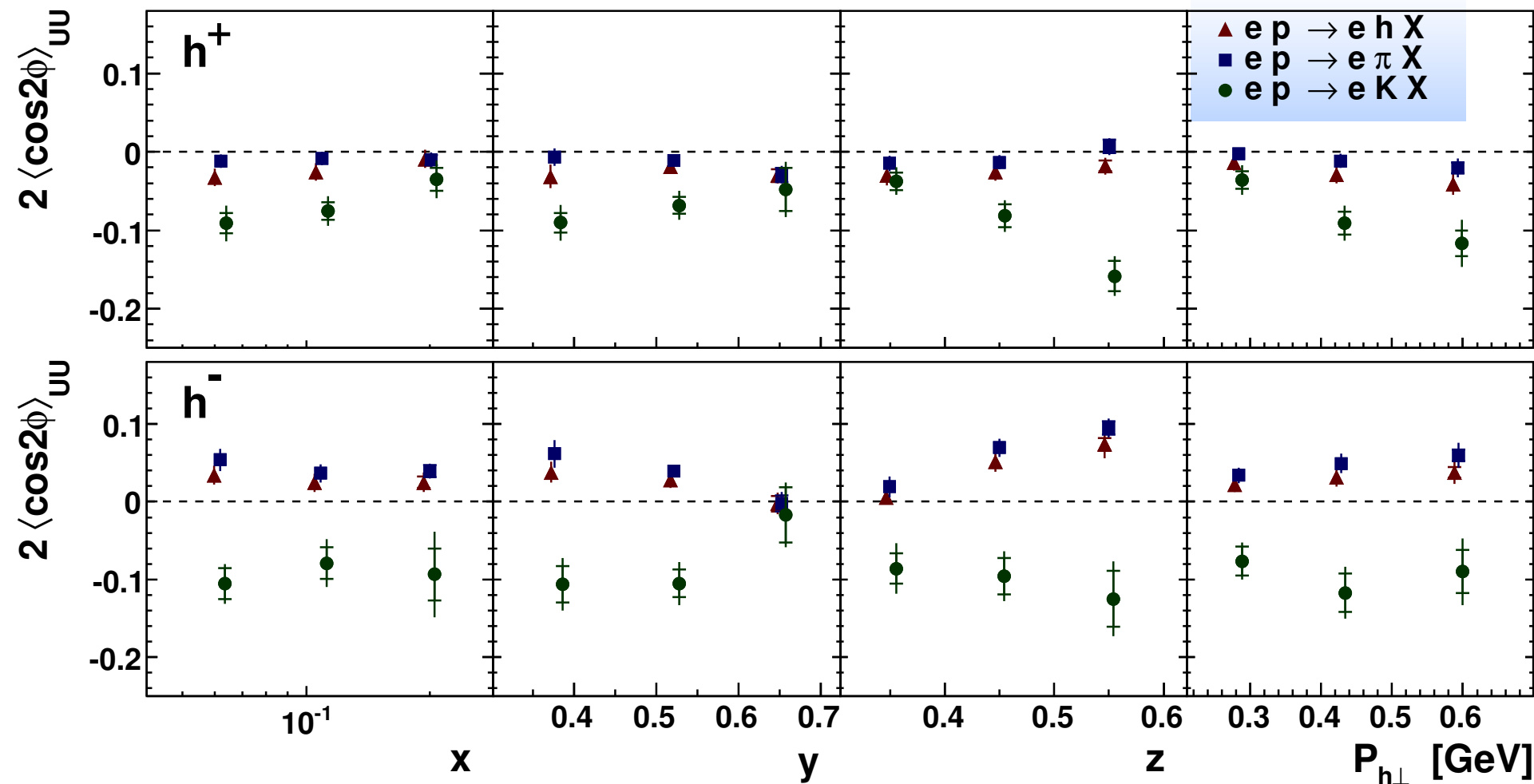
$$h_1^\perp =$$


The diagram shows a green sphere representing a nucleon. Inside, there are three quarks: a red one at the top, a blue one at the bottom left, and a green one at the bottom right. Each quark has a small yellow arrow pointing upwards, representing its transverse degree of freedom. The red quark's arrow is slightly curved, while the blue and green ones are straight.

quark's transverse degrees of freedom

$$\sigma_{UU} \propto h_1^\perp \otimes H_1^\perp$$

$$h_1^\perp =$$




- HERMES Collaboration-
Phys.Rev. D87 (2013) 012010

✓ negative asymmetry for π^+ and positive for π^-

➡ from previous publications ([PRL 94 \(2005\) 012002](#), [PLB 693 \(2010\) 11-16](#)):

$$H_1^\perp, u \rightarrow \pi^+ = -H_1^\perp, u \rightarrow \pi^-$$

➡ data support Boer-Mulders DF h_1^\perp of same sign for u and d quarks

✓ K^- and K^+ : striking differences w.r.t. pions

➡ role of the sea in DF and FF

beyond the leading twist

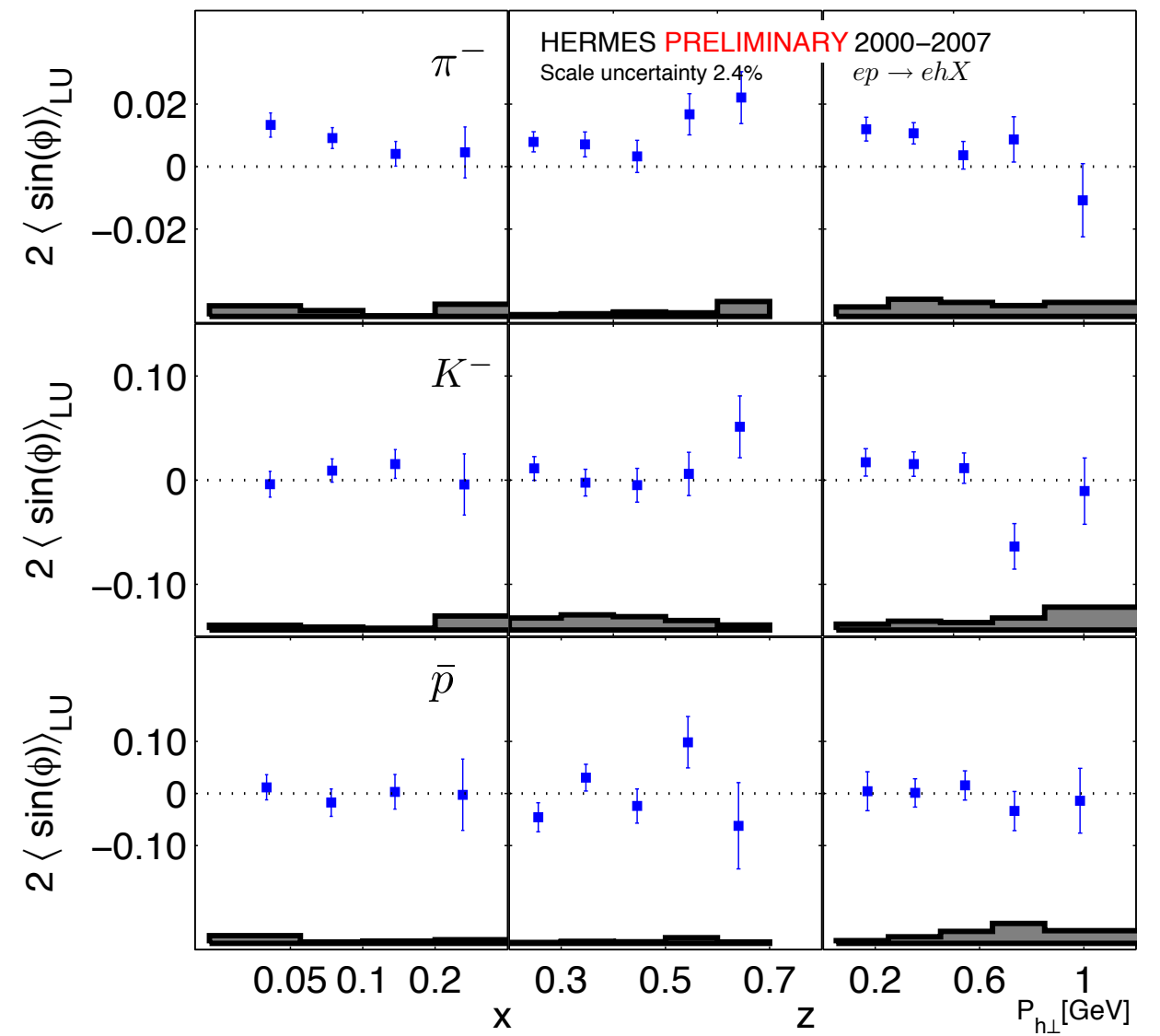
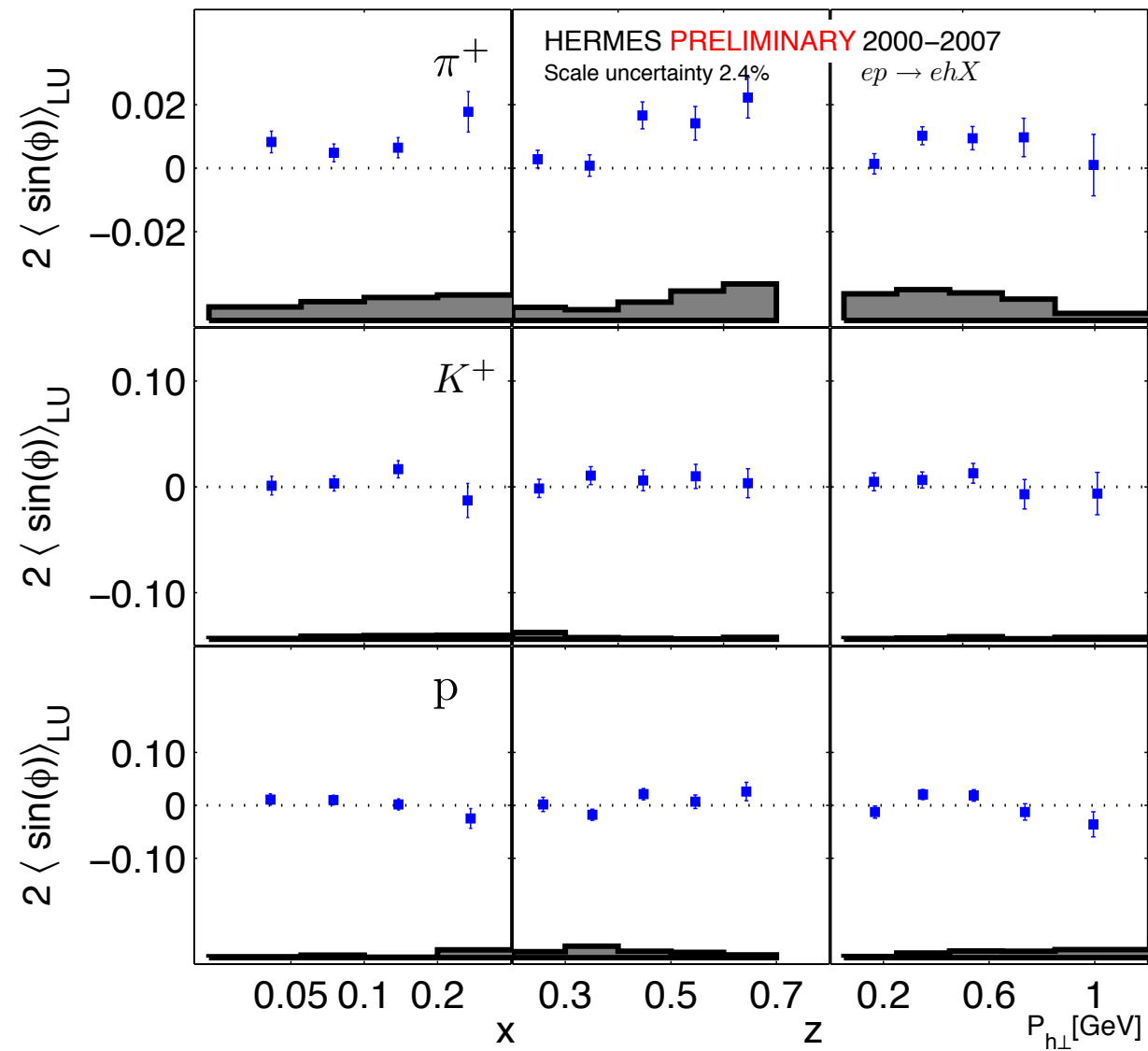
$$\frac{d^6 \sigma}{dx \, dy \, dz \, dP_{h\perp}^2 \, d\phi \, d\phi_s} \propto \left\{ F_{UU} + \dots + \lambda_e \left\{ \sqrt{2\epsilon(1-\epsilon)} F_{LU}^{\sin \phi} \sin \phi \right\} + \dots \right.$$

convolutions of twist-2 and twist-3 functions

beyond the leading twist

$$\frac{d^6\sigma}{dx dy dz dP_{h\perp}^2 d\phi d\phi_s} \propto \left\{ F_{UU} + \dots + \lambda_e \left\{ \sqrt{2\epsilon(1-\epsilon)} F_{LU}^{\sin\phi} \sin\phi \right\} + \dots \right.$$

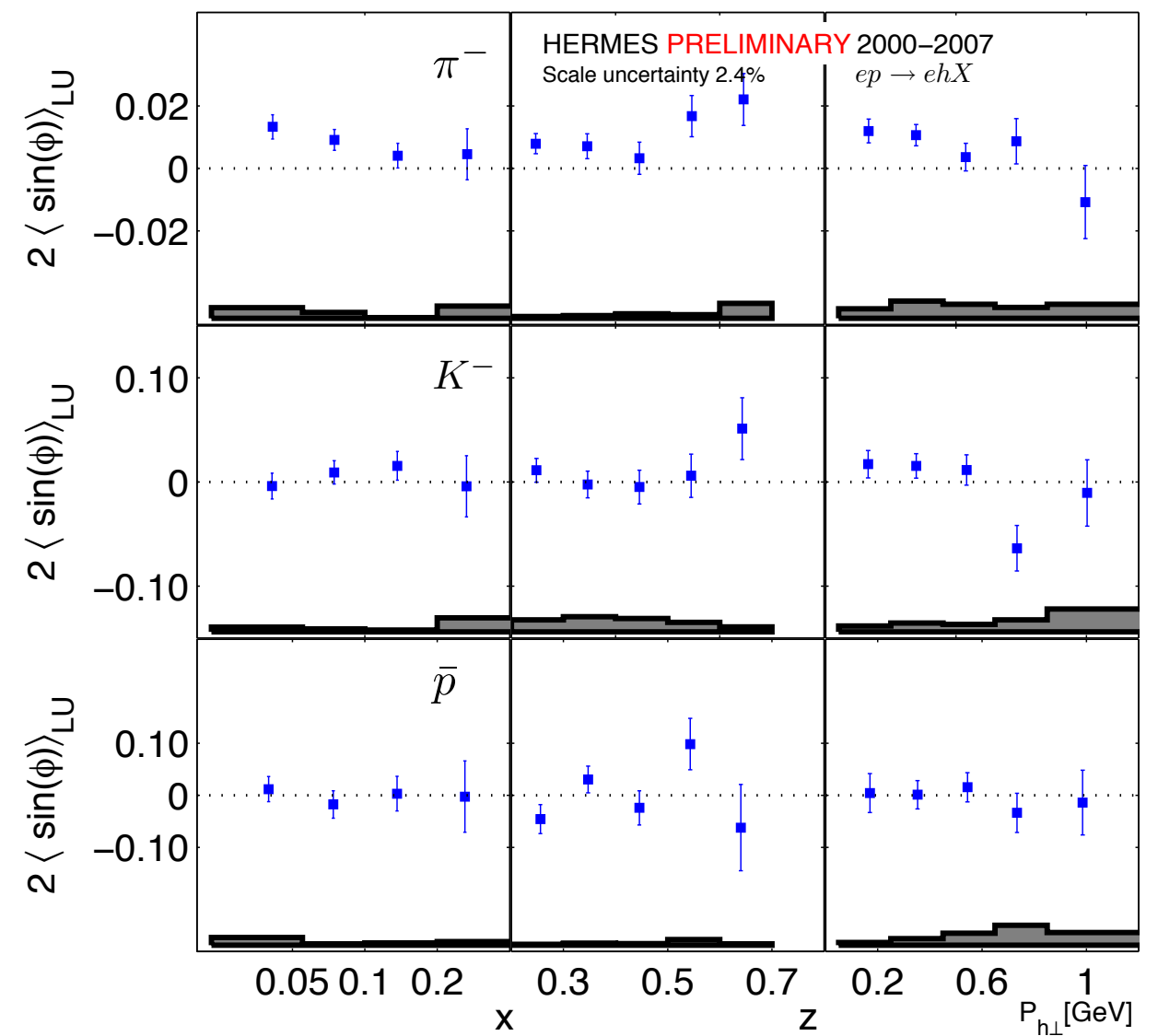
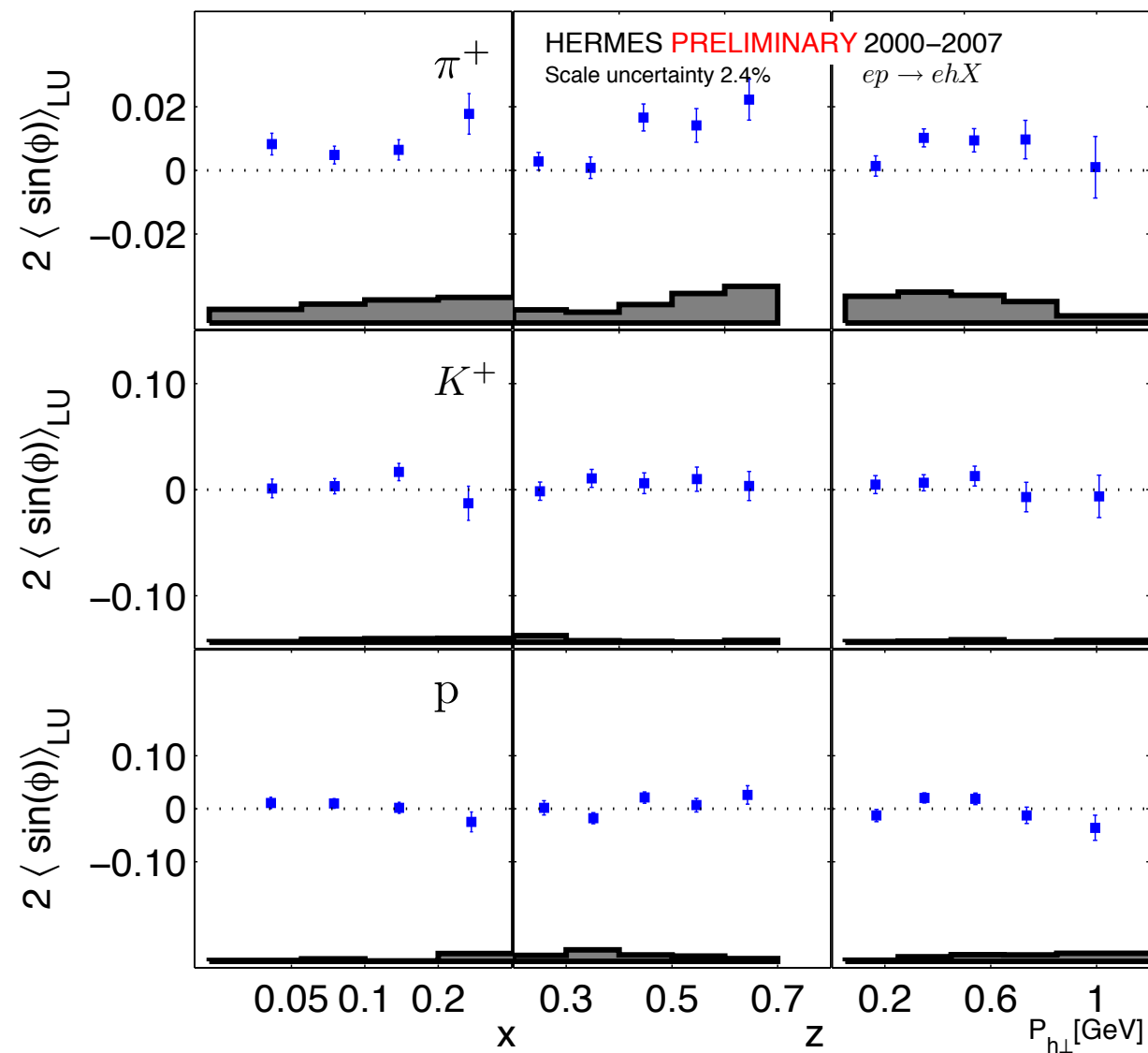
convolutions of twist-2 and twist-3 functions



beyond the leading twist

$$\frac{d^6\sigma}{dx dy dz dP_{h\perp}^2 d\phi d\phi_s} \propto \left\{ F_{UU} + \dots + \lambda_e \left\{ \sqrt{2\epsilon(1-\epsilon)} F_{LU}^{\sin\phi} \sin\phi \right\} + \dots \right.$$

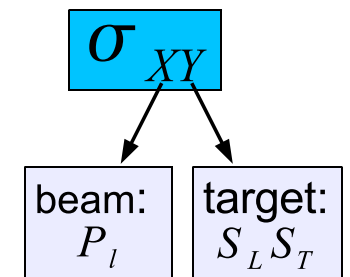
convolutions of twist-2 and twist-3 functions



π^+ and π^-

the role of the twist-3 DF or FF is sizeable

Collins effect

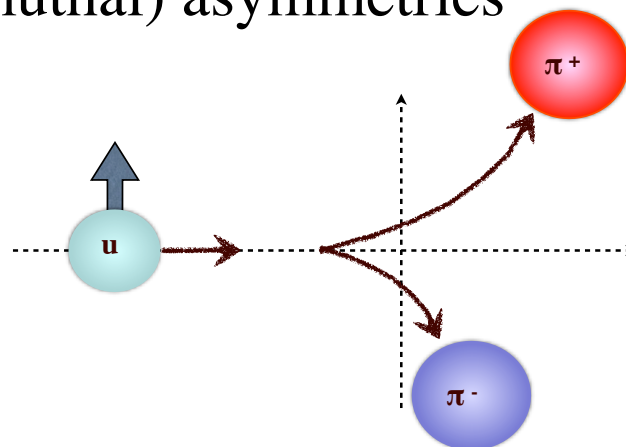
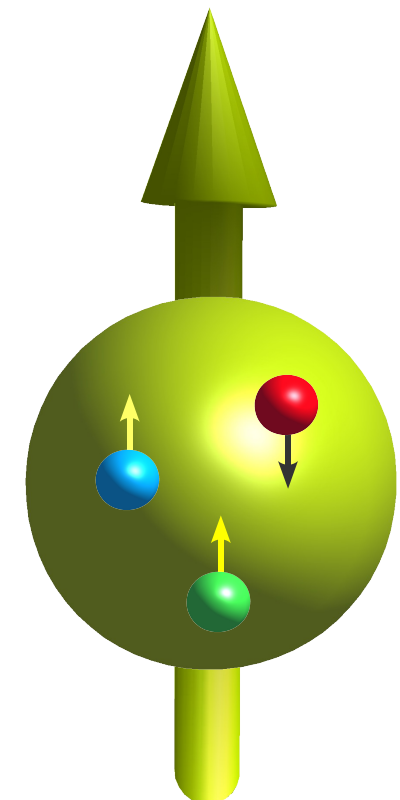


$$\begin{aligned}
 d\sigma = & d\sigma_{UU}^0 + \cos(2\phi)d\sigma_{UU}^1 + \frac{1}{Q}\cos(\phi)d\sigma_{UU}^2 + P_l\frac{1}{Q}\sin(\phi)d\sigma_{LU}^3 \\
 & + S_L\left[\sin(2\phi)d\sigma_{UL}^4 + \frac{1}{Q}\sin(\phi)d\sigma_{UL}^5 + P_l\left(d\sigma_{LL}^6 + \frac{1}{Q}\cos(\phi)d\sigma_{LL}^7\right)\right] \\
 & + S_T\left[\sin(\phi - \phi_s)d\sigma_{UT}^8 + \sin(\phi + \phi_s)d\sigma_{UT}^9 + \sin(3\phi - \phi_s)d\sigma_{UT}^{10} + \frac{1}{Q}\sin(2\phi - \phi_s)d\sigma_{UT}^{11} + \frac{1}{Q}\sin(\phi_s)d\sigma_{UT}^{12}\right. \\
 & \left. P_l\left(\cos(\phi - \phi_s)d\sigma_{LT}^{13} + \frac{1}{Q}\cos(\phi_s)d\sigma_{LT}^{14} + \frac{1}{Q}\cos(2\phi - \phi_s)d\sigma_{LT}^{15}\right)\right]
 \end{aligned}$$

☞ the transversity DF $h_1^q(x)$ is sensitive to the difference of the number densities of transversely polarized quarks aligned along or opposite to the polarization of the nucleon

☞ “Collins-effect” accounts for the correlation between the transverse spin of the fragmenting quark and the transverse momentum of the produced unpolarized hadron

☞ generates left-right (azimuthal) asymmetries

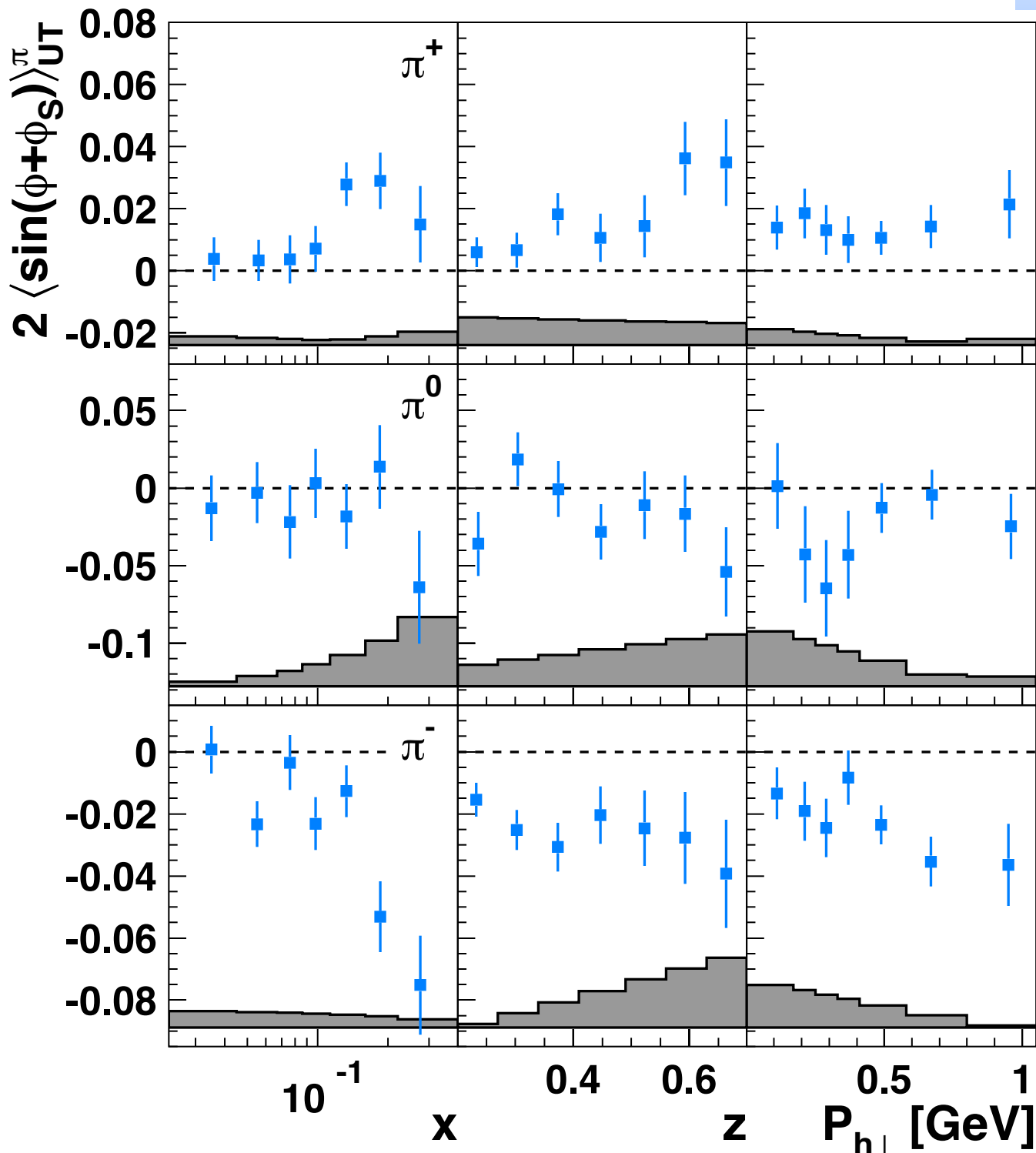


Collins amplitudes for pions

- HERMES Collaboration-
Phys. Lett. B 693 (2010) 11-16

- ☞ non-zero Collins effect observed!
- ☞ both Collins FF and transversity sizeable

$$2\langle\sin(\phi + \phi_s)\rangle_{UT} \propto \frac{\mathcal{C}\left[-\frac{\hat{\mathbf{P}}_{h\perp}\cdot\mathbf{k}_T}{M_h} h_1^q(x, p_T^2) H_1^{\perp q\rightarrow h}(z, k_T^2)\right]}{\mathcal{C}\left[f_1^q(x, p_T^2) D_1^{q\rightarrow h}(z, k_T^2)\right]}$$

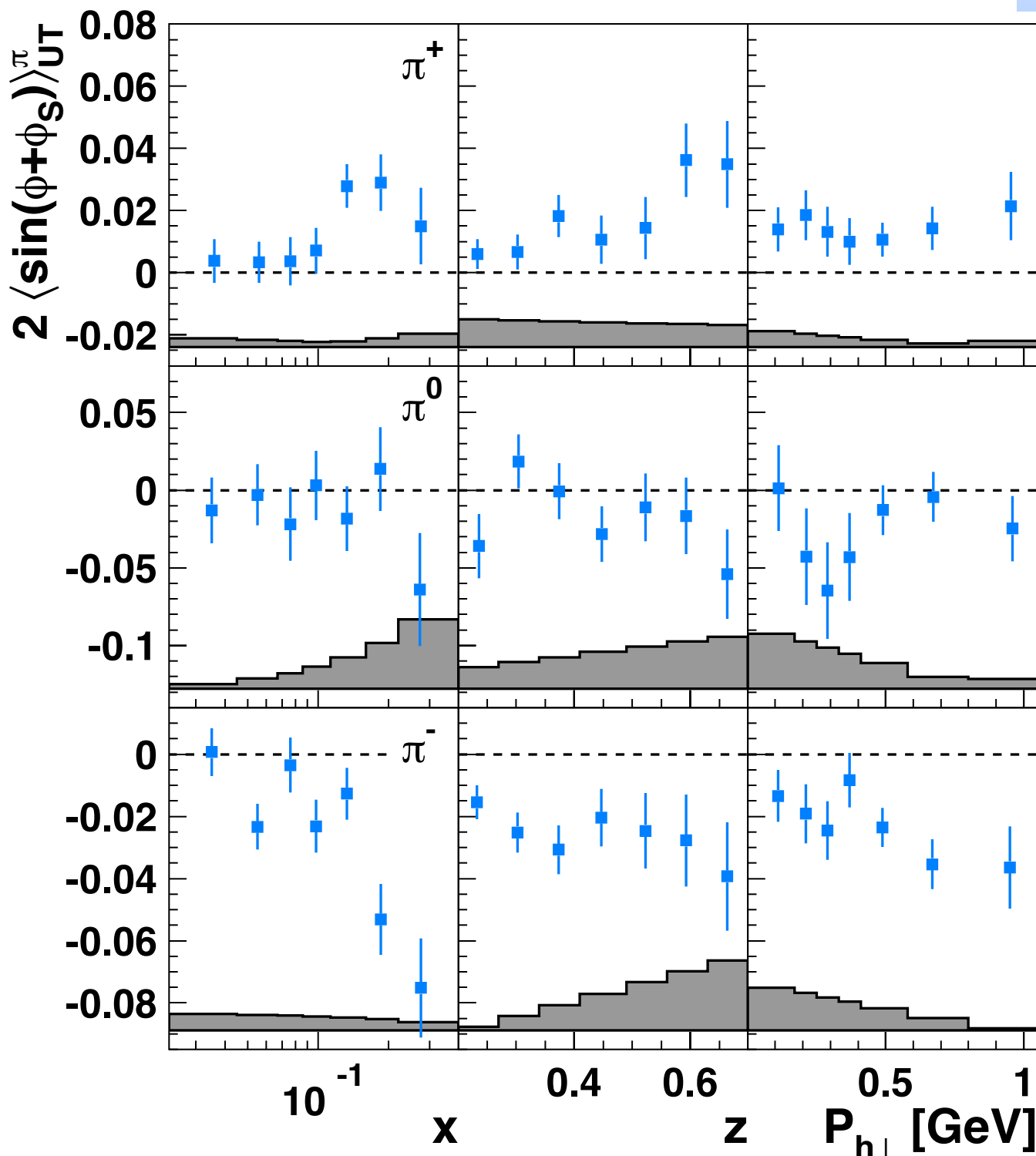


Collins amplitudes for pions

- HERMES Collaboration-
Phys. Lett. B 693 (2010) 11-16

- ☞ non-zero Collins effect observed!
- ☞ both Collins FF and transversity sizeable

$$2\langle\sin(\phi + \phi_s)\rangle_{UT} \propto \frac{\mathcal{C}\left[-\frac{\hat{\mathbf{P}}_{h\perp}\cdot\mathbf{k}_T}{M_h} h_1^q(x, p_T^2) H_1^{\perp q\rightarrow h}(z, k_T^2)\right]}{\mathcal{C}\left[f_1^q(x, p_T^2) D_1^{q\rightarrow h}(z, k_T^2)\right]}$$



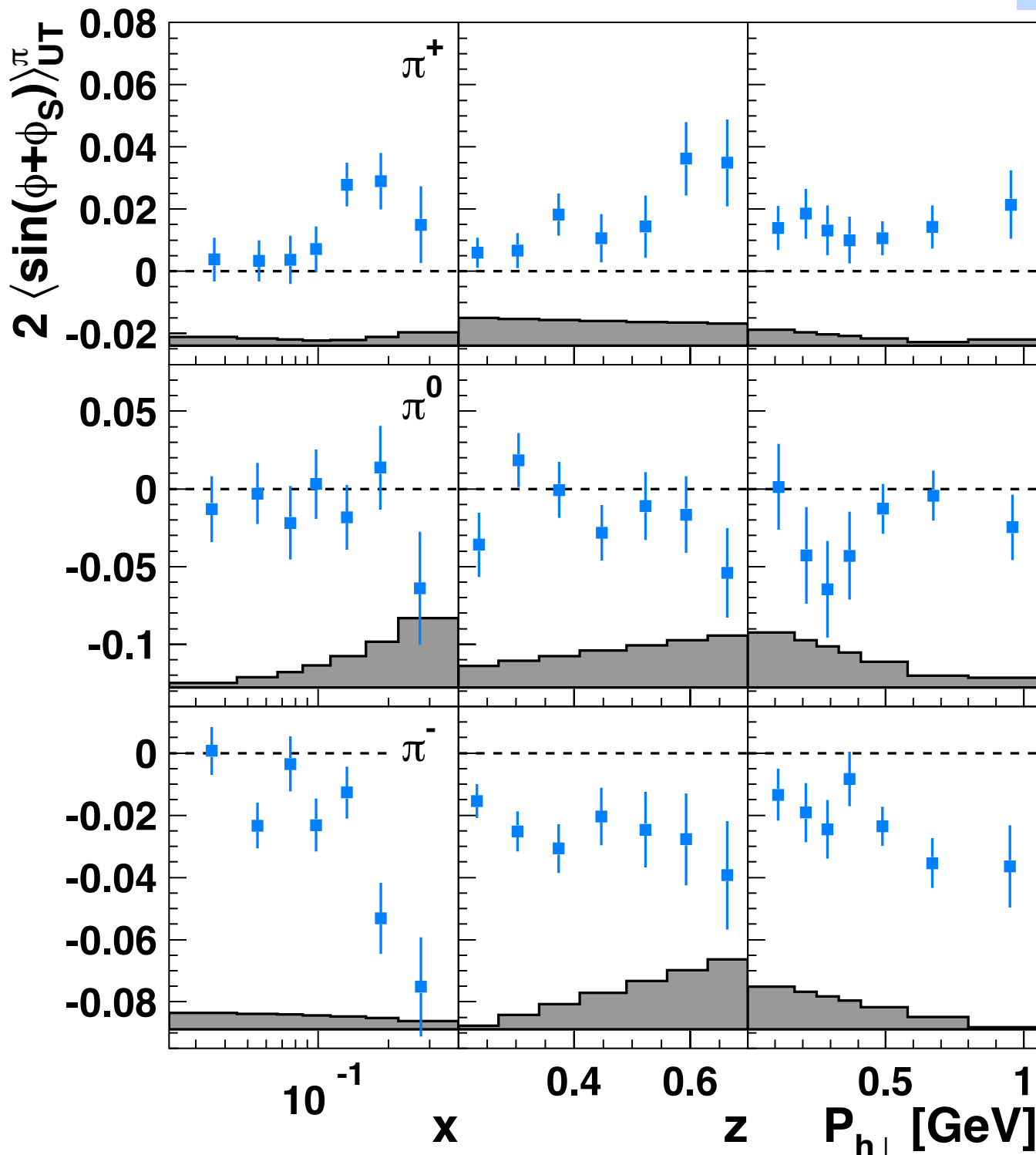
- ☞ positive amplitude for π^+
- ☞ compatible with zero amplitude for π^0
- ☞ large negative amplitude for π^-
- ☞ increase in magnitude with x
 - ☞ transversity mainly receives contribution from valence quarks
- ☞ increase with z
- ☞ in qualitative agreement with BELLE results

Collins amplitudes for pions

- *HERMES Collaboration*
Phys. Lett. B 693 (2010) 11-16

- ☞ non-zero Collins effect observed!
- ☞ both Collins FF and transversity sizeable

$$2\langle\sin(\phi + \phi_s)\rangle_{UT} \propto \frac{\mathcal{C}\left[-\frac{\hat{\mathbf{P}}_{h\perp}\cdot\mathbf{k}_T}{M_h} h_1^q(x, p_T^2) H_1^{\perp q\rightarrow h}(z, k_T^2)\right]}{\mathcal{C}\left[f_1^q(x, p_T^2) D_1^{q\rightarrow h}(z, k_T^2)\right]}$$



- ☞ positive amplitude for π^+
- ☞ compatible with zero amplitude for π^0
- ☞ large negative amplitude for π^-
- ☞ increase in magnitude with x
- ☞ transversity mainly receives contribution from valence quarks
- ☞ increase with z
- ☞ in qualitative agreement with BELLE results
- ☞ positive for π^+ and negative for π^-

☞ role of disfavored Collins FF:

$$\mathbf{H}_1^{\perp, \text{disfav}} \approx -H_1^{\perp, \text{fav}}$$

$$u \Rightarrow \pi^+; \quad d \Rightarrow \pi^- (\text{fav})$$

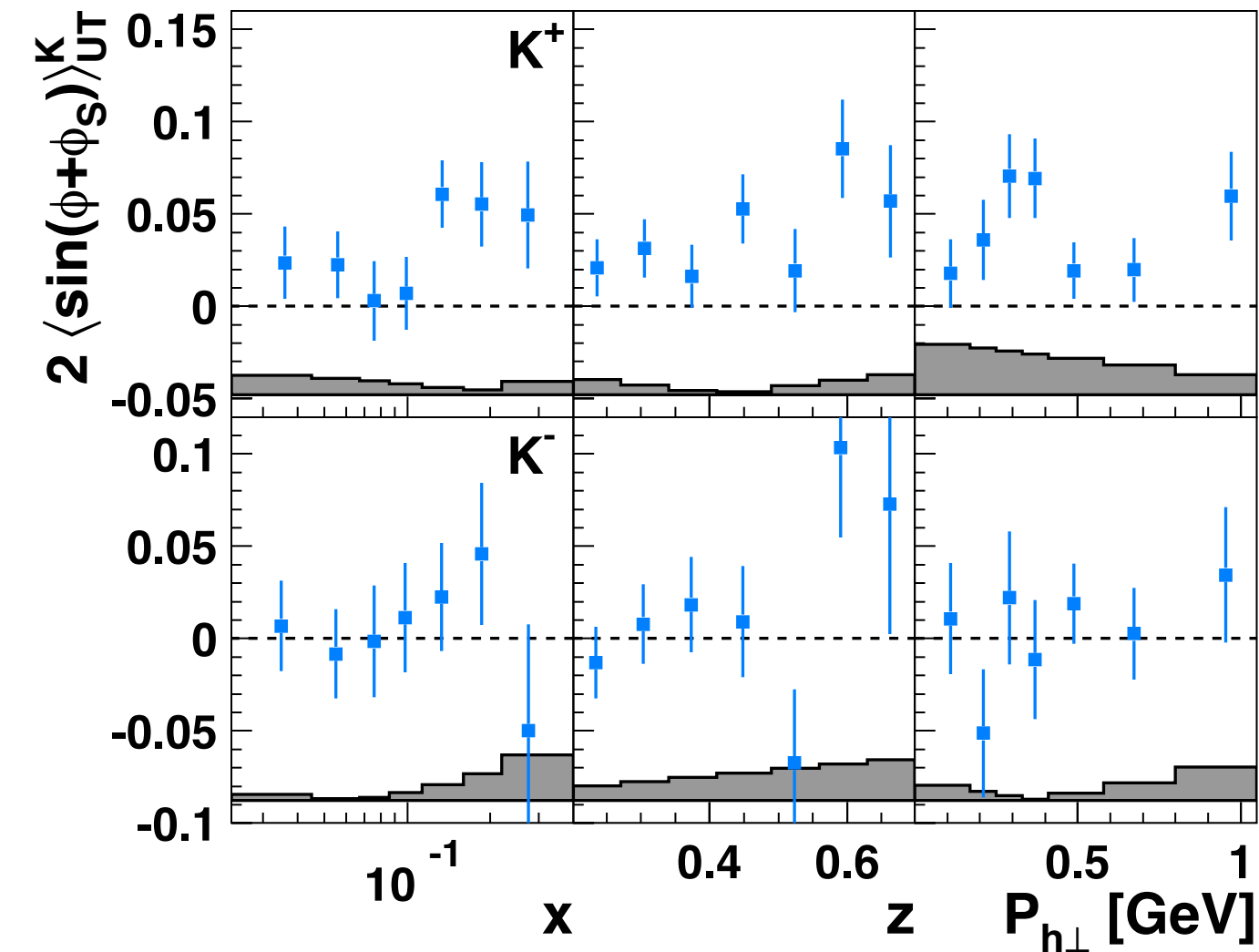
$$u \Rightarrow \pi^-; \quad d \Rightarrow \pi^+ (\text{disfav})$$

$$h_1^u > 0$$

$$h_1^d < 0$$

Collins amplitudes for kaons

- HERMES Collaboration-
Phys. Lett. B 693 (2010) 11-16



$$2\langle\sin(\phi + \phi_s)\rangle_{UT} \propto \frac{\mathcal{C}\left[-\frac{\hat{\mathbf{P}}_{h\perp} \cdot \mathbf{k}_T}{M_h} h_1^q(x, p_T^2) H_1^{\perp q \rightarrow h}(z, k_T^2)\right]}{\mathcal{C}\left[f_1^q(x, p_T^2) D_1^{q \rightarrow h}(z, k_T^2)\right]}$$

K^+

☞ K^+ amplitudes are similar to π^+ as expected from the u-quark dominance

☞ K^+ are larger than π^+

K^-

☞ consistent with zero amplitudes

☞ $K^- (\bar{u}s)$ is all sea object

Collins amplitudes for kaons

- HERMES Collaboration-
Phys. Lett. B 693 (2010) 11-16

$$2\langle \sin(\phi + \phi_s) \rangle_{UT}^K \propto \frac{\mathcal{C}\left[-\frac{\hat{\mathbf{P}}_{h\perp} \cdot \mathbf{k}_T}{M_h} h_1^q(x, p_T^2) H_1^{\perp q \rightarrow h}(z, k_T^2)\right]}{\mathcal{C}\left[f_1^q(x, p_T^2) D_1^{q \rightarrow h}(z, k_T^2)\right]}$$

K^+

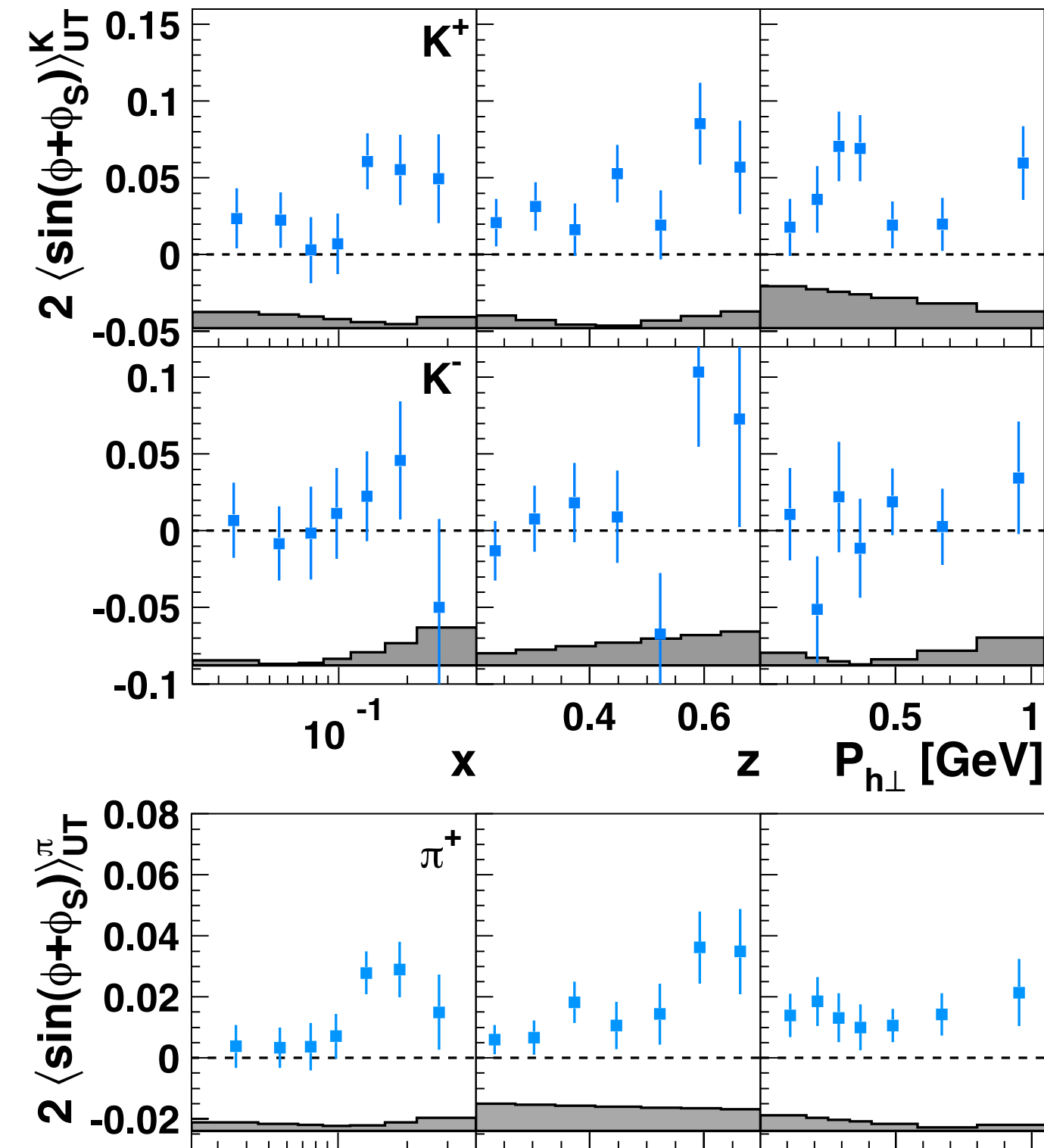
☞ K^+ amplitudes are similar to π^+ as expected from the u-quark dominance

☞ K^+ are larger than π^+

K^-

☞ consistent with zero amplitudes

☞ $K^- (\bar{u}s)$ is all sea object



Collins amplitudes for kaons

- HERMES Collaboration-
Phys. Lett. B 693 (2010) 11-16

$$2\langle \sin(\phi + \phi_s) \rangle_{UT} \propto \frac{\mathcal{C} \left[-\frac{\hat{\mathbf{P}}_{h\perp} \cdot \mathbf{k}_T}{M_h} h_1^q(x, p_T^2) H_1^{\perp q \rightarrow h}(z, k_T^2) \right]}{\mathcal{C} \left[f_1^q(x, p_T^2) D_1^{q \rightarrow h}(z, k_T^2) \right]}$$

K^+

☞ K^+ amplitudes are similar to π^+ as expected from the u-quark dominance

☞ K^+ are larger than π^+

K^-

☞ consistent with zero amplitudes

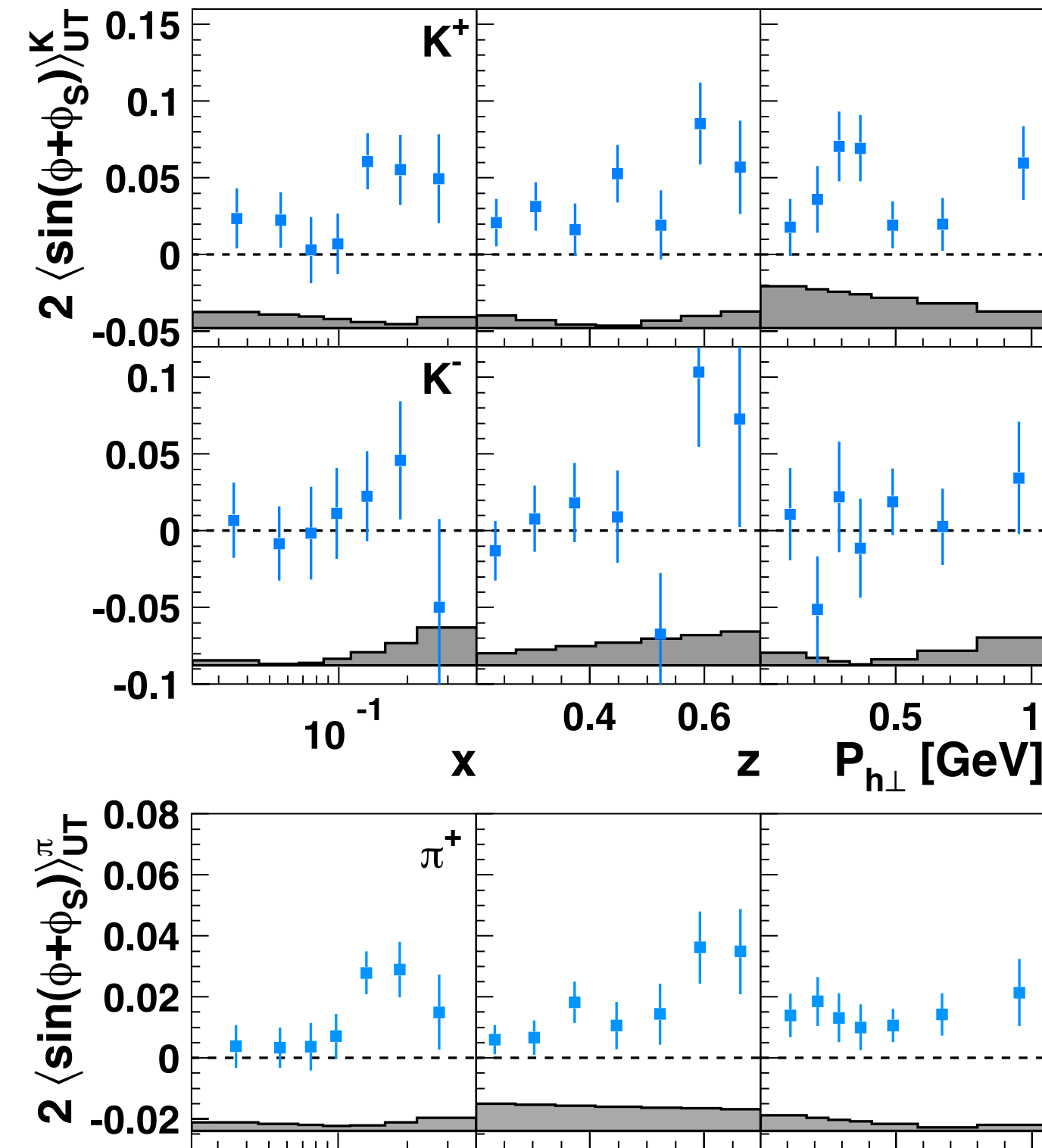
☞ $K^- (\bar{u}s)$ is all sea object

differences between K^+ and π^+ amplitudes

☞ role of sea quarks in conjunction with possibly large FF

☞ various contributions from decay of semi-inclusively produced vector-mesons

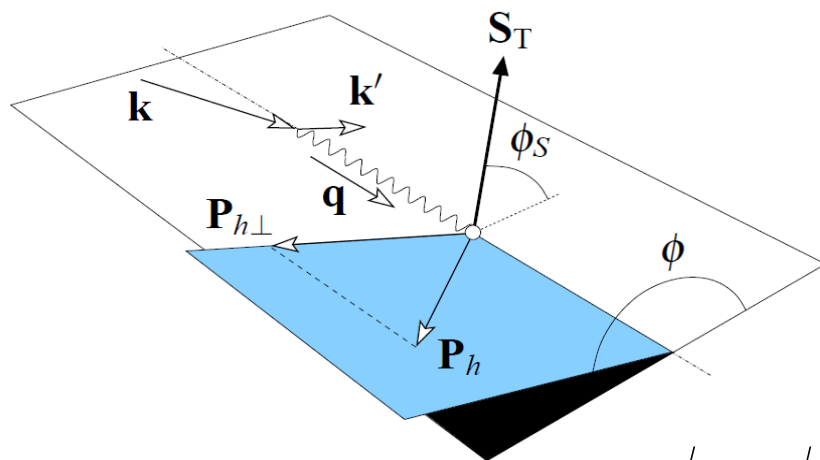
☞ the k_T dependences of the fragmentation functions



inclusive hadron measurements

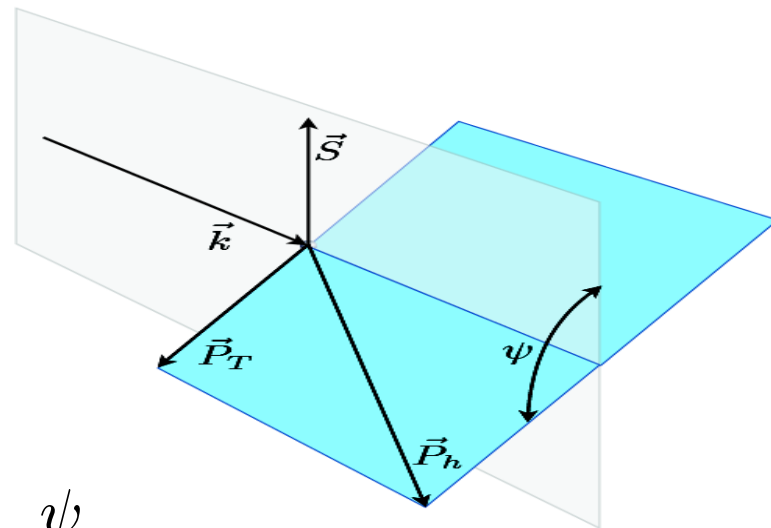
Inclusive transverse target spin asymmetries

semi-inclusive DIS $lp^\uparrow \rightarrow l'hX$



$$\phi - \phi_S \longrightarrow \psi$$

inclusive hadrons $lp^\uparrow \rightarrow hX$



inclusive transverse target spin asymmetry

$$d\sigma = d\sigma_{UU} [1 + S_\perp A_{UT}^{\sin(\psi)} \sin(\psi)]$$

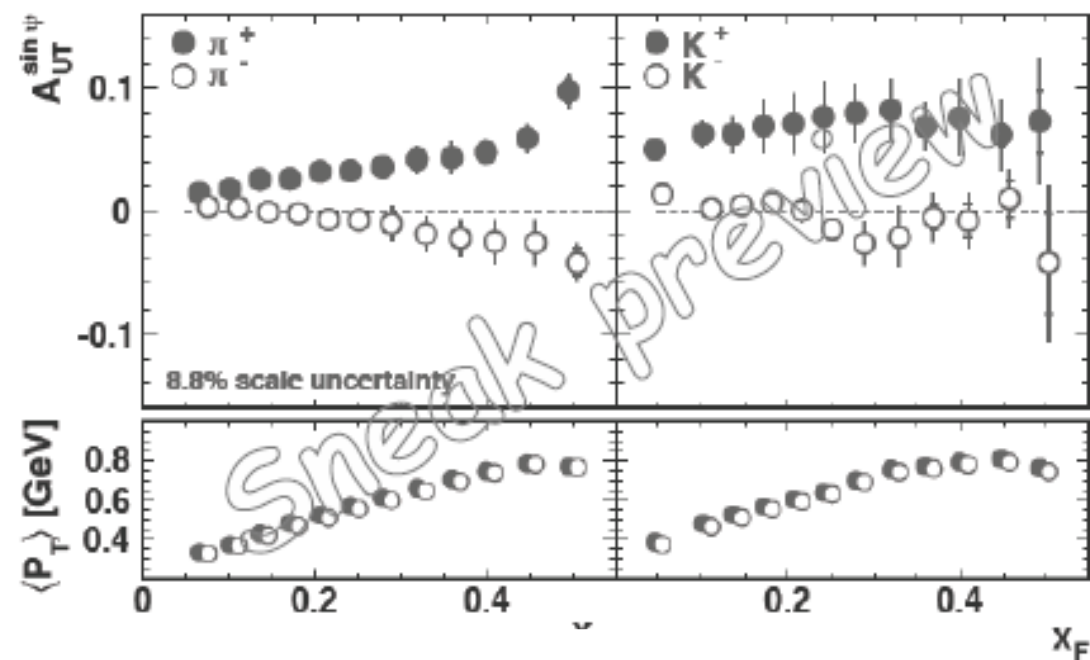
no info on Q^2

data dominated by $Q^2 \approx 0$

SIDIS only small subsample

Inclusive transverse target spin asymmetries

 x_F dependence




π^+

 positive, increase nearly linearly with x_F

π^-


 negative, decrease nearly linearly with x_F

 x_F behavior of pions similar to what observed in hadron-hadron collisions

K^+

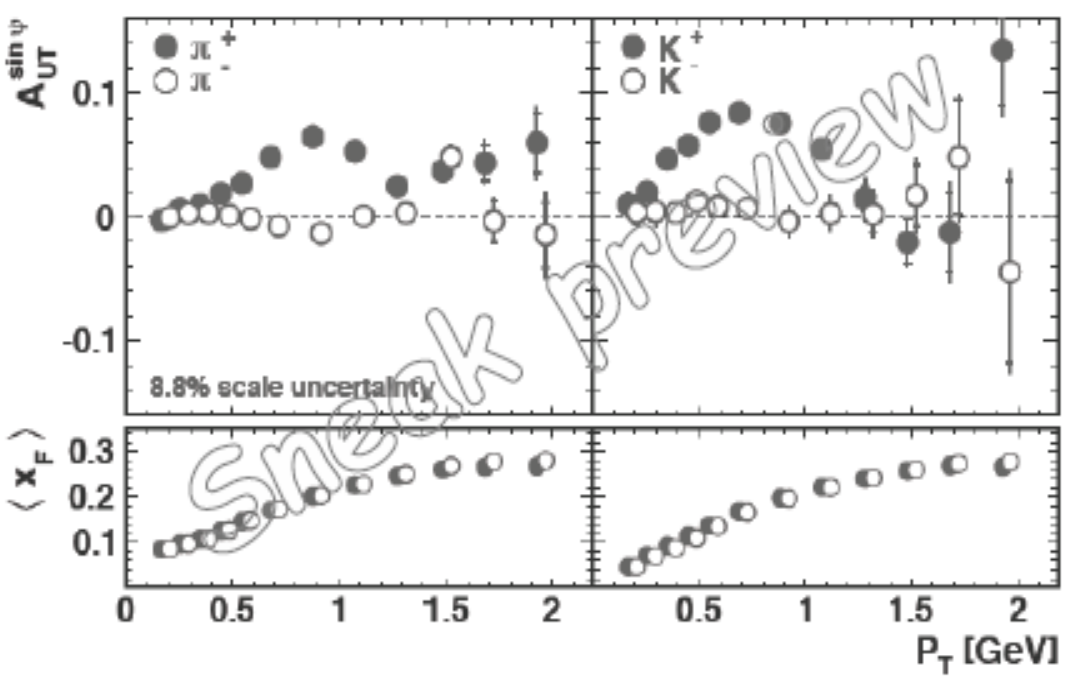
 positive, approximately constant with x_F

K^-


 compatible with zero, with small variation over x_F

Inclusive transverse target spin asymmetries

 p_T dependence




π^+

 positive, increase to approximately 0.06, and then decrease with p_T


π^-

 small, varyingly positive and negative

K^+

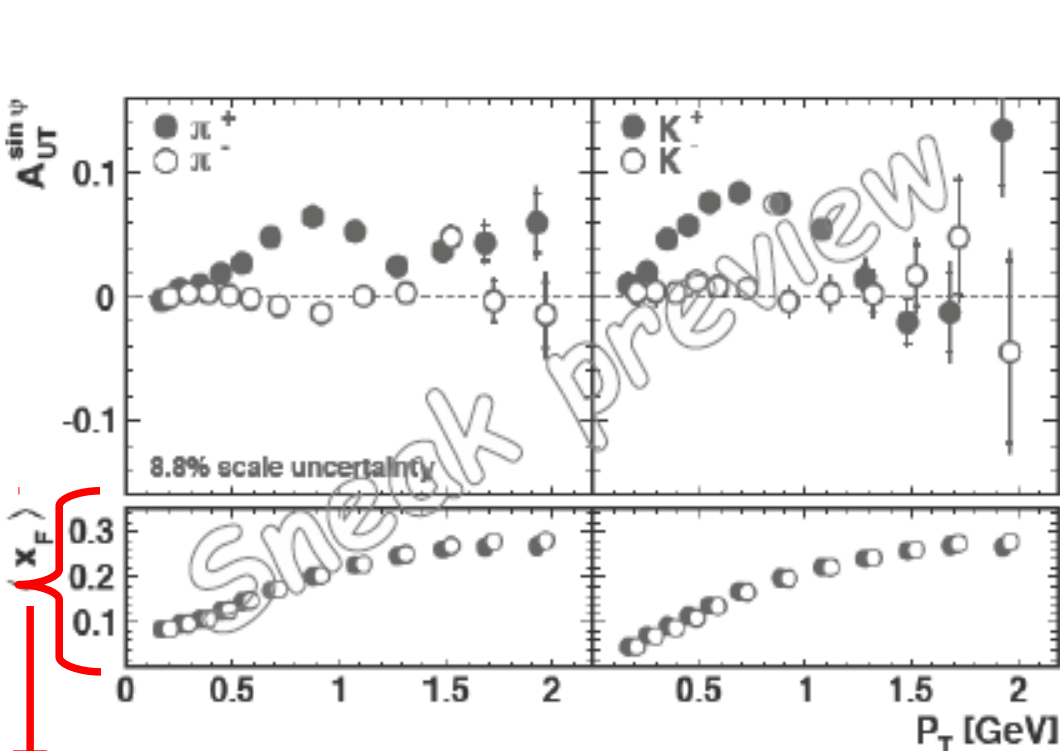
 positive, increase to approximately 0.08, and then decrease with p_T

K^-


 small, positive

Inclusive transverse target spin asymmetries

 p_T dependence




π^+

 positive, increase to approximately 0.06, and then decrease with p_T

π^-


 small, varyingly positive and negative

K^+

 positive, increase to approximately 0.08, and then decrease with p_T

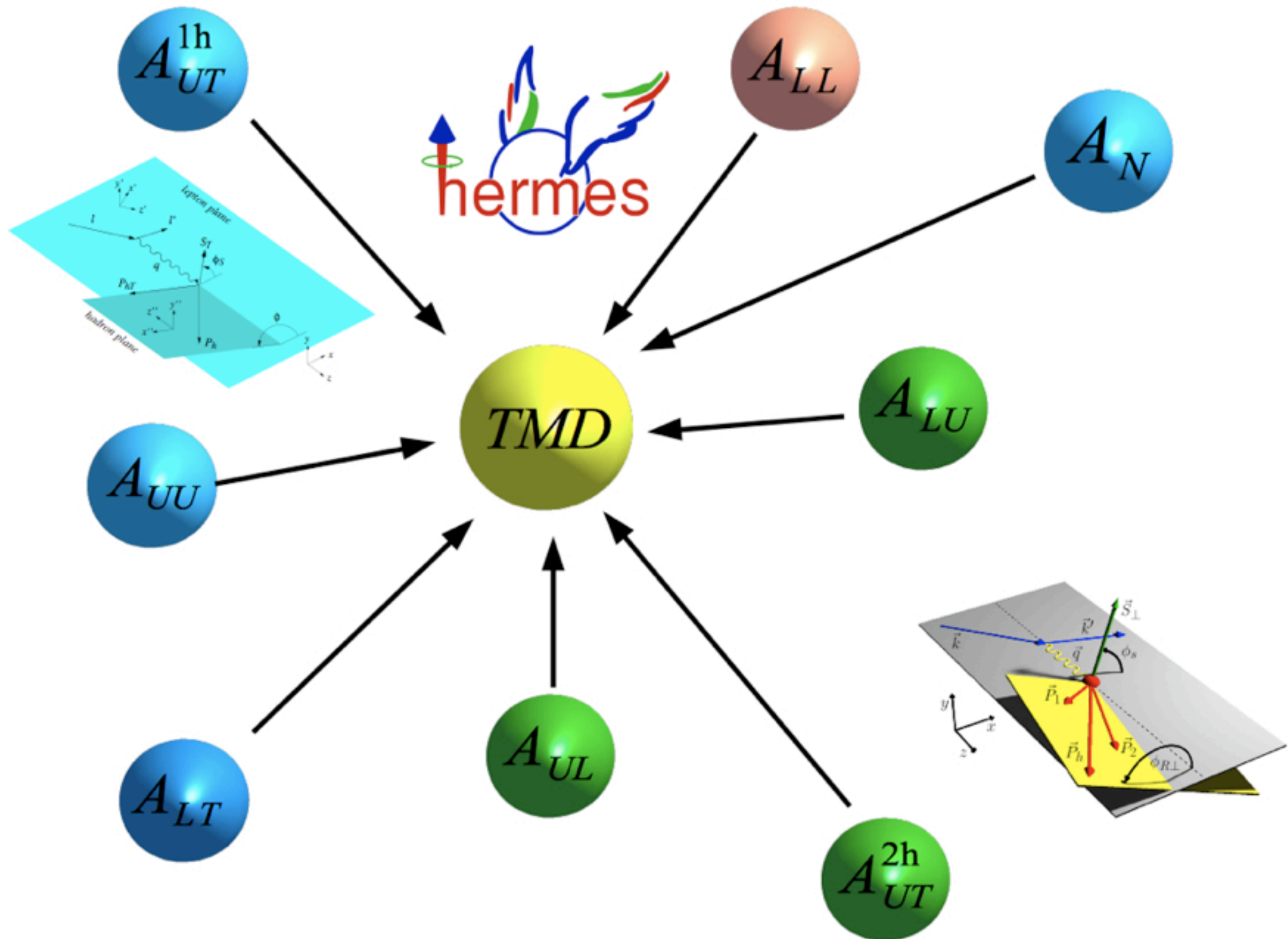
K^-

 small, positive

 disentangling of $x_F - p_T$ correlation: 2D asymmetries

 disentangling of different data samples:
with and without scattered-electron tagging, and different kinematic regions

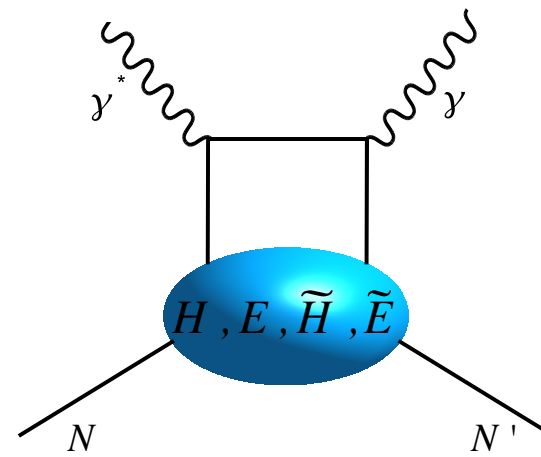
to appear very soon on the arXiv!



exclusive measurements
(probing GPDs)

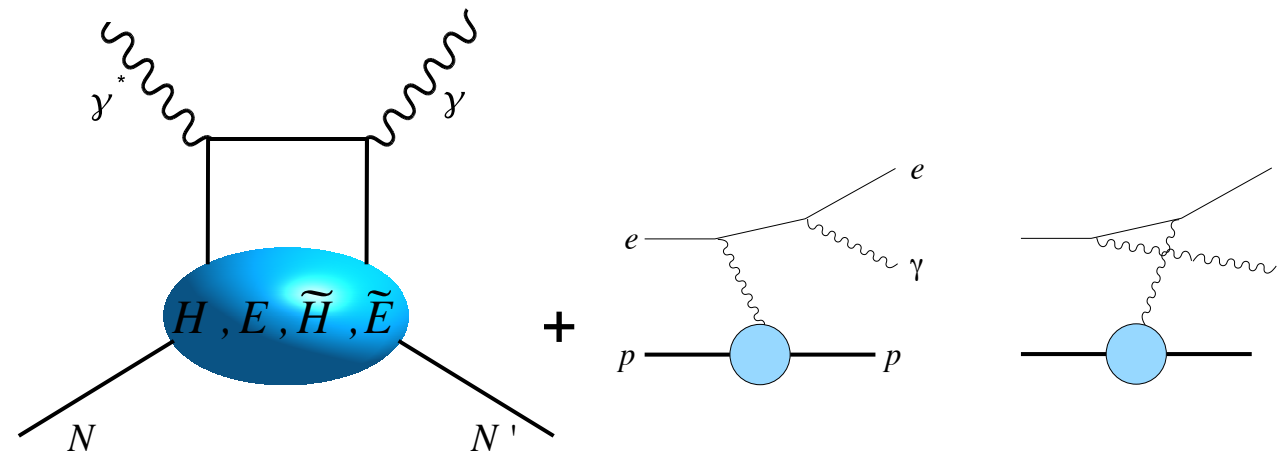
☞ theoretically the cleanest probe of GPDs

$$\gamma^* N \rightarrow \gamma N : H, E, \tilde{H}, \tilde{E}$$



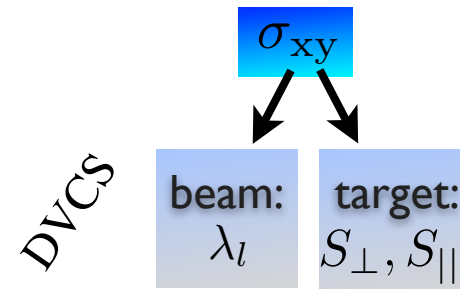
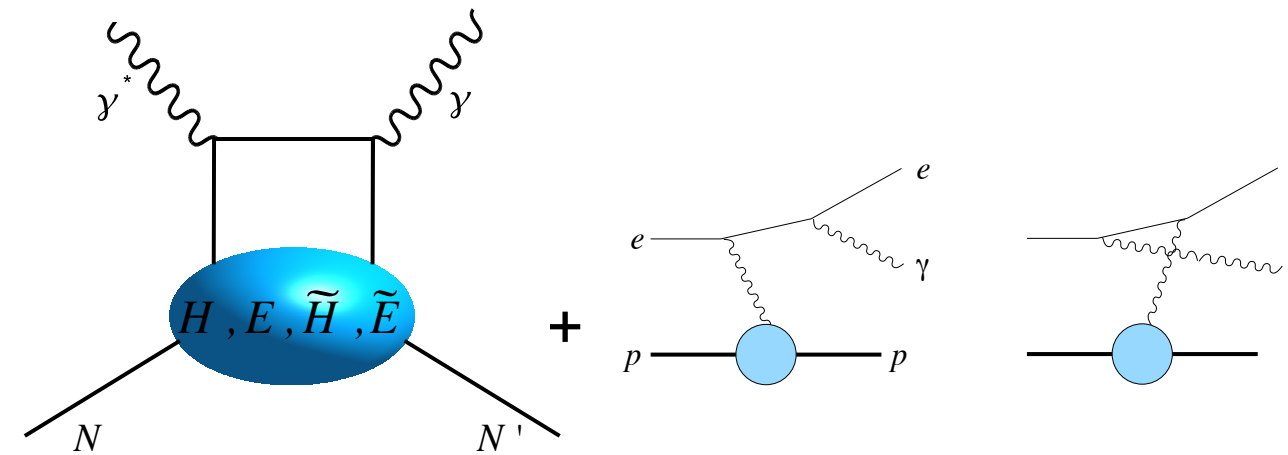
☞ theoretically the cleanest probe of GPDs

$$\gamma^* N \rightarrow \gamma N : H, E, \tilde{H}, \tilde{E}$$



☞ theoretically the cleanest probe of GPDs

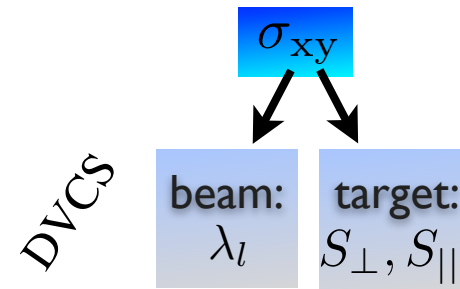
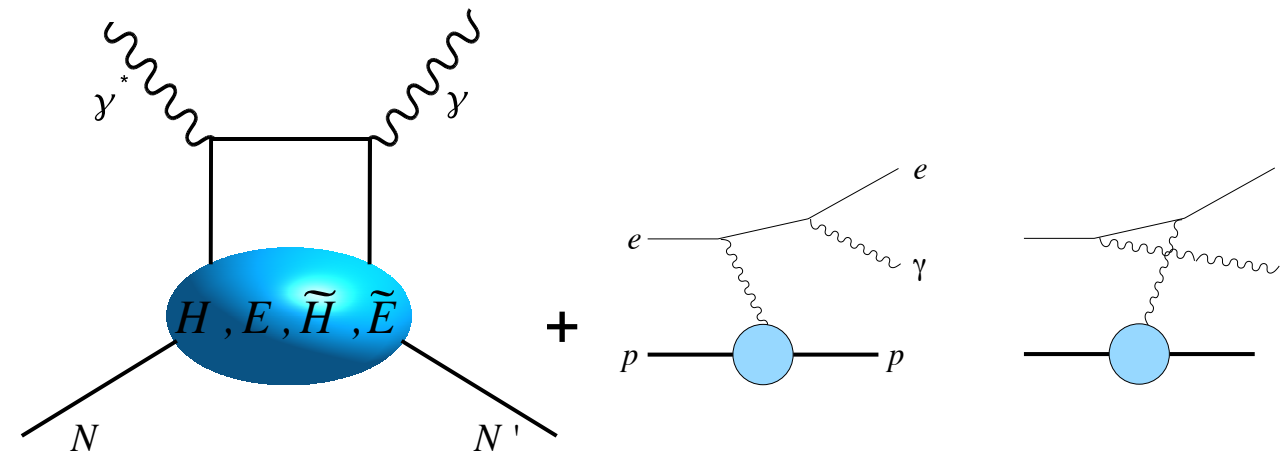
$$\gamma^* N \rightarrow \gamma N : H, E, \tilde{H}, \tilde{E}$$



Bethe-Heitler		interference		DVCS
$d\sigma \sim d\sigma_{UU}^{BH}$	+	$e_\ell d\sigma_{UU}^I$	+	$d\sigma_{UU}^{DVCS}$
	+	$e_\ell \lambda_\ell d\sigma_{LU}^I$	+	$\lambda_\ell d\sigma_{LU}^{DVCS}$
	+	$e_\ell S_{ } d\sigma_{UL}^I$	+	$S_{ } d\sigma_{UL}^{DVCS}$
	+	$e_\ell S_{\perp} d\sigma_{UT}^I$	+	$S_{\perp} d\sigma_{UT}^{DVCS}$
$+ \lambda_\ell S_{ } d\sigma_{LL}^{BH}$	+	$e_\ell \lambda_\ell S_{ } d\sigma_{LL}^I$	+	$\lambda_\ell S_{ } d\sigma_{LL}^{DVCS}$
$+ \lambda_\ell S_{\perp} d\sigma_{LT}^{BH}$	+	$e_\ell \lambda_\ell S_{\perp} d\sigma_{LT}^I$	+	$\lambda_\ell S_{\perp} d\sigma_{LT}^{DVCS}$

☞ theoretically the cleanest probe of GPDs

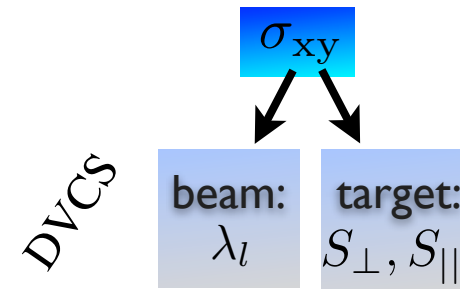
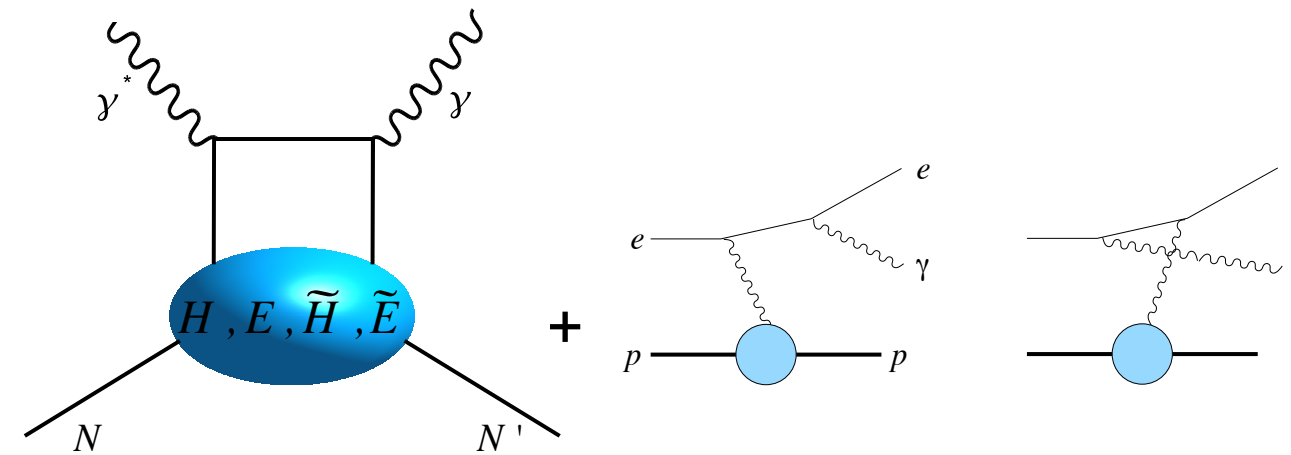
$$\gamma^* N \rightarrow \gamma N : H, E, \tilde{H}, \tilde{E}$$



Bethe-Heitler	beam charge: e_ℓ	interference	
	↓		
$d\sigma \sim d\sigma_{UU}^{BH}$ $+ \lambda_\ell S_{ } d\sigma_{LL}^{BH}$ $+ \lambda_\ell S_{\perp} d\sigma_{LT}^{BH}$	$+ e_\ell d\sigma_{UU}^I$ $+ e_\ell \lambda_\ell d\sigma_{LU}^I$ $+ e_\ell S_{ } d\sigma_{UL}^I$ $+ e_\ell S_{\perp} d\sigma_{UT}^I$ $+ e_\ell \lambda_\ell S_{ } d\sigma_{LL}^I$ $+ e_\ell \lambda_\ell S_{\perp} d\sigma_{LT}^I$	$+ d\sigma_{UU}^{DVCS}$ $+ \lambda_\ell d\sigma_{LU}^{DVCS}$ $+ S_{ } d\sigma_{UL}^{DVCS}$ $+ S_{\perp} d\sigma_{UT}^{DVCS}$ $+ \lambda_\ell S_{ } d\sigma_{LL}^{DVCS}$ $+ \lambda_\ell S_{\perp} d\sigma_{LT}^{DVCS}$	

☞ theoretically the cleanest probe of GPDs

$$\gamma^* N \rightarrow \gamma N : H, E, \tilde{H}, \tilde{E}$$

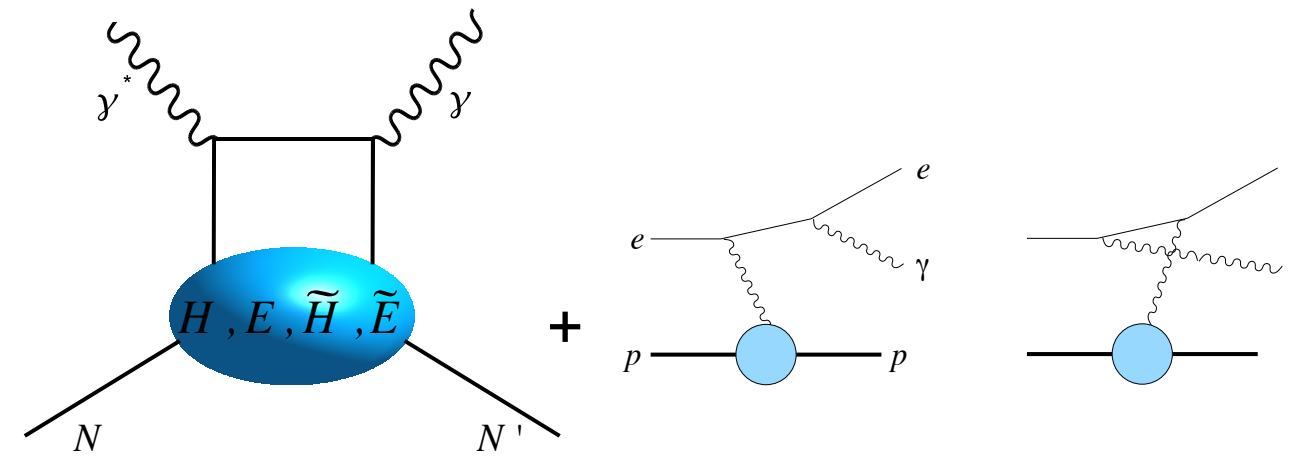


Bethe-Heitler	beam charge: e_ℓ	interference	
	↓		
$d\sigma \sim d\sigma_{UU}^{BH}$ $+ \lambda_\ell S_{ } d\sigma_{LL}^{BH}$ $+ \lambda_\ell S_{\perp} d\sigma_{LT}^{BH}$	$+ e_\ell d\sigma_{UU}^I$ $+ e_\ell \lambda_\ell d\sigma_{LU}^I$ $+ e_\ell S_{ } d\sigma_{UL}^I$ $+ e_\ell S_{\perp} d\sigma_{UT}^I$ $+ e_\ell \lambda_\ell S_{ } d\sigma_{LL}^I$ $+ e_\ell \lambda_\ell S_{\perp} d\sigma_{LT}^I$	$+ d\sigma_{UU}^{DVCS}$ $+ \lambda_\ell d\sigma_{LU}^{DVCS}$ $+ S_{ } d\sigma_{UL}^{DVCS}$ $+ S_{\perp} d\sigma_{UT}^{DVCS}$ $+ \lambda_\ell S_{ } d\sigma_{LL}^{DVCS}$ $+ \lambda_\ell S_{\perp} d\sigma_{LT}^{DVCS}$	

✓ HERMES measured complete set of beam helicity, beam charge and target polarization asymmetries

☞ theoretically the cleanest probe of GPDs

$$\gamma^* N \rightarrow \gamma N : H, E, \tilde{H}, \tilde{E}$$



Bethe-Heitler
beam charge:
 e_ℓ
interference

DVCS
 σ_{xy}
beam:
 λ_l
target:
 S_\perp, S_\parallel

$$\begin{aligned} d\sigma \sim & d\sigma_{UU}^{BH} + e_\ell d\sigma_{UU}^I + d\sigma_{UU}^{DVCS} \\ & + e_\ell \lambda_\ell d\sigma_{LU}^I + \lambda_\ell d\sigma_{LU}^{DVCS} \\ & + e_\ell S_\parallel d\sigma_{UL}^I + S_\parallel d\sigma_{UL}^{DVCS} \\ & + e_\ell S_\perp d\sigma_{UT}^I + S_\perp d\sigma_{UT}^{DVCS} \\ & + \lambda_\ell S_\parallel d\sigma_{LL}^{BH} + e_\ell \lambda_\ell S_\parallel d\sigma_{LL}^I + \lambda_\ell S_\parallel d\sigma_{LL}^{DVCS} \\ & + \lambda_\ell S_\perp d\sigma_{LT}^{BH} + e_\ell \lambda_\ell S_\perp d\sigma_{LT}^I + \lambda_\ell S_\perp d\sigma_{LT}^{DVCS} \end{aligned}$$

☞ unpolarized target

$$F_1 \mathcal{H} + \frac{x_B}{2 - x_B} (F_1 + F_2) \tilde{\mathcal{H}} - \frac{t}{4M^2} F_2 \mathcal{E}$$

☞ longitudinally polarized target

$$\begin{aligned} & \frac{x_B}{2 - x_B} (F_1 + F_2) \left(\mathcal{H} + \frac{x_B}{2} \mathcal{E} \right) \\ & + F_1 \tilde{\mathcal{H}} - \frac{x_B}{2 - x_B} \left(\frac{x_B}{2} F_1 + \frac{t}{4M^2} F_2 \right) \tilde{\mathcal{E}} \end{aligned}$$

☞ transversely polarized target

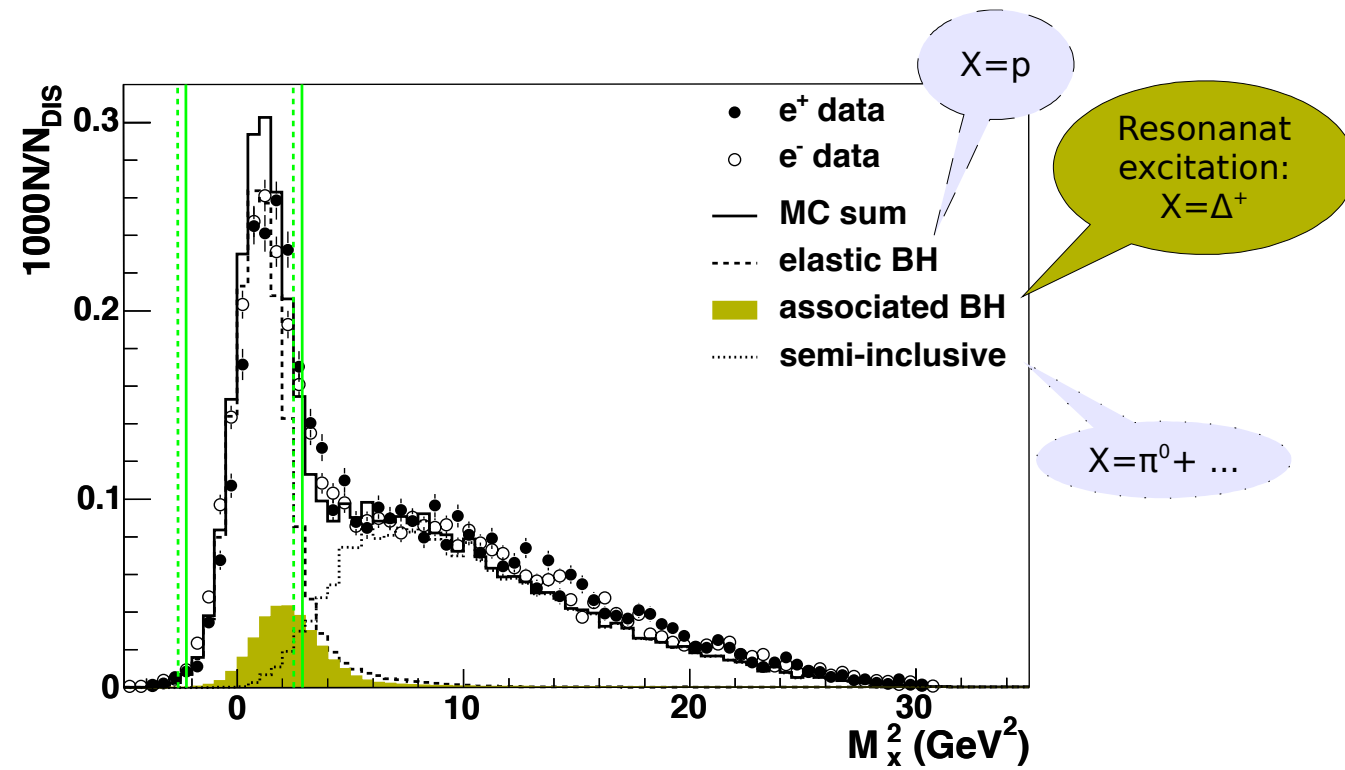
$$\frac{t}{4M^2} \left[(2 - x_B) F_1 \mathcal{E} - 4 \frac{1 - x_B}{2 - x_B} F_2 \mathcal{H} \right]$$

✓ HERMES measured complete set of beam helicity, beam charge and target polarization asymmetries

$$ep \rightarrow e' \gamma X$$

DVCS measurements

(without recoil detector)



👉 missing mass technique

$$M_X^2 = (p + e - e' - \gamma)^2$$

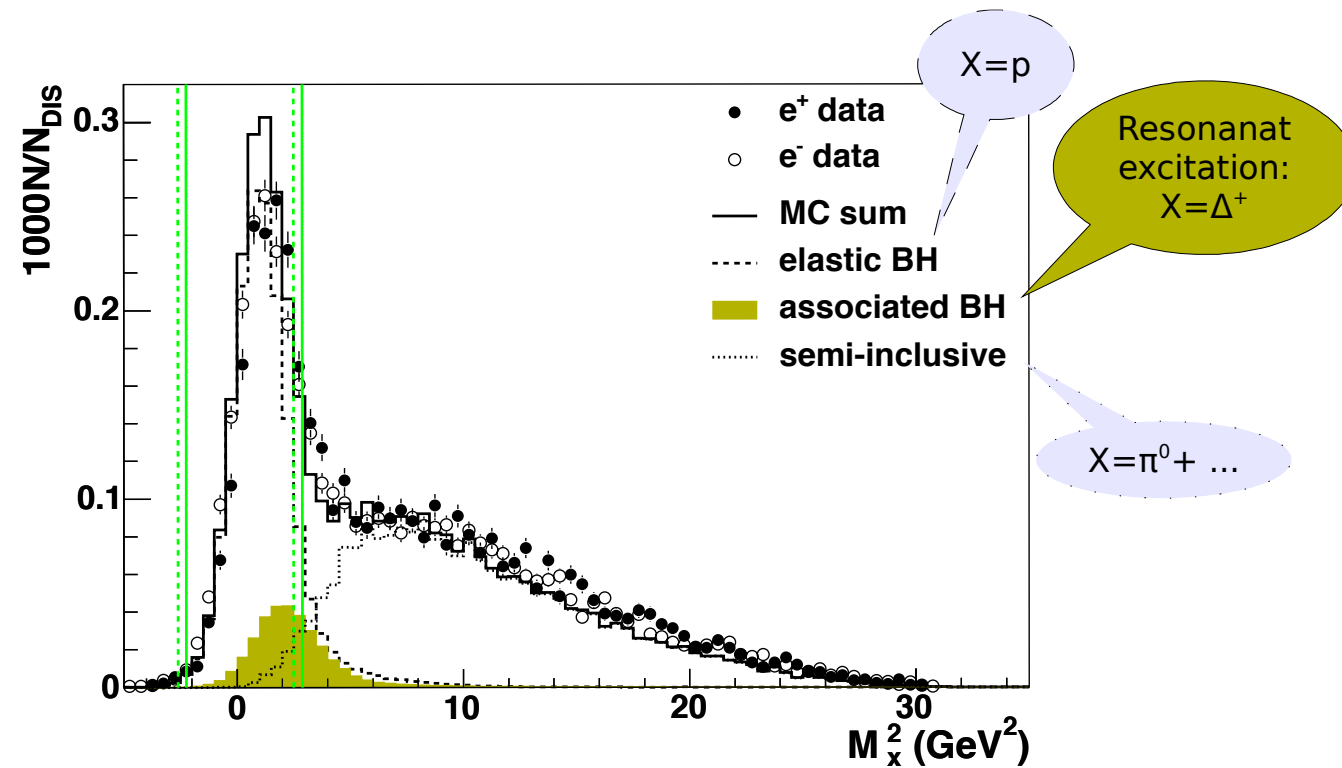
$$ep \rightarrow e' \gamma X$$

DVCS measurements

$$ep \rightarrow e' \gamma p'$$

(without recoil detector)

(with recoil detector)



👉 missing mass technique

$$M_X^2 = (p + e - e' - \gamma)^2$$

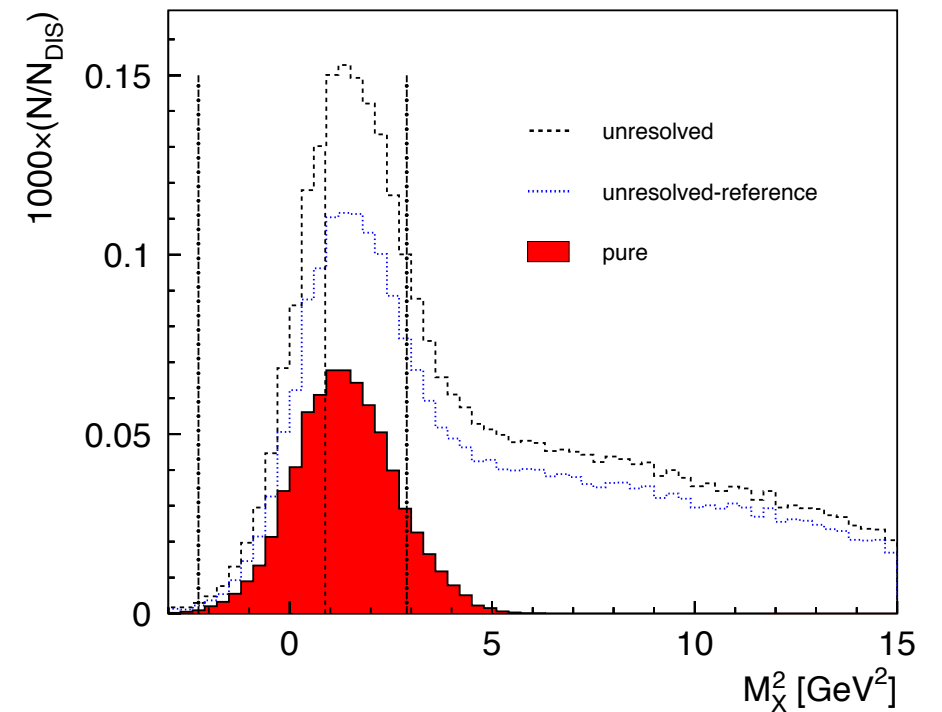
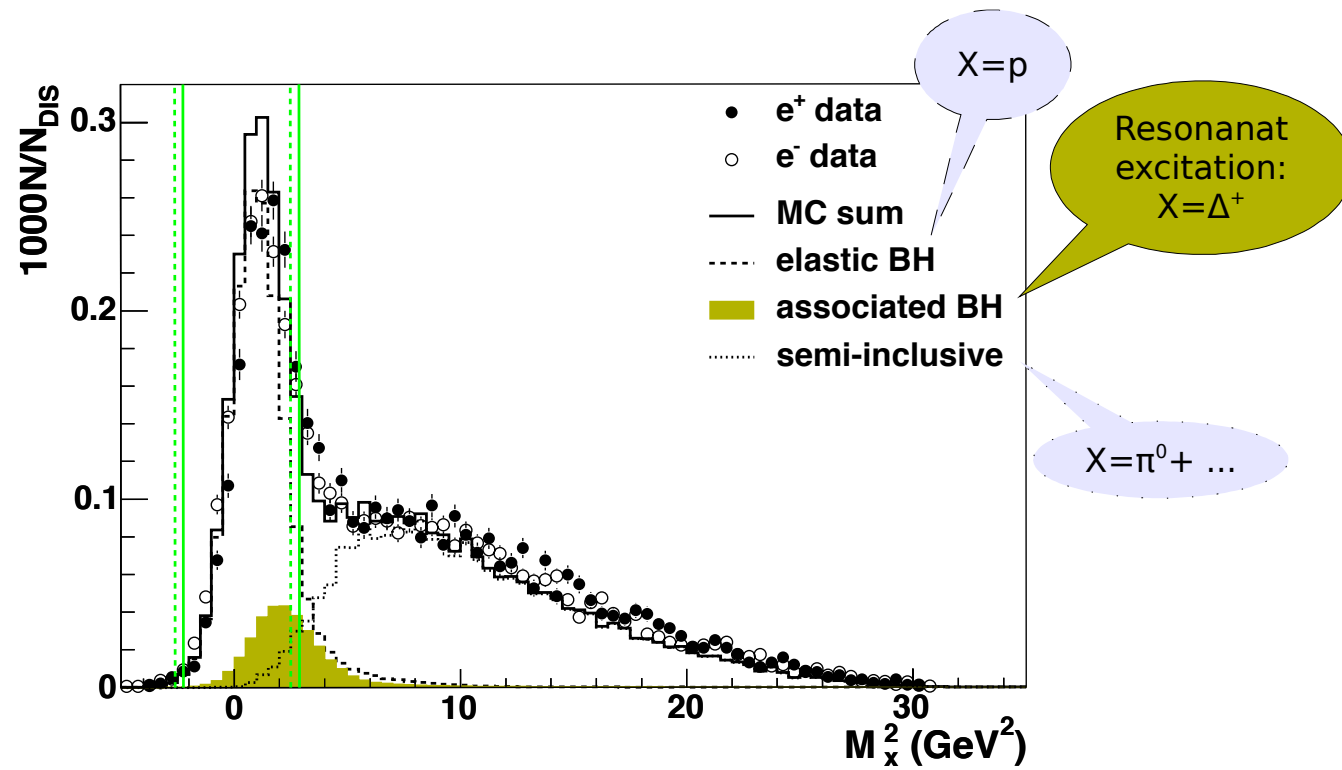
$$ep \rightarrow e' \gamma X$$

DVCS measurements

$$ep \rightarrow e' \gamma p'$$

(without recoil detector)

(with recoil detector)



👉 missing mass technique

$$M_X^2 = (p + e - e' - \gamma)^2$$

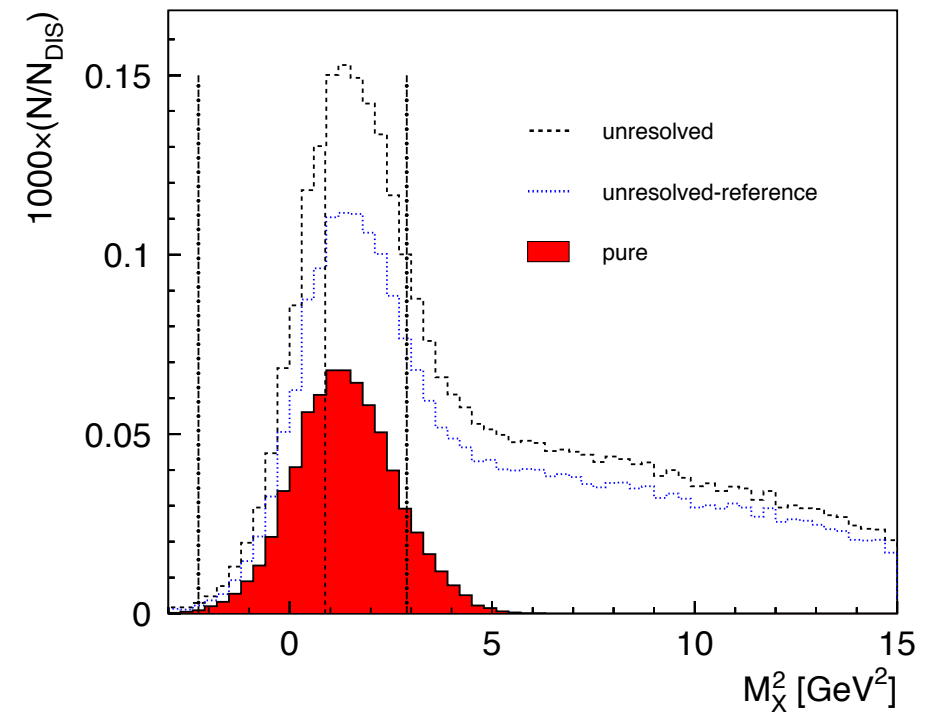
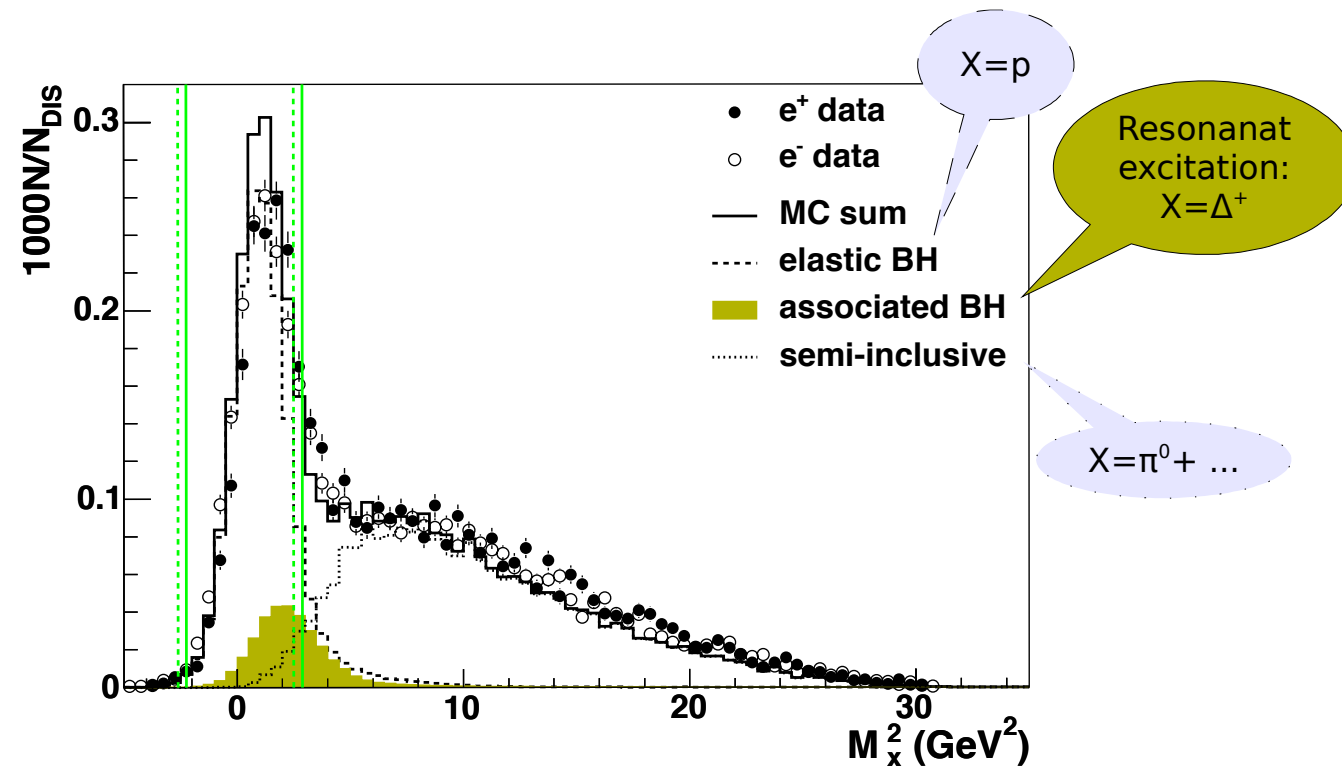
$$ep \rightarrow e' \gamma X$$

DVCS measurements

$$ep \rightarrow e' \gamma p'$$

(without recoil detector)

(with recoil detector)



✎ missing mass technique

$$M_X^2 = (p + e - e' - \gamma)^2$$

✓ unresolved and unresolved-reference samples: $ep \rightarrow e' \gamma X$

✎ use missing mass technique

✎ for comparison only

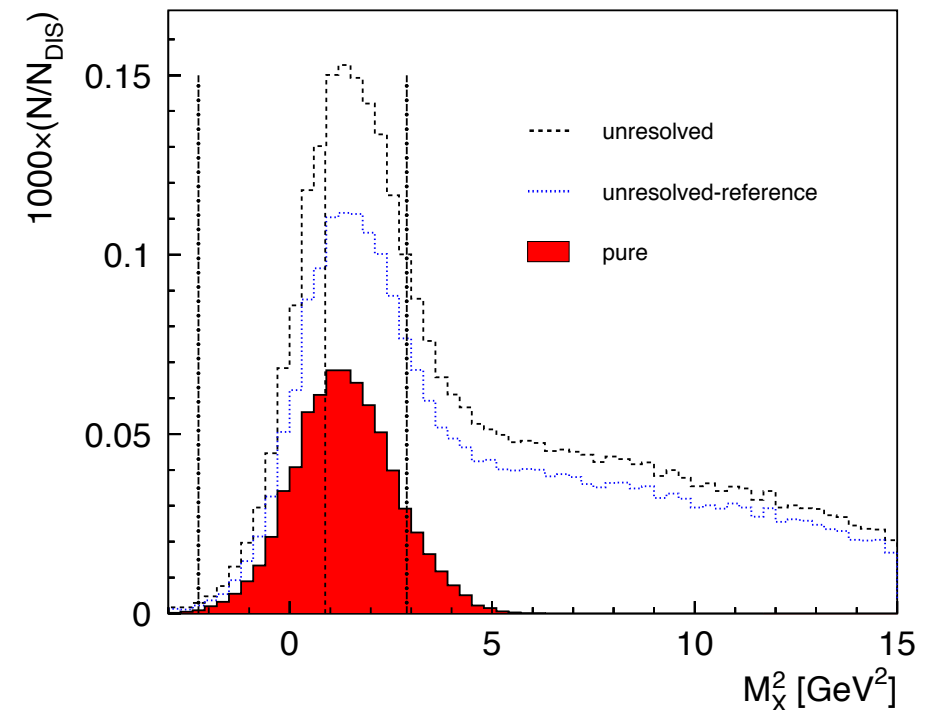
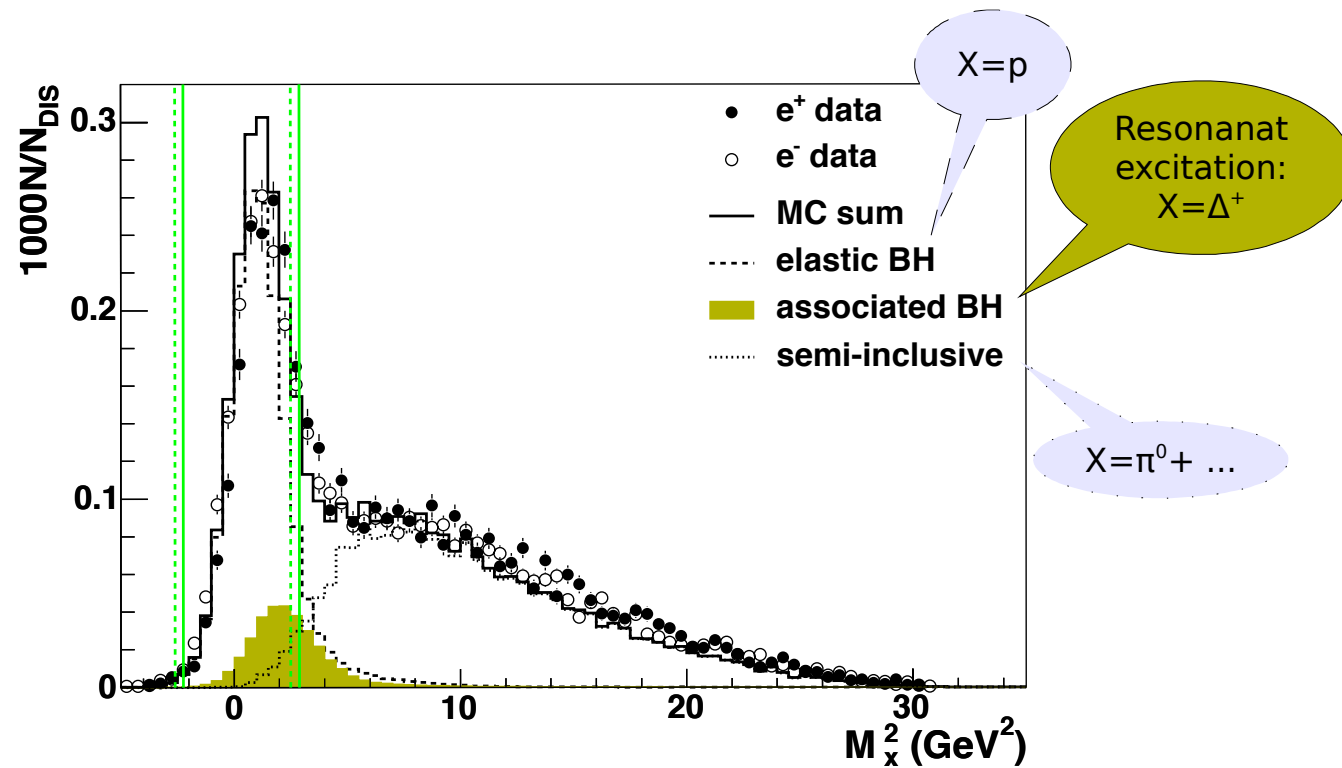
$$ep \rightarrow e' \gamma X$$

DVCS measurements

$$ep \rightarrow e' \gamma p'$$

(without recoil detector)

(with recoil detector)



✎ missing mass technique

$$M_X^2 = (p + e - e' - \gamma)^2$$

✓ unresolved and unresolved-reference samples: $ep \rightarrow e' \gamma X$

✎ use missing mass technique

✎ for comparison only

✓ pure sample: $ep \rightarrow e' \gamma p'$

✎ all particles in the final state are detected

✎ kinematic event fit

✎ BH/DVCS events with 83% efficiency

✎ background contamination from semi-inclusive and associated processes less than 0.2%

$ep \rightarrow e' \gamma X$
(pre-recoil data)

GPD H: unpolarized hydrogen target

-HERMES Collaboration- : JHEP 07 (2012) 032

$$\sigma(\phi, P_\ell, e_\ell) = \sigma_{UU}(\phi) \times [1 + P_\ell \mathcal{A}_{LU}^{DVCS}(\phi) + e_\ell P_\ell \mathcal{A}_{LU}^I(\phi) + e_\ell \mathcal{A}_C(\phi)]$$

✓ full hydrogen dataset used (incl. 2006/2007 data)

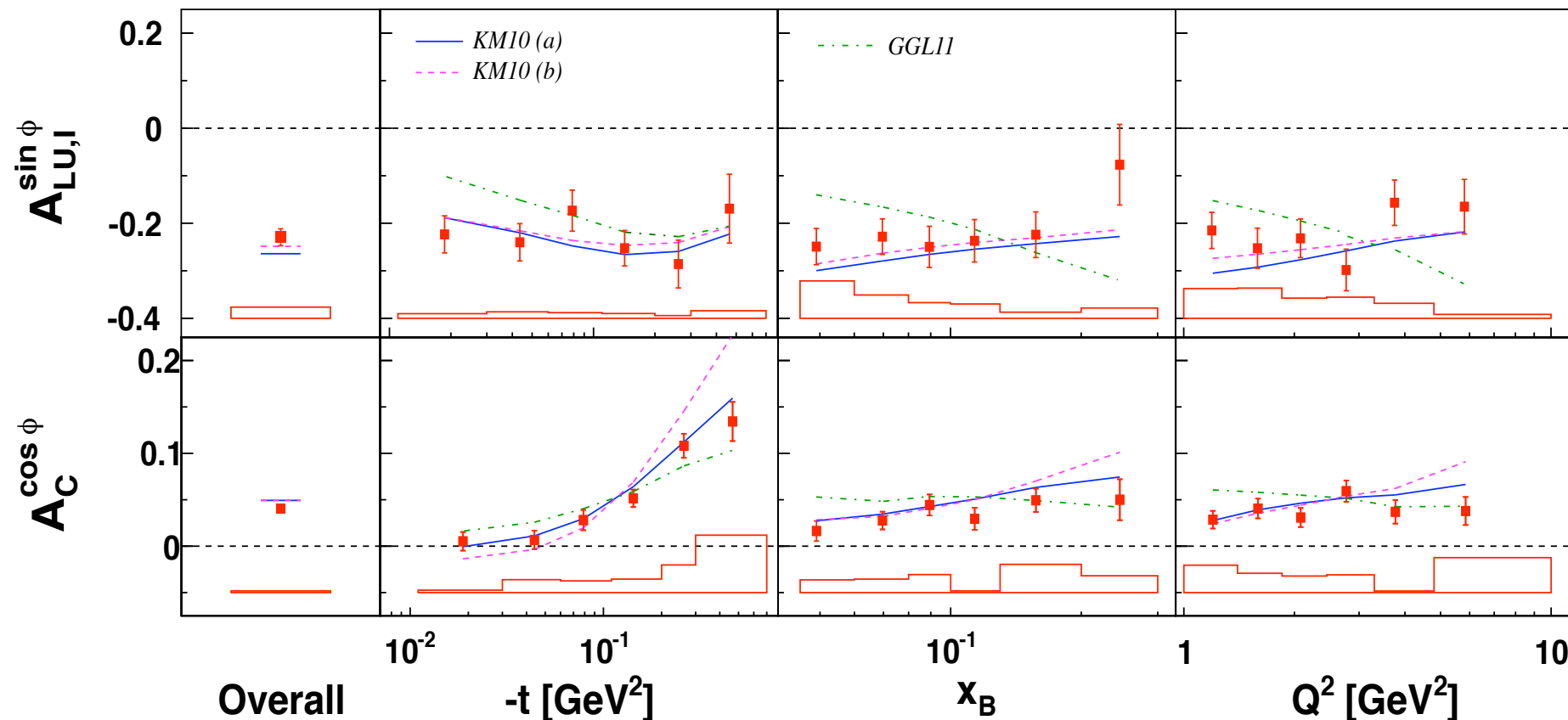
✓ sensitivity to Re and Im parts of CFF H

$$\mathcal{A}_C(\phi) = \sum_{n=0}^3 A_C^{\cos(n\phi)} \cos(n\phi)$$

$$\mathcal{A}_{LU}^I(\phi) = \sum_{n=1}^2 A_{LU,I}^{\sin(n\phi)} \sin(n\phi)$$

$$A_C^{\cos \phi} \propto \text{Re}[F_1 \mathcal{H}]$$

$$A_{LU,I}^{\sin \phi} \propto \text{Im}[F_1 \mathcal{H}]$$



charge-difference beam helicity
asymmetry

➡ large overall value

➡ no kin. dependencies

beam charge asymmetry

➡ strong t-dependence

➡ no x_B or Q^2 dependencies

$$ep \rightarrow e' \gamma p'$$

(recoil data)

GPD H: unpolarized hydrogen target

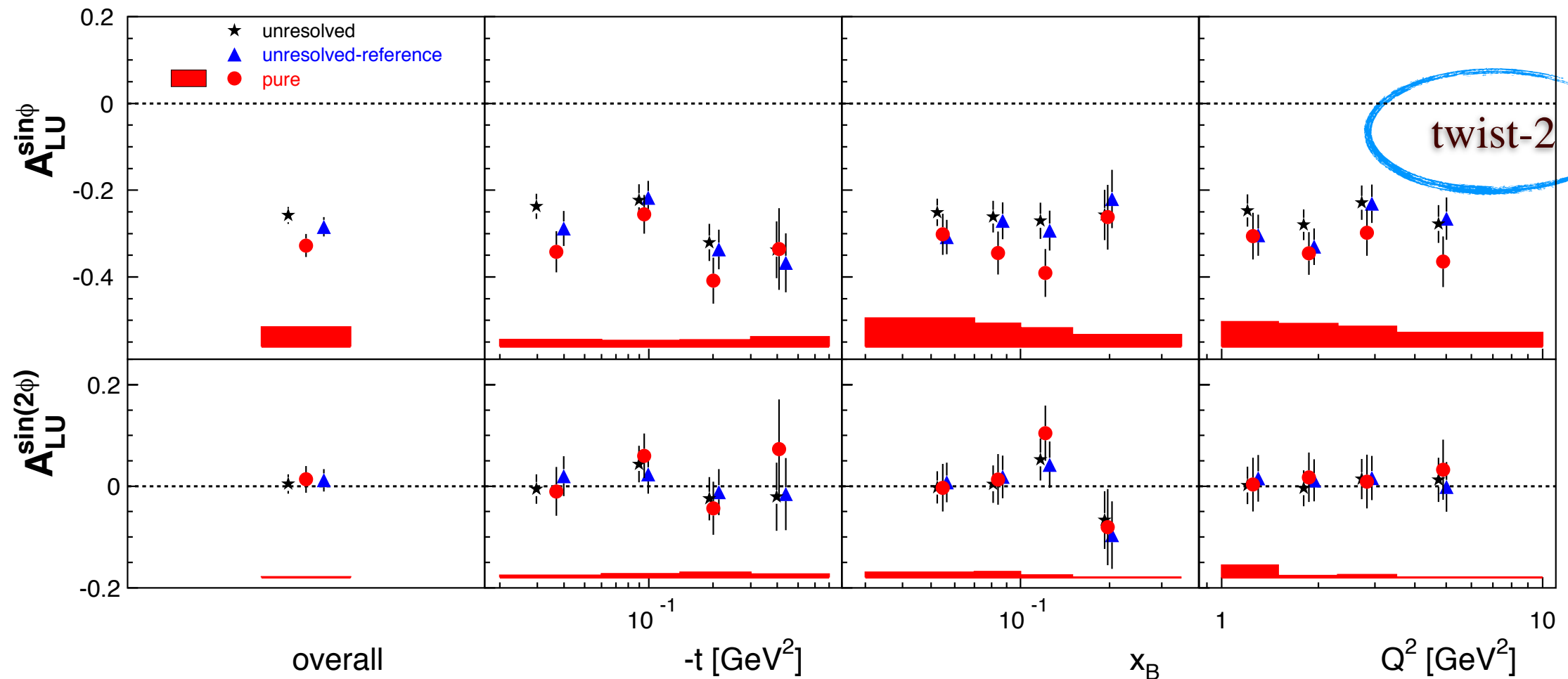
$$\sigma(\phi, P_\ell, e_\ell) = \sigma_{UU}(\phi) \times [1 + P_\ell \mathcal{A}_{LU}^{DVCS}(\phi) + e_\ell P_\ell \mathcal{A}_{LU}^I(\phi) + e_\ell \mathcal{A}_C(\phi)]$$

- HERMES Collaboration-
JHEP 10 (2012) 042

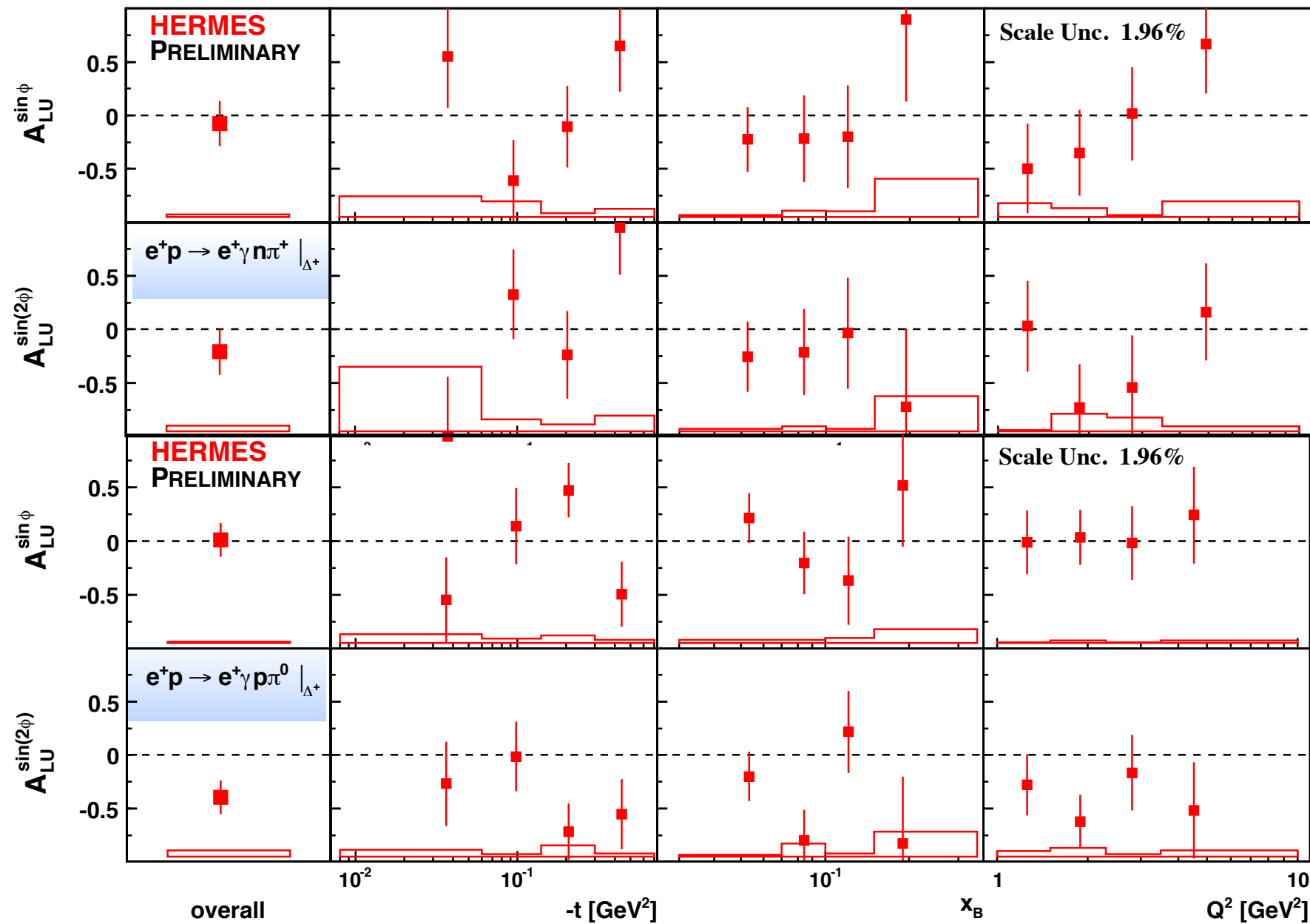
$$\mathcal{A}_{LU}(\phi) \simeq \sum_{n=1}^2 A_{LU}^{\sin(n\phi)} \sin(n\phi)$$

➡ extraction of single-charge beam-helicity asymmetry amplitudes for elastic (pure) data sample

➡ no separate access to DVCS and interference terms



➡ indication for slightly larger magnitude of the leading amplitude for elastic process compared to the one in the recoil detector acceptance (unresolved-reference)



Fractional purity
 Associated: DVCS/BH - 85.7 ± 1.8
 Elastic DVCS/BH ($ep \rightarrow e\gamma p$): 1.1 ± 0.1
 SIDIS: 13.2 ± 1.9

Fractional purity
 Associated DVCS/BH: 75.6 ± 2.6
 Elastic DVCS/BH ($ep \rightarrow e\gamma p$): 0.1 ± 0.1
 SIDIS: 24.4 ± 3.4

- consistent with zero result for both channels
- associated DVCS is mainly dilution in the analysis using the missing mass technique
- in agreement with the DVCS results on pure sample

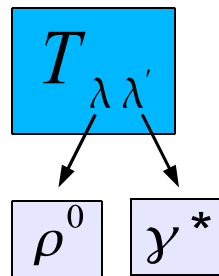
vector meson production

$$\frac{d\sigma}{dx_B dQ^2 dt d\phi_s d\phi d\cos\vartheta d\varphi} \sim \frac{d\sigma}{dx_B dQ^2 dt} W(x_B, Q^2, t, \phi_s, \phi, \cos\vartheta, \varphi)$$

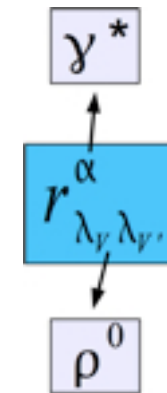
➡ production and decay angular distributions W decomposed:

$$W = W_{UU} + P_L W_{LU} + S_L W_{UL} + P_L S_L W_{LL} + S_T W_{UT} + P_L S_T W_{LT}$$

➡ parametrized by helicity amplitudes



➡ or alternatively by SDMEs:



-Schilling, Wolf (1973)-

helicity amplitudes or SDMEs describe

➡ the helicity transfer from virtual photon to the vector meson

➡ the parity of the diffractive exchange process

➡ natural parity is related to H and E

➡ unnatural parity is related to \tilde{H} and \tilde{E}



unnatural parity exchange observation

✓ At large Q^2 and W the **unnatural** parity exchange should be suppressed by M_V/Q

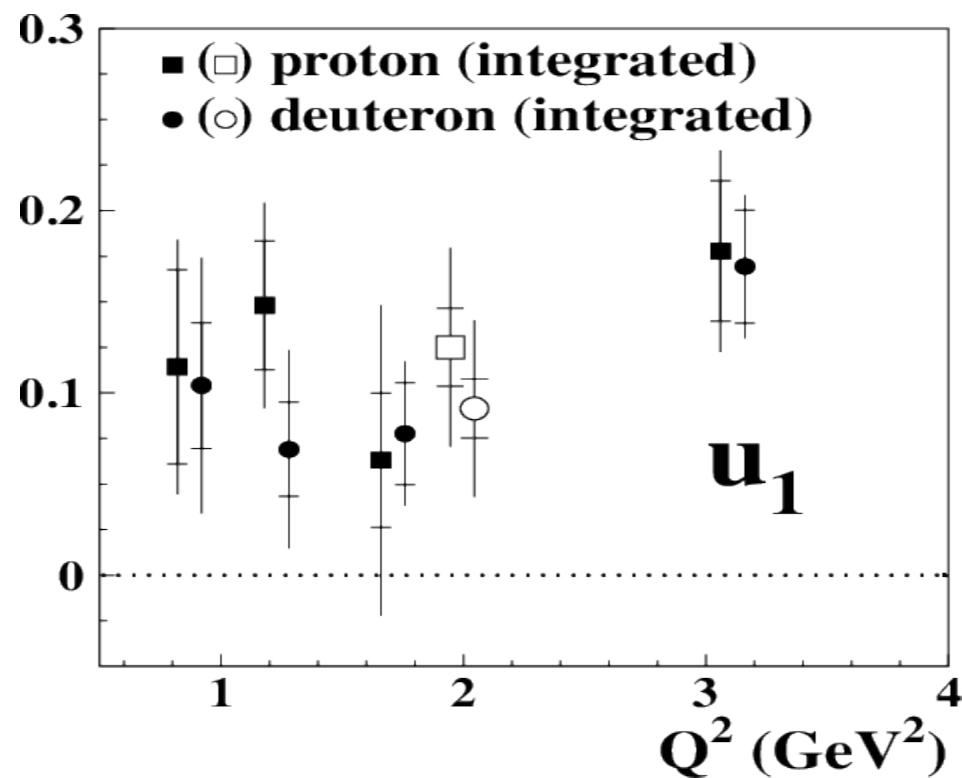
✓ The combinations of SDMEs expected to be zero in case of natural parity exchange dominance:

$$u_1 = 1 - r_{00}^{04} + 2r_{1-1}^{04} - 2r_{11}^1 - 2r_{1-1}^1$$

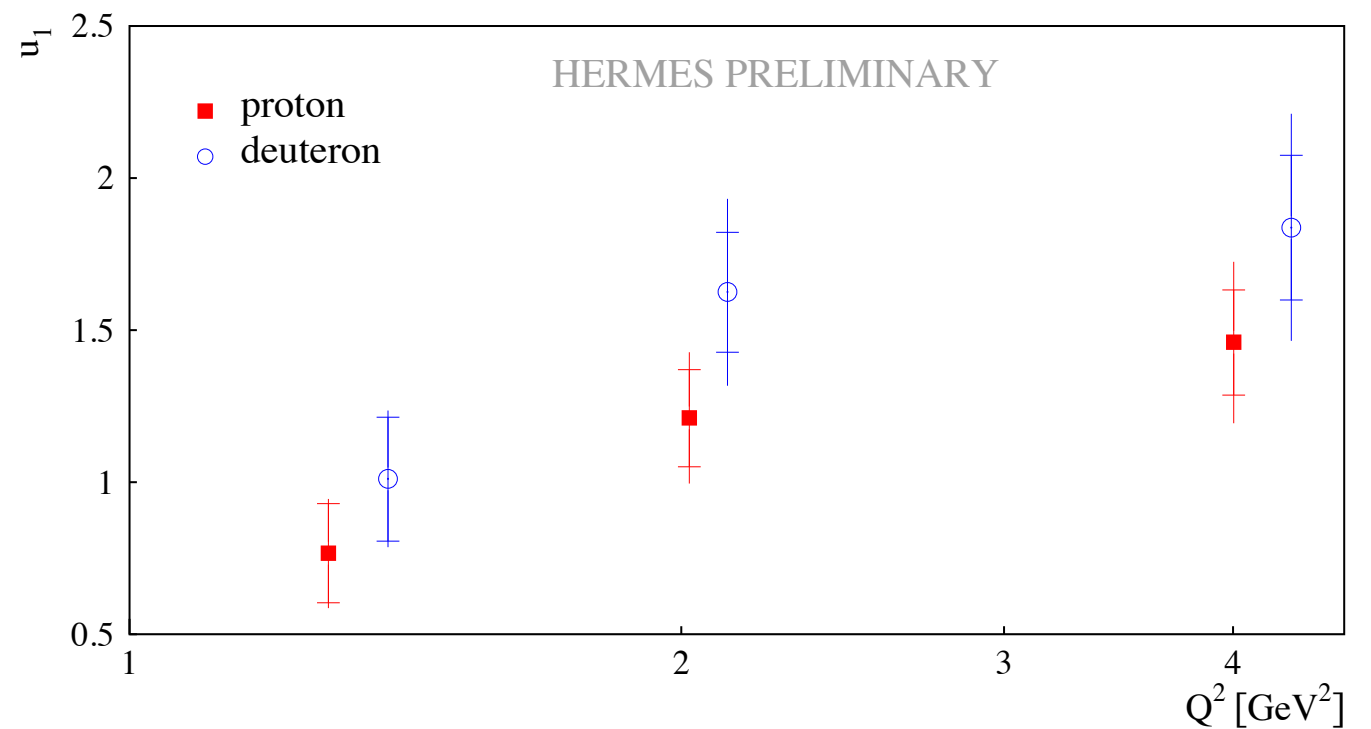
$$u_2 = r_{11}^5 + r_{1-1}^5$$

$$u_3 = r_{11}^8 + r_{1-1}^8$$

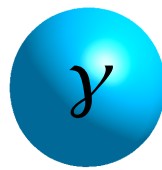
ρ^0 : non-zero UPE signal (3σ)



ω : dominant UPE signal!

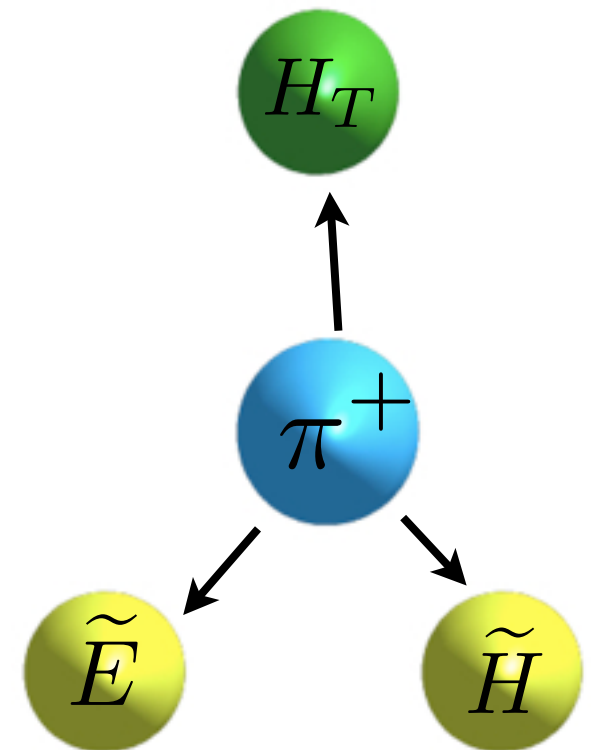
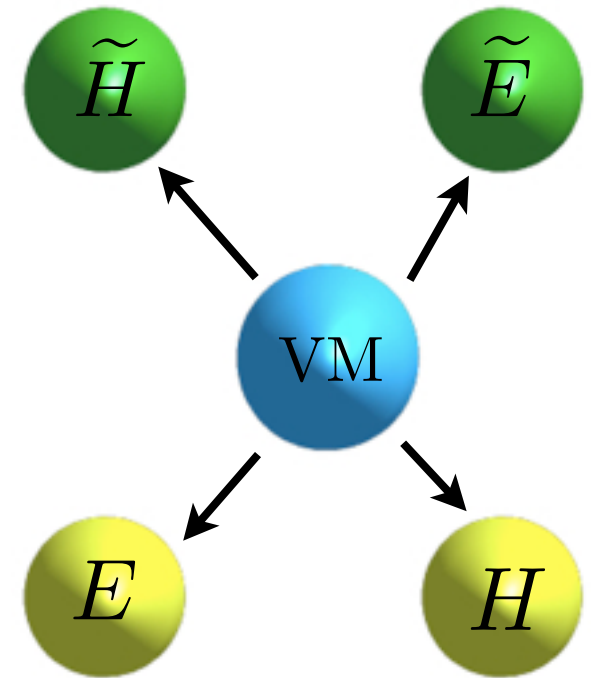
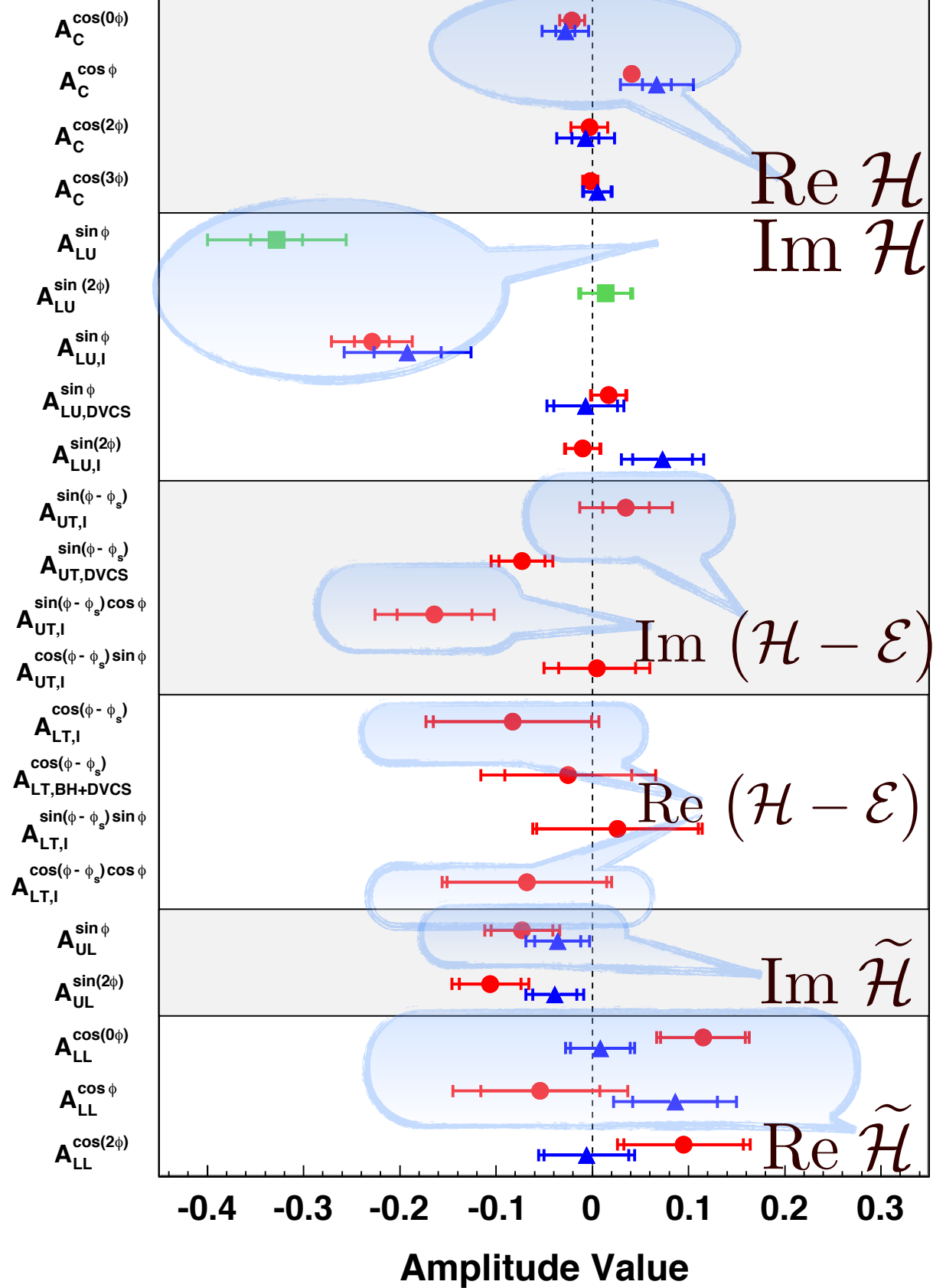


possible access to GPD \tilde{H} !



HERMES DVCS

- Hydrogen
- ▲ Deuterium
- Hydrogen Pure





The Spin Community And The World

- ➡ HERMES has been the pioneering collaboration in TMD and GPD fields
- ➡ still very important player in the field of nucleon (spin) structure
 - ➡ polarized $e^{+/-}$ beams
 - ➡ pure gas target
 - ➡ good particle identification
 - ➡ recoil detector